ARTICLE INFO
Article ID: 03-15-01-0004

doi:10.4271/03-15-01-0004

Knock: A Century of Research

Daire James Corrigan[1] and Stefano Fontanesi[2]
[1]Ferrari SpA, Italy
[2]University of Modena and Reggio Emilia, Italy

Abstract

Knock is one of the main limitations on increasing spark-ignition (SI) engine efficiency. This has been known for at least 100 years, and it is still the case today. Knock occurs when conditions ahead of the flame front in an SI engine result in one or more autoignition events in the end gas. The autoignition reaction rate is typically much higher than that of the flame-front propagation. This may lead to the creation of pressure waves in the combustion chamber and, hence, an undesirable noise that gives knock its name. The resulting increased mechanical and thermal loading on engine components may eventually lead to engine failure. Reducing the compression ratio lowers end-gas temperatures and pressures, reducing end-gas reactivity and, hence, mitigating knock. However, this has a detrimental effect on engine efficiency.

Automotive companies must significantly reduce their fleet carbon dioxide (CO_2) values in the coming years to meet targets resulting from the 2015 Paris Agreement. One path towards meeting these is through partial or full electrification of the powertrain. However, the vast majority of automobiles in the near future will still feature a gasoline-fueled SI engine; hence, improvements in combustion engine efficiency remain fundamental.

As knock has been a key limitation for so long, there is a huge amount of literature on the subject. A number of reviews on knock have already been published, including in recent years. These generally concentrate on current understanding and status. The present work, in contrast, aims to track the progress of research on knock from the 1920s right through to the present day. It is hoped that this can be a useful reference for new and existing researchers of the subject and give further weight to occasionally neglected historical activity, which can still provide important insights today.

History

Received: 30 Jan 2021
Revised: 17 Apr 2021
Accepted: 24 Jun 2021
e-Available: 28 Jul 2021

Keywords

Knock, Engine efficiency, CO_2, Compression ratio, Detonation, Combustion, Octane, Gasoline

Citation

Corrigan, D. and Fontanesi, S., "Knock: A Century of Research," *SAE Int. J. Engines* 15(1):2022, doi:10.4271/03-15-01-0004.

ISSN: 1946-3936
e-ISSN: 1946-3944

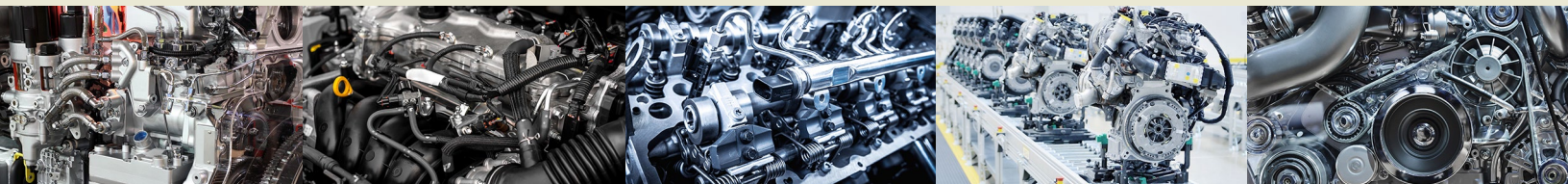

Introduction

In December 2015, an international treaty on climate change was agreed as part of the United Nations Framework Convention on Climate Change. This is now known as the Paris Agreement [1]. Its goal was to limit the increase in global average temperatures to within a maximum of 2°C, and ideally to within 1.5°C, of preindustrial levels. In order to respect this, all signatories must reduce greenhouse gas emissions significantly. The European Union (EU) set targets for its automotive manufacturers to reduce carbon dioxide (CO_2) emissions as shown in Figure 1 [2]. It can be seen that the 2030 target is just 50% of the 2015 status. Electrification of the fleet is expected to play a major role in achieving these targets. The year 2020 was a record year for Extended Range Electric Vehicles (ECV[1]) sales in the EU, as shown in Figure 1, but the total market share was just 10% [3]. Around half of these were plug-in hybrids, which also feature a combustion engine. Diesel engines do not suffer from end-gas knock as combustion primarily occurs in locally rich regions in an otherwise very lean chamber. They tend to have higher oxides of nitrogen (NO_x) and particulate matter emissions as a result and, hence, require more expensive aftertreatment systems than typical homogeneous charge stoichiometric Spark-Ignition (SI) engines. While in 2015 diesel engine vehicle sales made up 52% of the European market, following the 2015 Volkswagen "Dieselgate" emissions scandal [4], equivalent sales had reduced to just 28% by 2020. Alternative fuels such as Liquefied Petroleum Gas (LPG), Natural Gas (NG), and 85% ethanol blends (E85) accounted for less than 2% of sales. Vehicles with gasoline-fueled SI engines, therefore, dominated the market in 2020 and are expected to continue to do so in the near future. If CO_2 targets are to be met, significant gains in SI engine efficiency are therefore required.

SI engines operate on the Otto cycle. The thermal efficiency of this cycle is a function of the Expansion Ratio, which is well known. For the basic Otto cycle, the Compression Ratio is equal to the expansion ratio. The compression ratio should therefore be maximized in order to minimize CO_2 output. The primary limitation on how high the compression ratio can be raised is knock.

FIGURE 1 EU fleet CO_2/km target and achieved values for new passenger cars [2] and ECV sales [3].

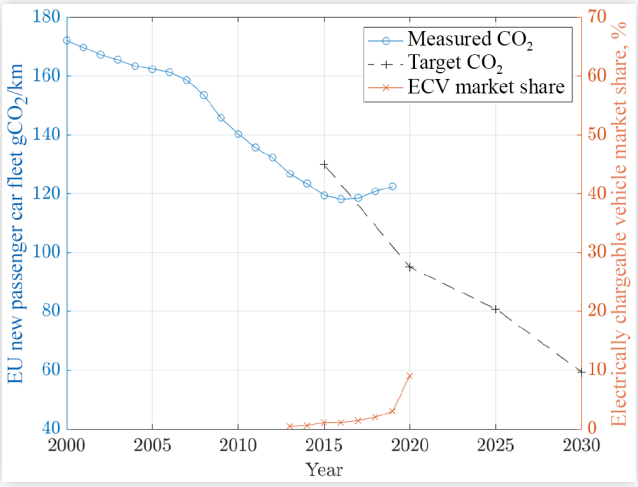

Data taken from Refs. [2] and [3]. © SAE International

[1]ECVs are defined as Battery Electric Vehicles (BEV), Fuel Cell Electric Vehicles (FCEV), Plug-in Hybrid Vehicles (PHEV), and Range Extender Vehicles (EREV).

Knock Description

"Knock" was the name given by early engine researchers to a certain abnormal combustion noise made by an Internal Combustion Engine (ICE). It was a sharp, metallic sound that could easily be discerned by the human ear. Sir Dugald Clerk [5] in a 1921 paper referred back to the problem in the 1870s. Knock has therefore been a recognized issue since at least around the time of Otto's famous 1876 patent for a compressed charge four-cycle engine. It was noted that knock occurred shortly after ignition timing and so was a distinct phenomenon to preignition. H.R. Ricardo [6] in 1922 said that knock was what limited the compression ratio of an engine and hence its performance and efficiency. Ricardo also described the phenomenon of knock as being caused by spontaneous ignition of the unburnt charge, ahead of the flame front.

A number of theories of the origin and nature of knock have been proposed in the meantime, but the basics of current understanding are not far removed from Ricardo's description. The theory has, however, been significantly refined as will become clear in the main body of this work. A brief summary of the phenomenon, in any case, will now be given. Knock in an SI engine occurs when a region of the unburnt charge ignites ahead of an advancing flame front. The autoignition almost always begins at one or a number of localized regions known as hot spots, or exothermic centers. Once a localized autoignition event takes place, what happens next depends on the size of this exothermic center and the reactivity gradient around it. A pressure wave is frequently, but not always, generated. For moderate knocking, this propagates at sonic velocity across the chamber and is then reflected by the chamber boundary. Standing waves result, whose frequencies depend on the acoustic modes of the combustion chamber volume. These cause vibrations in the engine structure that give rise to the characteristic sound. It is also possible that the initial pressure wave becomes coupled with local autoignition chemistry and, thus, generates a reaction front traveling at well above sonic velocities. This results in very strong pressure wave behavior, and hence is likely to cause engine damage. This phenomenon is sometimes referred to as "super-knock" and is an example of Developing Detonation.

Knock in the present article refers to end-gas autoignition. This definition separates it from Low-Speed PreIgnition (LSPI), which is generally thought to be driven by solid particles detached from the combustion chamber walls or liquid droplets of oil/fuel mixture separated from the liner or the

piston rings. These may go on to form relatively large exothermic centers, which can cause strong autoignition events that cannot be controlled by retardation of spark timing. This problem is most likely to occur at low speed and high load in modern Gasoline Direct Injection (GDI) engines and is a large field of research in itself. The current article will not comment upon LSPI in detail as it is somewhat distinct from what may be called "conventional knock" behavior, which is the main focus of the current work. Controlled AutoIgnition (CAI) engines will be referred to, but only where there are important links to current SI knock understanding, for example, pressure wave behavior following autoignition or Spark-Assisted Compression Ignition (SACI) combustion systems.

Recent Knock Literature Reviews

The current article is far from the first literature review on the subject of knock, and indeed a number of high-quality reviews have been published in recent years. These will now be commented upon and the motivation for a new review paper explained.

In 1998 Towers and Hoekstra [7] of the University of Central Florida published their paper titled "Engine Knock, A Renewed Concern in Motorsports—A Literature Review." The background was the proposed introduction of unleaded fuel in Winston Cup NASCAR racing. A wide-ranging review was performed including basic theory, damage mechanisms, and design considerations. Although some historic works were commented upon, in particular, the visualization activity of Miller in the 1930s, almost two-thirds of the 46 papers cited were from only the preceding two decades.

In 2012 Zhen et al. [8] of Tianjin University published their work "The Engine Knock Analysis—An Overview." The knocking phenomenon was described, as were detection, quantification, and visualization techniques. Simulation and chemical kinetics models were also discussed as were methods of knock suppression. A total of 70 papers were reviewed, but once again the majority of these were from the preceding 20 years—over 90%.

A large-scale literature review on knock titled "Knocking Combustion in Spark-Ignition Engines" was published as recently as 2017 by Wang and Liu of Tsinghua University and Reitz of the University of Wisconsin-Madison [9]. Both conventional knock and super-knock resulting from oil droplets and solid particles were discussed in detail, as were analysis methods, suppression and control strategies, and future research directions. Over 300 works were cited, but once more over 90% of these were from the two decades preceding publication.

Also in 2017, Gautam Kalghatgi [10] published his review "Knock Onset, Knock Intensity, Super-Knock and Preignition in Spark Ignition Engines." Of the articles published, a large majority were from the preceding 20 years, in this case, three-quarters of the total of 60.

A paper from 2015 entitled "A Literature Review of Abnormal Ignition by Fuel and Lubricant Derivatives" by Chapman and Costanzo [11] did make a concerted effort to study historical work, making comparisons of abnormal combustion observed in earlier periods with that seen with modern engines. Less than a third of citations were from the 20 years leading up to publication with the majority concentrated on older activities. This work, however, focused on preignition rather than knock and, more specifically, preignition sensitivity to oil and fuel derivatives.

The above comments on existing knock review papers should not be seen as a criticism of the approach taken by the relevant authors, as each work has made a significant contribution to our understanding of the subject. However, the period from 1920 to 1990 has not been covered in great detail in these papers (with the exception of the work by Chapman et al. on preignition) despite the importance of the early period in explaining how we have arrived at our modern understanding and approach. This is shown in Figure 2. The current paper, therefore, seeks to fill this gap in the literature by describing the contributions that have been made in each decade from the 1920s up until the present day. This is intended to be complementary to existing recent surveys of knock.

Paper Structure

The article aims to take the reader from a starting point 100 years ago through to the present day, commenting on significant works over the decades. The conclusion section will summarize our current understanding based on this accumulated learning with particular emphasis on knock mitigation techniques. Suggestions are also made for future research activity.

FIGURE 2 Number of works cited from each year by some recent literature reviews on knock.

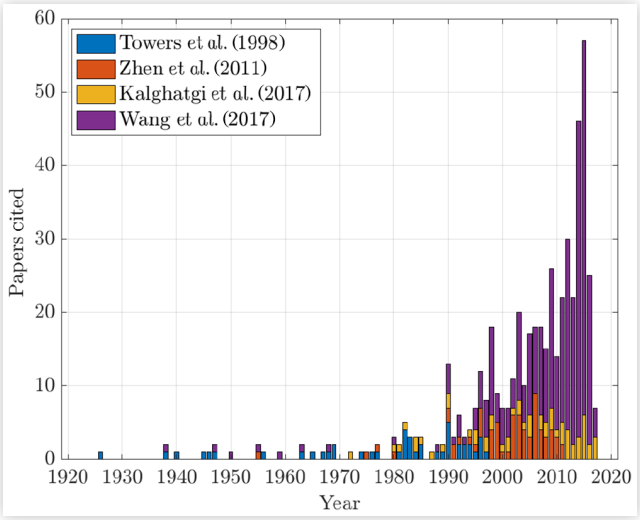

Paper Selection

It is relatively easy to survey the relevant literature in the early period, but the volume of work has increased significantly in the last years. The first database of literature investigated was that of the Society of Automotive Engineers (SAE). Papers from the early decades were found by searching for "knock" or "detonation" in the SAE database, either in the title or full text. As the years progressed, a more selective approach had to be taken in order to render realistic completion of the review within the available time. In the more recent years, papers were primarily identified from having "knock" in the title and since 2007 from having achieved journal publication. Other key works in journals including *Combustion and Flame*, *Proceedings of the Royal Society*, and *Proceedings of the Combustion Institute*, together with relevant textbooks, have also been referred to. In order to give a broader overview, related engine development, scientific progress, and societal and regulatory changes have also been commented upon.

Despite the significant effort made, undoubtedly important works have been overlooked for which the authors apologize in advance. It is hoped that enough activity has been covered to give a general overview of the research progress over the decades and to point the reader towards sources where more detailed information can be found.

The 1920s: Fuel Shortages, New Experimental Methods, and Tetra-Ethyl Lead

A number of detailed studies on knock were already published in the 1920s. The driving interest was a shortage of high-quality fuels following the First World War in comparison to a greatly increasing number of vehicles on the road, as described by Kettering [12]. Knock was already a well-known issue to these engineers, with Sir Dugald Clerk [5] (a pioneer of early two-stroke engines) referring back to the problem in the 1870s. Knock was an issue because of its unpleasant noise and the possibility of engine failure. The ignition timing was typically adjusted by the driver to avoid the knocking sound. Motorists were therefore highly aware of the phenomenon and the impact of variable fuel quality. Gasoline was produced at the time through fractional distillation of crude oils and shale oils with boiling temperatures in the range 50-200°C. The knock resistance of the fuel was heavily dependent on the source of the crude oil. Certain oil fields, such as Pennsylvania, produced oil high in paraffins (alkanes). Oil from Borneo, on the other hand, was high in aromatics [13]. Clerk also cited some methods of managing knock that have enjoyed a resurgence in recent years: cooled Exhaust Gas Recirculation (EGR) and water injection. Horning [14] of the Waukesha Motor Company noted the knock mitigation effects of fuel enrichment and the importance of charge and component temperature reduction, in particular avoiding hot spots in the combustion chamber from the valves and spark plug, maintaining piston temperatures low, and having an effective water jacket. Note that heating of the inlet manifold was typically required at the time to achieve adequate vaporization of the available fuels, with obvious deleterious impact on the compression ratio that could be tolerated.

Knock was also discussed in some detail in a seminal paper by the esteemed engineer Harry R. Ricardo in 1922, where he stated that it was the main limit on spark-ignited engine performance and efficiency [6]. Ricardo also suggested that the fundamental cause of knock originated from an autoignition event in the end gas. This theory had actually originally come from his professor at Cambridge University, Hopkinson, as Ricardo himself would later describe. The influence of temperature, pressure, turbulence, mixture strength, and fuel type was considered. A Rapid Compression Machine (RCM) was constructed, together with his colleagues Tizard and Pye, in order to more properly understand the underlying dependencies. It was found that for a given fuel and equivalence ratio, whether autoignition occurred depended on a critical temperature being reached in the machine. Both rich and lean mixtures were shown to be beneficial for knock in an engine, as shown in Figure 3. For homogeneous gasoline mixtures, enleanment was only possible in a narrow range, due presumably to combustion instability. Hydrogen, as a fuel, was shown to permit further enleanment and knock benefits. A stratified charge engine making use of a prechamber was also built. This extended the lean limit with gasoline and was shown to be advantageous from a knocking point of view. OverHead Valve (OHV) and "L-head" (side valve) engines were compared. OHV engines gave superior knock resistance and better volumetric efficiency. The importance of minimizing the distance from the spark plug to the furthest extreme of the combustion chamber was stressed. Compression ratios studied in the work ranged from 4.0 to 7.5 using a

FIGURE 3 Knock-limited compression ratio variation with mixture strength for aromatic-free gasoline as measured by Ricardo, from Ricardo [6].

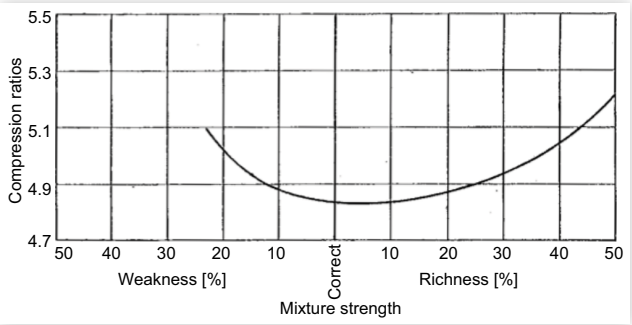

variable compression ratio engine to rate different fuel types.[2] Alcohols and aromatics were most resistant to autoignition while paraffins were the worst, although there was considerable variability within the same hydrocarbon (HC) family. The knock limit was detected by the human ear only, but this was judged to be very repeatable. The Indicated Thermal Efficiency (ITE) with aromatic-free gasoline was around 30%.

Alternative methods of recognizing knock were already available, and indeed, cylinder pressure curves during knocking were presented in this period by a number of researchers including Kettering [12], Dickinson [16], and Midgley [17]. These came from optical indicating devices where a beam of light is focused by a mirror onto a photographic film. An issue with such systems was separating vibration effects of the instrument from pressure oscillations due to knock. The natural frequencies of the instruments were between 1200 Hz and 1700 Hz [18]—too low to measure typical knock-driven pressure oscillations. An alternative system was a string galvanometer constructed by Professor Augustus Trowbridge [19] of Princeton University, which recorded the rate of change of cylinder pressure on the photographic film. Ion-current measurements were developed by MacKenzie and Honaman [20] at the Bureau of Standards. This enabled flame-speed measurement in an ICE for the first time by making use of multiple spark plugs. Flame velocities from 1 m/s to 4 m/s were observed. Knocking cycles were seen to feature rapid combustion. Clark [21], an applied chemist at the Massachusetts Institute of Technology (MIT), applied ultraviolet (UV) spectroscopy using a crank-angle synchronous shutter to an engine running on different fuels in knocking and non-knocking conditions. Greater spectral content in the UV range was seen for knocking cycles in the early stages of combustion.

A method that would later become a standard was the so-called Dickinson Bouncing Pin. H.C. Dickinson also worked at the Bureau of Standards, Washington. The pin rested on a piston, which was exposed to combustion chamber pressure. During knocking combustion, the pin would jump clear of the piston as high as 1.5 inches. Midgley [17], working at General Motors (GM) Research Corporation on fuels research, added an integration device to this instrument by having the jumping of the pin close a circuit that performed electrolysis on dilute sulfuric acid mixture. The resulting gas was collected and the flow rate used to indicate the severity of the knock. The instrument is shown in Figure 4. A review of the range of methods of knock determination and fuel rating in use at the time was given by H.K. Cummings [22] of the Bureau of Standards in 1927. The bouncing pin was said to be the most common device in use. In 1928, a new electrical indicator was described by Martin and Caris [18] of GM. This enabled registering of single cycles on photographic film at frequencies of several kilohertz. It was based on the pressure in the engine varying the resistance of two carbon pile rheostats and could be connected to a cathode-ray oscilloscope.

FIGURE 4 Dickinson/Midgley bouncing pin knock indicator, from Cummings [22].

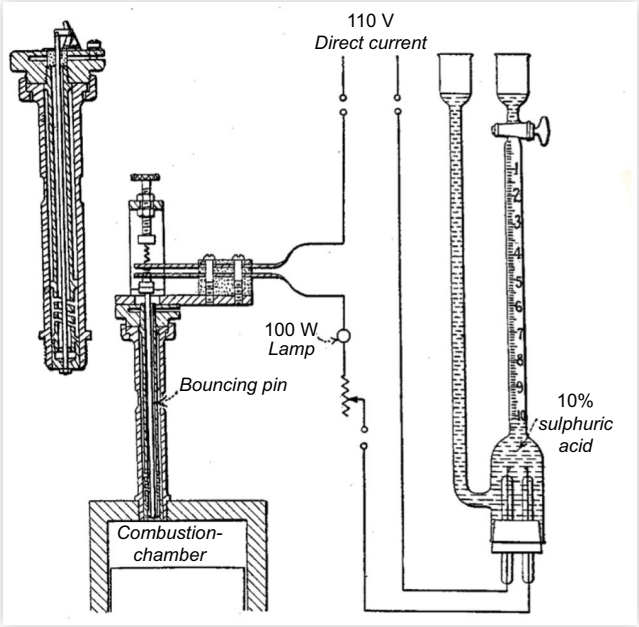

The frequency bandwidth was said to be high, but was not quantified. Another electrical instrument, a condenser-based device created by Obata and Yosida of Tokyo Imperial University, could measure up to 12,000 Hz and so was capable of measuring knocking pressure oscillations.

Midgley [23] published not only on experimental methodology but also theoretical analysis of knock physics and chemistry. He is regarded as being one of the key figures behind the introduction of Tetra-Ethyl Lead (TEL) [24]. His colleague, C.F. Kettering, published on similar themes, discussing the molecular structure of various HCs, their knock propensity, and distillation characteristics [12]. TEL allowed for remarkable improvements in knock behavior when added in small quantities to gasoline. It was manufactured by the Ethyl Gasoline Corporation, which was formed by GM and Standard Oil of New Jersey. Treat rates of 3 cubic centimeters (cc) per gallon were typical. This enabled a significant increase in compression ratio, and hence fuel efficiency for a given fuel cost. However, health risks were noted at an early stage.

Eleven people involved in the manufacture of TEL died between 1923 and 1925 due to acute lead poisoning, as documented by Hamilton et al. [25] in the *Journal of the American Medical Association* in 1925.[3] This was likely through skin contact. Sale was banned and new precautions were taken in manufacturing facilities to reduce exposure risk. A second potential issue was chronic lead poisoning through inhalation of exhaust fumes over extended periods from engines

[2]The most popular car of the period, the Ford Model-T, featured a side-valve four-cylinder engine of 3.98:1 compression ratio [15].

[3]Alice Hamilton was recognized as being a leading expert on lead poisoning and industrial toxicology [26] and was also the first woman appointed to the faculty of Harvard University.

operating on fuel containing TEL. GM Research Corporation requested and paid for an investigation into this by the United States (US) Bureau of Mines in 1923. An interim update on this work was given in 1924 by Sayers et al. [27] and did not demonstrate a link between inhalation and lead poisoning. The report was criticized in terms of its methodology and conclusions by, among others, Hamilton et al., who suggested further investigations should be performed and in the meantime to suspend the use of TEL in gasoline. Testing continued until 1925, although the final report was not published until 1927 by Sayers et al. [28]. The Surgeon General organized an independent study in the meantime [26]. The resulting report in 1926 by Leake et al. [29] found insufficient evidence for prohibiting the use of TEL. However, a longer-term independent study was recommended. TEL returned to the market, and it would be many years before the issue would once again return to the public consciousness.

TEL was a commercially successful product as it improved the antiknock resistance of fuels, and such fuels were sought after by consumers. An objective rating scale of knock resistance of commercial gasolines was required. This was the task of the Cooperative Fuel Research (CFR) group. It was Edgar Graham [30] of the Ethyl Gasoline Corporation who suggested the use of iso-octane (2,2,4-trimethyl pentane) and n-heptane as the scale against which all other gasolines could be compared. It was stated that commercial fuels of the time behaved similarly in knocking terms to a mixture of 40-60% iso-octane in n-heptane. Iso-octane/n-heptane mixtures are now known as Primary Reference Fuels (PRF), with the following number that corresponds to the percentage iso-octane content. Thermal cracking was becoming more popular as a refinery process, meaning more olefinic HCs (alkenes) were being used in gasoline [13].

At the end of the decade, Robert N. Janeway [31], a consulting engineer in Detroit, stated that it was generally accepted that knock was primarily driven by maximum unburnt gas temperature. He also derived mathematical relationships between flame-front propagation, inflamed volume, and cylinder pressure.

The 1930s: The Research Octane Number and Motor Octane Number Methods, Flame-Front Visualization, and Knock Frequencies

In the early 1930s, work continued to refine a standardized method of rating the knock resistance of fuel, led by the CFR group. There was general agreement that a knock-prone and a knock-resistant HC should form the basis of the scale. Normal heptane had already been suggested by Ricardo as being an adequately knock-prone reference. There was some discussion, however, on what should be the knock-resistant fuel. Some laboratories, such as that of the Asiatic Petroleum Co. in London, continued for a time with the suggestion of Ricardo in using benzene [32].[4] Iso-octane, as suggested by Graham [30], was preferred by Campbell, Lovell, and Boyd of GM, primarily as it had similar physical properties to n-heptane. This meant they mixed well, and hence there was little risk of the components separating in the intake system of an engine. Campbell et al. [33] tested a number of candidate pure HCs mixed with n-heptane in a variable compression ratio OHV 3.25 bore engine at 600 rpm with no inlet heating. This low engine speed was used both because it made knock easier to hear, and also it increased knock propensity. Testing was performed with spark timing for maximum power (according to tabulated values against compression ratio) and with mixture ratio for maximum performance. The results are shown in Figure 5. The authors noted that perhaps iso-octane was not adequately knock resistant to cover all potential future fuels. Despite this concern, the laboratories converged on an n-heptane/iso-octane scale. This was said to give greater variation in knock intensity and more consistency than the main alternative considered, benzene, as documented by Barton et al. [34]. This scale is still in use to this day.

Work was carried out in parallel on the development of a dedicated CFR knock rating engine to facilitate quick and accurate testing, as described by Kegerreis [35]. Investigations were performed and recommendations made for water jacket temperature by Graham [36] and for carburetor setting and ignition timing by Campbell et al. [37] at GM. The Air-Fuel Ratio (AFR) was to be swept for maximum knock.[5]

FIGURE 5 Knock-limited compression ratio of various HCs in n-heptane mixtures, as measured by Campbell et al. [33].

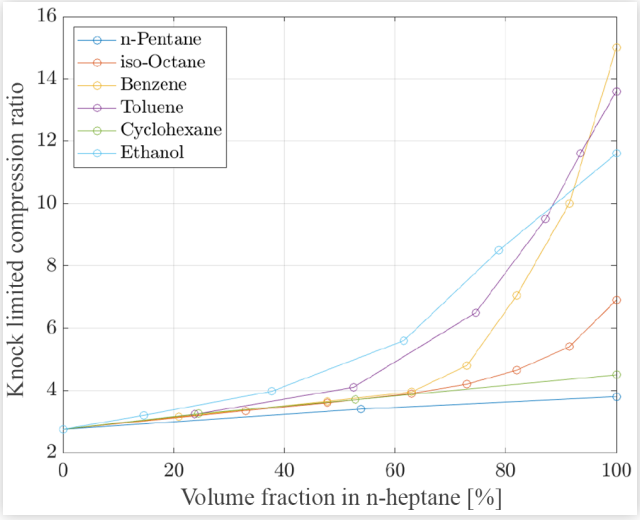

Data taken from Ref. [33]. © SAE International

[4] Ricardo also experimented with toluene in his own laboratories.

[5] It was found that most fuels had a maximum knocking tendency at an AFR of 13-14:1.

The compression ratio would be adjusted in testing, as had been suggested by Ricardo, to obtain a target amount of knock as judged by the bouncing pin. It was initially recommended that the theoretical best ignition timing for each compression ratio be used. It was shown by Huf [38] of the Atlantic Refining Co. that the exact knock intensity at which fuels were rated was not critical, providing that it was consistent over the duration of the test activity and that the reference and test fuels had a similar knock propensity. This work would form the basis of what is still known as the Research Octane Number (RON) test procedure, and this was approved by the American Society for Testing and Materials (ASTM) in 1931. Some details are shown in Table 1 from the 1932 CFR Committee report [39]. Note that in the approved version the spark timing was fixed at 13° Before Top Dead Center (BTDC) rather than being variable with compression ratio, as suggested by Campbell et al. An electronic knockmeter was used with the bouncing pin indicator—taking the place of the earlier electrolysis device. This procedure, with some minor modifications, is now known as ASTM D2699 [40].

The problem of fuel rating appeared to have been solved. It was noticed, however, that the ranking of fuels in road testing did not fully agree with the results of the RON test. A large-scale study was again coordinated by the CFR group as described by Veal et al. [41] in 1933. A total of 14 companies, from both fuel and automotive backgrounds, took part. Testing took place at Uniontown. A total of 15 different vehicles were used with reported compression ratios from 4.9 to 7.0. A total of 15 fuels were tested in a blind manner. Testing took place over a range of vehicle speeds with the knocking tendency tending to die out as the car accelerated. Charts were therefore produced of knock intensity, judged aurally, against vehicle speed. It was decided, however, that the maximum knock would be taken as the criterion against which to judge a reference fuel, irrespective of the speed at which it occurred. Over 2500 test runs were performed. It was noted that different engines had different so-called "sensitivities" to different fuels. The same fuels were then tested on the CFR engine using the RON procedure. Modifications were implemented both to the engine and the procedure, with a view to improving correlation with the road-test results. A shrouded intake valve was introduced in order to create swirl, with the aim of producing more consistent knock measurements. An improved vapor condenser was also installed. The water jacket circulation pump was removed to increase wall temperatures. The test speed was moved to 900 rpm and an air/fuel mixture temperature of 300°F was stipulated (149°C). The key changes are summarized in Table 2. This would form the basis of the CFR Motor method. This gave the Motor Octane Number (MON) of a fuel. Correlation was much improved with road test results of the period. This procedure is now known as ASTM D2700 [42].

TABLE 1 1931 CFR research method test conditions, from the 1932 CFR Committee Report [39].

Engine type	Waukesha CFR OHV
Bore/stroke	3.25″/4.5″
Compression ratio	4-18:1
Piston	Cast iron
Engine speed	600 rpm
Intake air temperature	52°C
Coolant temperature	100°C
Spark advance	13°BTDC
Carburetor adjustment	Maximum knock
Knock feedback	Bouncing pin with knockmeter

Data taken from Ref. [39]. © SAE International

TABLE 2 1933 CFR motor method modifications from the research method, from Veal et al. [41].

Engine speed	900 rpm
Air/fuel mixture temperature	149°C
Spark advance	Variable with compression ratio

Data taken from Ref. [41]. © SAE International

A follow-up report by the CFR group was published in 1935, once again by Veal [43]. Good, though not perfect, correlation was again demonstrated between MON values and on-road measurements on a wide range of cars and fuels. The concept of fuel sensitivity "S" was defined as RON − MON. A car-dependent index known as the "Engine Severity Factor" attempted to weigh how close the road rating corresponded to MON and RON values, as shown in Equation 1. This can be seen as a forerunner of the modern "K-factor" approach.

$$\text{Severity factor} = \frac{\text{RON} - \text{Road rating}}{\text{RON} - \text{MON}} \qquad \text{Eq. (1)}$$

A further review of road knock tests was published in 1938, this time by Boyd [44] of GM. This featured around three times the number of cars in comparison to the prior study and 38 fuels covering both summer and winter grades. The MON test was again shown to be closest to the road test results. Statistical analysis of this dataset was also performed by Campbell et al. [45] at GM focusing on the probability of error in road and lab octane tests. It was shown that the variability in road testing was three to six times higher than for CFR engine tests.

At around the same time, work was also being performed by Beale and Stansfield [46] at the Anglo-Iranian Oil Company on an alternative method of knock feedback on the CFR engine. This was based on block vibrations measured using an electromagnetic pickup. The signal was rectified and amplified and then displayed on a knockmeter with adjustable damping. No details of the frequency bandwidth of the instrument were given. This was known as the Sunbury Knock Indicator and became an alternative to the bouncing pin method for CFR testing. It was relatively new in 1939 when the CFR group performed an international review of the precision of laboratory knock testing. The lead author was Brooks [47] of the National Bureau of Standards. It was not found to improve precision in comparison to the bouncing pin, although it was noted that this may have been simply due to the immaturity of the technique. In general, the standard

deviation of octane measurements between around 100 laboratories was less than 0.5 by the end of the decade.

Optical techniques to track flame-front propagation were being applied in this period by Marvin [48] of the National Bureau of Standards. Multiple small windows were made in an L-head engine, and stroboscopic techniques allowed tracking of typical flame-front positions at a given crank angle over a number of cycles. The technique recalls somewhat the fiber-optic method, which is commonly used today. Different fuels and knock conditions were compared and optical filters were used to study infrared emissions in bandwidths for carbon particles, CO_2 and H_2O. Flames were seen far from the spark plug at an earlier point in the cycle when knock occurred. Radiation also peaked at earlier crank angles.

Perhaps the most famous researchers on flame-front measurements at this time were Rassweiler and Withrow [49] at GM. In 1935, they published on gas temperature measurements in an ICE, for both knocking and non-knocking conditions, using the sodium line reversal method. As well as observing higher temperatures during knocking combustion, they also noted an increased heat transfer rate, which was attributed to higher turbulence caused by pressure oscillations. Sudden increases in luminosity were observed at the moment of knock. Pressure waves traveling in the combustion chamber following knock were also mentioned. In 1936 Withrow and Rassweiler [50] used a quartz plate on an L-head engine to have a complete view of the combustion chamber. A camera was used, which could take 5000 pictures per second. The propagation of the flame front could be clearly tracked. The high luminosity from incandescent carbon—a result of burning decomposed lubricating oil—was noted. A fast sampling valve was also used to confirm the chemistry in unburnt, burning, and burnt zones. The knocking cycles photographed demonstrated the presence of an autoignition event far away from the advancing flame front (rather than a sudden acceleration of the flame front, an alternative theory of knock at the time) as shown in Figure 6. The autoignition was correlated to preflame reactions, confirmed by the absorption spectra taken in this zone prior to knock. The knock initiation location was seen to vary, which was taken as evidence that it was not driven by surface hot spots in the combustion chamber.

Rassweiler and Withrow's [51] most famous work, however, was correlating flame-front propagation with pressure indication in 1938. The transparent L-head engine was again employed. Plaster casts of the combustion chamber at various piston positions were made. Photographs of the inflamed area as viewed through the transparent window were projected onto the casts as shown in Figure 7. The casts were then separated into "burnt" and "unburnt" regions and weighed. Single cycles, where the ignition was cut, were used to generate data of unburnt pressure versus total volume. It was found that there was a polytropic relationship between these values. The volume inflamed, based on the photographs and plaster casts, could be corrected to the original volume of this charge at ignition timing, through the polytropic relationship. Given that, at ignition timing, charge density is assumed to be spatially uniform, the volume fraction equals the mass fraction. This approach can be applied for each photograph in order to convert from volume fraction to Mass Fraction Burned (MFB). Of course, what is desirable is the possibility to obtain these data without optical access. A method was derived based on separating pressure differences due to piston movement, which can be calculated assuming a polytropic process, from those due to combustion. The pressure rises due to combustion at a given volume were furthermore adjusted to the pressure rise that would have occurred at the initial combustion chamber volume at ignition timing. The result of the analysis is shown in Equation 2.

FIGURE 6 High-speed images of six knocking combustion cycles at 900 rpm, from Withrow and Rassweiler [50].

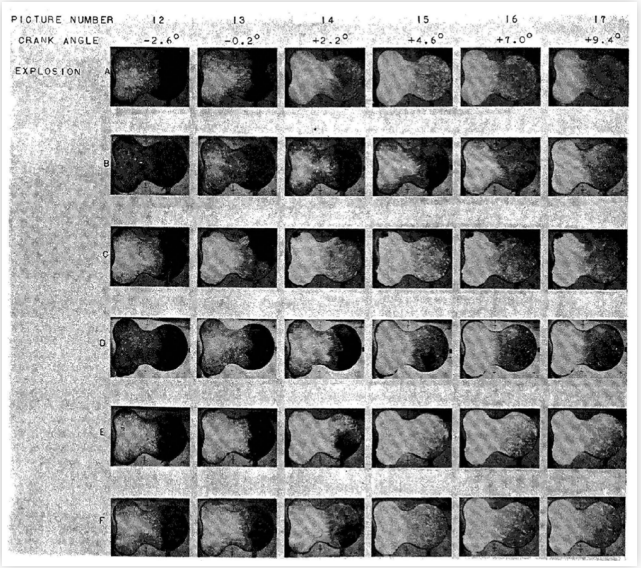

$$\mathrm{MFB} = \frac{\bar{P}_t^{1/n} V_t - \bar{P}_{ti}^{1/n} V_{ti}}{\bar{P}_{tf}^{1/n} V_{tf} - \bar{P}_{ti}^{1/n} V_{ti}} \qquad \text{Eq. (2)}$$

FIGURE 7 Plaster casts with flame area projections used by Rassweiler and Withrow to determine flame volume [51].

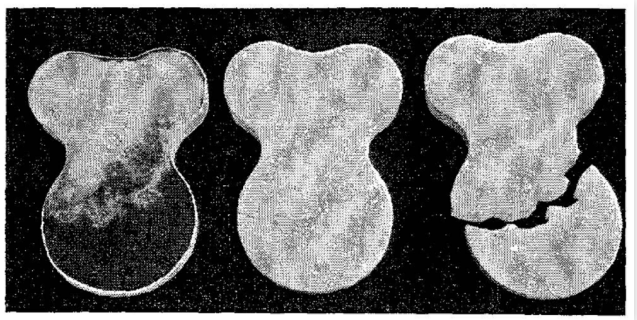

where

P is the combustion chamber pressure
V is the combustion chamber volume
ti is the state at ignition timing
t is any time between the start and end of combustion
tf is the state at end of combustion
n is the polytropic coefficient

Equation 2 is still employed in combustion analysis to this day. A summary paper of work at the GM laboratory was published by Boyd [52] in 1939. This was notable for showing the identical frequency of pressure oscillations in the combustion chamber and acoustic measurements just outside the engine. Preflame reactions in knocking cycles were also evidenced by differences in emission spectra and UV absorption in comparison to non-knocking combustion. Formaldehyde (HCHO) was seen to form ahead of the flame front for knocking cycles.

Advances were also being made in indication technology enabling characteristic frequencies of knock in-cylinder pressure traces and sound recordings to be identified. MacCoull [53] used a condenser microphone together with an electronic instrument that could perform frequency analysis and high-pass filtering. Knock on the CFR OHV engine was shown to take place between 6 kHz and 7 kHz while, on an L-head engine, a lower peak at 3500 Hz was also observed, as shown in Figure 8. This is likely because L-head combustion chambers have a length of approximately twice their bore diameter, as exemplified in Figure 7.

Draper [54] used a moving coil indicator connected through a vacuum-tube amplifier to an oscillograph to measure pressure oscillations during knocking on a CFR engine in 1935. He also noted that frequencies of around 6500 Hz were dominant in a frequently cited National Advisory Committee for Aeronautics (NACA) paper. Draper explained why this frequency was present by deriving the fundamental frequencies of oscillation of a plain-ended cylinder. A frequency of 6500 Hz was characteristic of the transverse acoustic mode (with a single nodal plane) of the cylinder at the expected gas conditions. The fired engine measurements were complemented by stationary recordings in the same engine where a small explosive charge was set off. It was shown that, theoretically, many modes could potentially be excited. In general, pressure measurement equipment of the day only had a bandwidth of around 10 kHz, and hence only content at 6500 Hz was confirmed. Draper [55] published a follow-up paper with the Institute of Aeronautical Sciences in 1938 with a more extensive theoretical analysis where modal frequencies up to 50 kHz were calculated. In this new work, an electromagnetic indicator with a resonant frequency of 95 kHz was coupled to an amplifier-oscillograph system with an extended bandwidth—greater than 20 kHz. The predominant frequency observed was still around 6500 Hz. Draper noted that other frequencies were present, but that a higher film speed would be required to isolate them.

FIGURE 8 Characteristic acoustic frequencies of knocking L-head engine as measured by MacCoull [53].

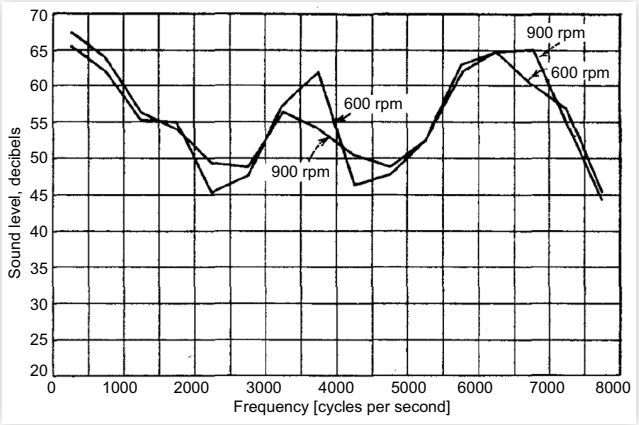

Reprinted with permission from Ref. [53]. © SAE International

Another significant activity for NACA was taking place at the time by Rothrock and Spencer [56] at Langley Field. They took schlieren photographs of the combustion chamber of a NACA research engine, initially at 1000 frames per second. The engine was of a fuel injection type, and indeed diffusion combustion, resulting from the sac volume, could be seen on the photographs. A similar phenomenon is frequently observed with modern GDI engines. Knock was apparent as a sudden increase in light intensity. A slight pressure rise was noted immediately prior to the knock event. Experiments were also performed charging a 2 μF condenser to 30 kV and then discharging it through a 0.004-inch copper wire in the combustion chamber. Although this produced a shock wave, it did not cause knock. This was to investigate one of the theories at the time that shock waves traveling through the combustion chamber were the cause of initial autoignition. This phenomenon is harnessed in shock-tube reactors to produce autoignition. It can also occur in engines if developing detonation takes place following an initial autoignition event. This would form a key avenue of research in later decades.

The octane value required to prevent knocking in automotive applications at this time was around 70 [43]. Gasoline octane had improved through the introduction of new refinery techniques such as polymerization and alkylation. Polymerization combines light olefins to give heavier olefins that can be used in gasoline. These tend to have high RON, but low MON. Alkylation produces iso-octane by catalytically reacting light olefins with iso-butane [13]. For military aero-engines, an octane value of 87 was targeted at the beginning of the decade. This required the use of aromatics and TEL as described by Heron [57], a research engineer for the Air Corps at Wright Field. Close to the outbreak of World War II (WWII), values of over 100 were becoming common for aviation fuels as noted by Du Bois and Cronstedt [58] of the Aviation Manufacturing Corp. The CFR group studied dedicated octane rating measurements for aviation gasoline. The objective, as described by Nutt [59] in 1933, was to develop a standard of knock rating for all types of aviation fuels that would be applicable to all engines. Veal [60] reported on status in 1936. Testing had been performed on four multicylinder

aero-engines, three of which were supercharged, made by Wright, Pratt and Whitney, and Lycoming. Testing was by sweeping the fuel flow from "full-rich" to "minimum-allowable" at a fixed throttle position. Cylinder temperatures, fuel flow, and power output were recorded, and each test fuel was bracketed with reference fuels. The point where cylinder temperature increased as fuel flow was reduced was used to define knocking behavior. The correlation with the Motor Octane method depended on the class of HCs in the base fuel. Further testing was reported in 1938 by Cummings [61]. The peak cylinder pressure was found to give a much better feedback on the knock-limited minimum fuel flow in comparison to the cylinder head temperature, as used in previous tests. Test fuels were bracketed by mixtures of technical iso-octane (Reference fuel S-1) and low-knock resistance Michigan Gasoline (Reference fuel M-1), rather than pure iso-octane and n-heptane, for cost reasons. TEL was used to extend the octane scale beyond 100 based on Indicated Mean Effective Pressure (IMEP) increases on a modified supercharged CFR engine as shown in Figure 9. A new laboratory method was suggested in 1939 by Stansfield and Taylor [62]. The CFR engine modifications included fitting an aluminum piston, improving engine volumetric efficiency through valve and carburetor modifications, and the use of a supercharger. Limitations of the bouncing-pin device were noted, where fast combustion with high-pressure rise rates could result in false detection of knock. The rate of change of pressure was therefore shown on an oscilloscope, and a knock index was developed based on the maximum rate of pressure rise of the first knocking oscillation of each cycle, observed over a minute of operation. Peak knock AFR was also identified using this method rather than the bouncing pin. The volumetric fuel flow was then increased by 25%, 35%, and 45% from this value. The compression ratio was adjusted at each AFR to give constant knocking for the reference fuel based on the oscilloscope method. This same compression ratio for each AFR was used also for the test fuels. The ratio of the knock signal for test and reference fuels against enrichment was then calculated. Different tendencies for different fuels were noted. The 45% rich setting was said to be representative of takeoff conditions. This combined activity would lead to the definition of the "Supercharge Rating of Spark-Ignition Aviation Gasoline"—now defined by ASTM D909 [63]. Some key details of the current standard are shown in Table 3. The procedure produces a knock-limited IMEP curve of the fuel over a range of AFRs from 0.08 to 0.12 with a fixed compression ratio. The manifold pressure is firstly adjusted to produce "standard knock"[6] at an AFR of 0.08. The mixture is then progressively enriched and manifold pressure increased to return to the same knock level. The IMEP of the test fuel is compared to the IMEP of the reference bracketing fuels at

FIGURE 9 Relative IMEP for reference fuels used in CFR aviation testing, from Cummings [61].

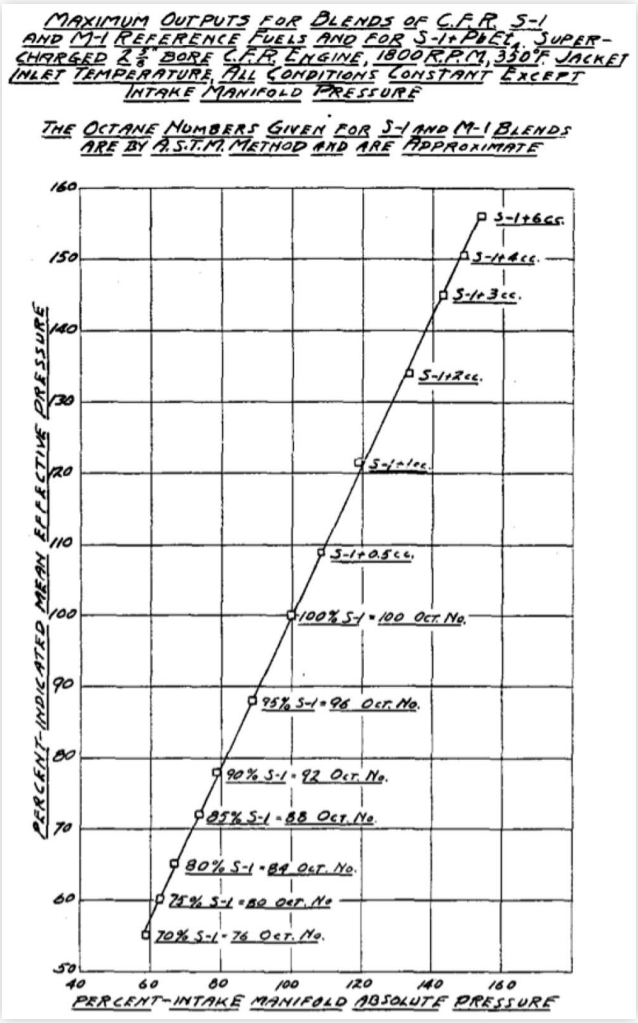

TABLE 3 Current standard test method for supercharge rating of SI aviation gasoline (ASTM D909-18e01) [63].

Engine type	CFR F-4
Bore/stroke	3.25″/4.5″
Engine speed	1800 rpm
Piston	Aluminum
Intake air temp. (Surge tank)	107°C
Supercharger pressure	Variable
Coolant temperature	191°C
Spark advance	45°BTDC
Compression ratio	7:1
Fuel system	Manifold injection 82-99 bar
Fuel-air ratio	0.08-0.12
Knock feedback	Determined by ear

[6]Despite the interesting studies on use of an oscilloscope for knock feedback, "standard knock" is still defined as trace or light knock as determined by ear in the modern procedure.

FIGURE 10 Supercharge performance number dependency on iso-octane in n-heptane and TEL concentration as defined by ASTM D909 [63].

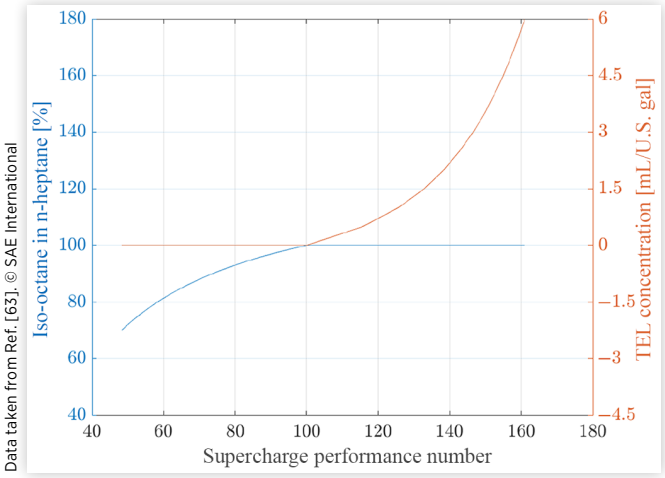

Data taken from Ref. [63]. © SAE International

the best mixture IMEP of the lower bracketing reference. Interpolation of these IMEP values gives the fuel rating. The rating scale for octane values above 100 was indeed based on the addition of TEL. A performance number was defined as shown in Figure 10.

Together with advances in combustion measurement techniques and improved octane fuel availability, engine technology was also evolving. Dillstrom and Torbjorn [64] of the Hesselman Motor Corporation published in 1934 on the use of fuel injection on an SI engine to permit a higher compression ratio. End of compression stroke injection was used and swirl employed to have adequate homogenization in full-load conditions. A stratified approach was employed at part load. A deep bowl was used in the piston to avoid fuel spray contacting the liner. A second goal of the fuel injection system was to reduce fuel volatility requirements. Compression ratios from 6:1 to 10:1 were discussed. For aviation applications, towards the end of the decade, the availability of fuels with octane values in excess of 100 permitted increases in compression ratio and supercharging as described by Du Bois et al. [58]. A paper by Tsien [65] at MIT discussed the limits of high-output piston engines of the day for aircraft applications. Typical engines at the time had a Brake Mean Effective Pressure (BMEP) of around 14 bar and piston speeds of around 14 m/s. A research engine is cited as having reached 40 bar BMEP with peak cylinder pressures of 107 bar at 2.6 bar absolute inlet pressure. This engine made use of water injection. High-performance aviation piston engine technology had developed during the Schneider Trophy era of 1913-1931. Engines were now being further developed for war. Extensive details of these engines have recently been revealed by Douglas [66]. These engines will be commented upon further in the next section.

The 1940s: High-Performance Aircraft Piston Engines, New Refinery Techniques, On-Board Knock Measurement, and High-Speed Photography

Considerable fuel and engine development took place in the late 1930s and early 1940s in a bid to extract more performance from military airplane engines for use in WWII. A number of new refinery techniques had become available, including catalytic cracking and alkylation as described by Risk [67] of Ethyl Corporation. This enabled more knock-resistant fuel components to be introduced and iso-octane to be manufactured at scale more cheaply. Catalytic reforming was also used, which improves octane numbers by producing aromatics from naphthenes (cycloalkanes) [13]. More complex branched molecules were studied, sacrificing volatility for aircraft applications in the quest for increased knock resistance, as noted by Barnard [68] of the Standard Oil Company of Indiana. The octane rating of aviation gasoline had increased to 100 by 1940, according to Hives et al. of Rolls-Royce [69]. By the beginning of the same decade, the MON values of premium motor gasoline were 80, up from around 70 in 1930, as pointed out by Hubner of Ethyl Corporation [70].

The ASTM MON was the most commonly used standard for automotive octane rating at the time, according to Risk [67]. However, confidence in how well it represented knocking tendencies on-road began to decrease in this period, including by the CFR group [71]. They began studying the effects of engine speed and ignition testing on typical cars of the day. It was found that some fuels performed better at low speed and others at high speed, but the so-called "Uniontown" road-rating method only gave a single value per acceleration run. The "Borderline" knock test method was therefore adopted by the CFR group in 1940. With this approach, a borderline ignition timing curve against engine speed is determined for the given fuel from multiple acceleration tests where the ignition angle is progressively adjusted. The Knock-Limited Spark Advance (KLSA) was generally nonlinear with engine speed while the distributor spark advance characteristic for vehicles at the time could not match this. This is shown in Figure 11. Significantly, L-head engines (an older design) were found to knock more at high speed and less at low speed in comparison to more modern "valve-in-head" (OHV) types [67].

Rothrock [72] at NACA proposed a more complex approach to fuel rating where curves of limiting end-gas density against temperature were plotted through varying boost, compression ratio, and inlet temperature. A number of suggestions were made for how to measure knock at octane

FIGURE 11 "Borderline" ignition timing showing knock region in comparison to distributor advance curve, from Risk [67].

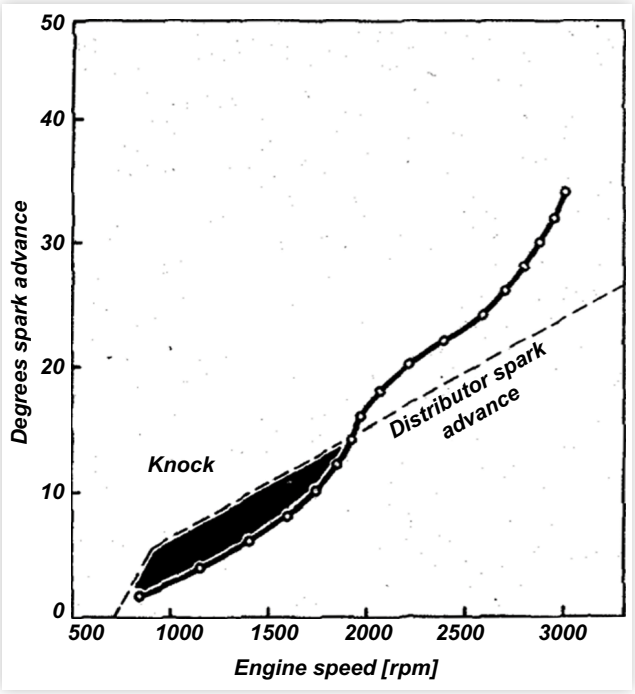

Reprinted with permission from Ref. [67]. © SAE International

FIGURE 12 Original Miller cycle concept explanation, based on [79]. Impact on charge pressure and temperature is shown as the charge makes its way through the engine. The new cycle (now known as 'Miller') featuring intercooling and in-cylinder expansion was compared to a standard Otto cycle with a blower. The Miller cycle reduces charge temperatures.

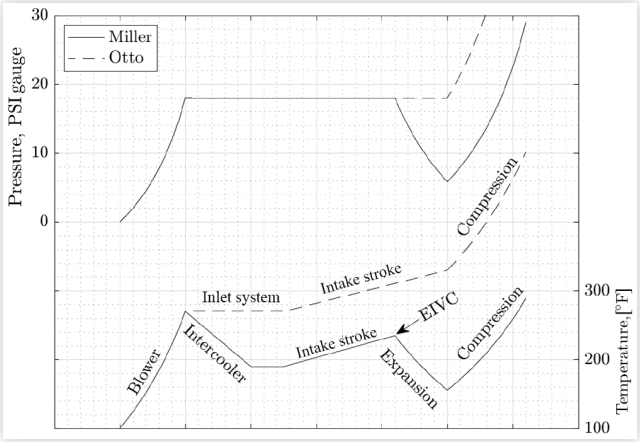

Based on Ref. [79]. © ASME

values greater than 100, as told by Brooks [73] of the CFR group, although there was no clear agreement. The use of TEL additive was proposed as was the use of triptane as a new reference knock-resistant base HC. The lack of a reference for octane values greater than 100 was increasingly problematic with the advent of synthetic fuels and increased sensitivity, commented upon respectively by Heron [74] and Gay [75], both of Ethyl Corporation.

Piston engine technology was being pushed forward by the military for aviation applications. This included the use of two-stage boosting with air-to-water charge cooling, four-valve cylinder heads, and sodium-cooled valves at Rolls-Royce, as described by Hives et al. [69]. Droegemueller et al. [76] of Pratt and Whitney commented on the knock benefits of charge cooling, water injection, and low exhaust backpressure—an advantage of mechanical supercharging over turbocharging leading to lower in-cylinder residuals. Rowe [77] of Wright Aeronautical Corporation presented results of water injection on a Wright Cyclone 9 and a CFR engine after the war in 1946. Pure water gave the strongest engine cooling while water/methanol mixture gave the highest knock-limited power output. Water/ethanol was less effective. Obert [78] of Northwestern University published on water injection in 1948. The fact that water slows combustion was noted. In testing on a CFR engine at 900 rpm and intake temperature of 143°C, it was estimated that less than 50% of injected water had evaporated by the end of compression. A 50% water in the fuel reduced the volumetric efficiency of the engine by 2%. Much activity of course did not make it into the academic literature during the war. Some of this has been recently revealed by Douglas [66]. German engines such as the Daimler-Benz 601 featured GDI at 90 bar pressure. BMW introduced a mechanical engine management system on the 800 engine, whose successor, the 801, powered the FW 190 fighter in 1941. The Jumo 211 featured water-cooled exhaust valve guides and variable inlet guide vanes (referred to as a "swirl throttle") on the compressor. Developments of much of this technology are still in use today, including in Formula 1.

One of the most significant contributions made to modern SI engine knock mitigation came, perhaps surprisingly, from the diesel engine locomotive industry in this period. In 1947, R.H. Miller [79] proposed a new cycle, which nowadays bears his name. Miller was Chief Engineer at Nordberg Manufacturing Company, and the suggested application of the cycle was for diesel engines. The concept is illustrated in Figure 12 and features a boosting system, an intercooler to bring temperatures down to an intermediate level, and then Early Intake Valve Closing (EIVC) and subsequent expansion in the remainder of the intake stroke to further cool the trapped charge. The objective was to lower the mean cycle temperature to allow a higher load for locomotive diesel engines. It was also mentioned that it could be used to increase the geometric compression ratio of an SI engine, and indeed this is frequently applied today.

The period was also notable for significant advances in knock instrumentation, again driven by military aircraft requirements. One instrument was the MIT Sperry Indicator, which came from activities carried out by Draper [80, 81]. This measured vibrations originating from knock in the range 5000-10,000 Hz. These were amplified by a device with automatic gain control and caused a light to flash in the cockpit of the aircraft when knock was detected. A closed-loop system was also introduced, which controlled the AFR to maintain the

engine at borderline knock both in takeoff (rich) and cruise (lean) conditions. This was but one of a number of devices available, based on the review by Bogen [82] of Universal Oil Products. They generally operated on similar principles and with various methods of handling other high-frequency noise sources apart from knock. It is perhaps no surprise that these devices were applied to automotive activity shortly after the war, as described by Goffe and Wheeler [83] of Sperry Gyroscope. At this stage, integration devices had also been introduced to allow a stable knock measurement over a number of cycles.

Fundamental engine combustion research was still taking place, as summarized by Fiock [84] of the Bureau of Standards, with significant activity undertaken by NACA and GM at the time. NACA notably carried out high-speed photography of combustion and knock. The first study, published in 1941 by A.M Rothrock, R.C. Spencer and C.D. Miller, was with a frame rate of 40,000 photographs per second [85]. As in their previous work, schlieren techniques were applied. Thermal gradients in the end gas shortly before knock onset were seen, suggesting exothermic reactions were already taking place. The knock event itself was found to take place over just 0.0005 seconds. This corresponded to two frames of their camera. A follow-up on the study was published in 1943 by the same group, this time authored by Miller and Olsen [86]. The simple autoignition theory of knock described by Ricardo was called into question and an experimental campaign performed to test if autoignition always preceded pressure oscillations, as measured by a piezoelectric transducer. On knocking cycles, a blurring of a region of the schlieren image was observed in the end gas, which corresponded to the start of knock as judged by the pressure transducer. It was determined to be a reaction covering just 25 μs—much faster than the slow autoignition events recorded by Withrow and Rassweiler a decade earlier. Mottling of the schlieren images was observed in the end gas before the blur appeared. This was considered by the researchers to be a form of combustion, but not that of a thin flame. They were possibly observing evidence of preflame reactions, but these would not be studied in detail until the following decade. A new experimental apparatus was developed by NACA in order to cover the timescales of the initial knock event. This device could take photographs at 200,000 frames per second. A report was published in 1946 by Miller et al. with 20 ultrahigh-speed photographs of a single knock event [87]. It was seen that the initial knocking reaction traveled through the charge at around twice the speed of sound. A follow-up work was published by the same group in 1948 [88]. This time a much greater body of data allowed firmer conclusions to be drawn. A new experimental approach allowed much clearer visualization of the end gas. Three different fuels were tested with different knocking tendencies. Both homogeneous autoignition and so-called "pin-point" autoignition were observed. The pin-point type was hypothesized to perhaps originate from particles but was seen, in any case, to respond to the fuel knock resistance. The pin-point type autoignition did not always result in significant pressure rise rates or knock. The homogeneous type, on the other hand, generally resulted in high pressure-rise rates and knocking combustion. A reaction front that moved at around twice the expected acoustic velocity was observed and was surmised to be a type of detonation wave, although it was thought that this was of an unstable type and did not last for very long. This is now described as Developing Detonation. Knock was revealing itself to be a more complex phenomenon than had been supposed just some years earlier.

At around the same time, a very large-scale fuel study was taking place, organized by the American Petroleum Institute. This was known as the American Petroleum Institute Research Project 45. A total of 225 pure HCs were tested in 29 different operating conditions in an engine. Some highlights were presented by Lovell [89] of GM. This generated a wealth of data for the future on the relationship between fuel molecular structure and knock tendency. An example is shown in Figure 13.

Although general tendencies for different types of HC were found, the knocking tendencies were seen to overlap between classes, as had also been noted by Ricardo in more limited studies in the 1920s [6]. It was shown that it was necessary to evaluate pure components over a range of conditions, or at least RON and MON, instead of just a single test point. An important HC that was used during WWII was triptane (trimethyl butane). Kettering [90] of GM told the story of this highly knock-resistant fuel, which was first tested in an engine at GM in 1926. It allowed a 50% power output over iso-octane in supercharged engines. A special plant was constructed to produce triptane in quantity for the war effort in 1943. This

FIGURE 13 Relationship between critical compression ratio and molecular structure for paraffinic hydrocarbons, from Lovell [89].

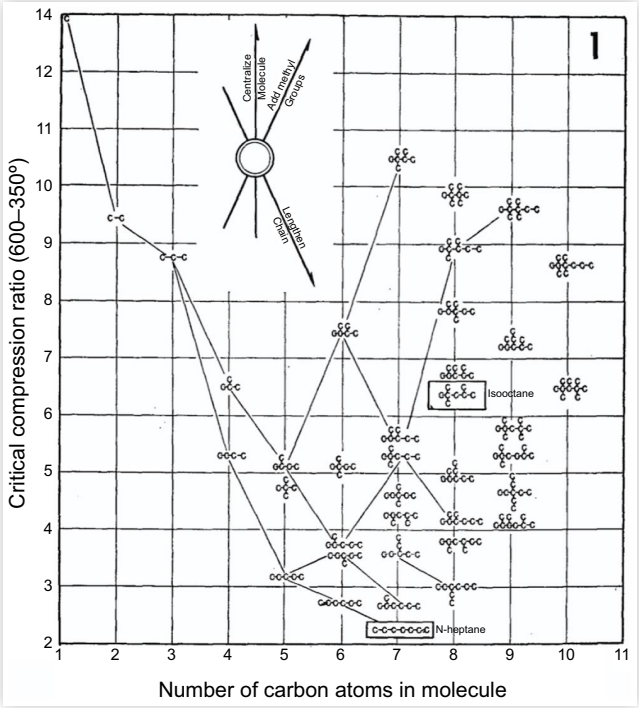

HC would still find many applications today, in particular for modern Formula 1 boosted engines. However, it is no longer commercially available in large quantities.

The 1950s: The Beginnings of a Chemical Kinetics Approach and New Combustion Problems

In the early part of the 1950s, a new approach to knock investigations emerged. This was to use a motored engine with conditions tailored to approach that of fired engine end gas. Retailliau et al. [91] at Esso Laboratories ran a CFR engine in motored conditions with PRF 75 as the fuel. The exhaust gas was collected and condensed, and distillation was performed to identify which HCs were present. Half of the original fuel had undergone reactions. Subsequent testing was performed on this blend and also pure iso-octane and pure benzene. A temperature plug in the engine indicated heat release during motoring above a certain compression ratio for the paraffinic fuels, but not for benzene. Fired engine testing indicated a correlation between these so-called "pre-reactions" and knock onset. TEL appeared to reduce the extent of pre-reactions in paraffinic fuel. Pastell [92] at Du Pont reported on similar activity on a CFR engine at their laboratory.[7]

Here the pre-reaction work was identified on pressure/volume diagrams. This was then characterized against mixture temperature, compression ratio, and manifold pressure. An example is shown in Figure 14. Here a region is clearly visible where the increasing temperature does not increase pre-reaction heat release. This is non-Arrhenius behavior. The reactions occurring were noted to be of the cool-flame type and could also be observed using a photomultiplier tube sensitive in the range 200-700 nm. Photomultiplier tubes were also used to characterize such reactions in a fired engine by Cornelius and Caplan [93] of GM. A narrower band device with peak sensitivity around 400 nm was used as cool flames were expected to be in the range 340-450 nm. Pre-reaction heat release was again characterized using cylinder pressure measurements. Peak reaction rates were found to be BTDC on PRF 80 suggesting the existence of a Negative Temperature Coefficient (NTC) region. This NTC region was said to be that of cool-flame reactions, and indeed a pale blue luminescence could be seen for fuels exhibiting this behavior. A number of HCs were tested with cool-flame behavior correlating with the presence of normal paraffins as expected. However, the companion

[7]In the discussion of this article, Learny and Livengood of MIT mentioned that the CFR engine could operate in a stable manner on a low-octane fuel without a spark and remarked that this cycle could be interesting for the future. They were describing what would later be known as Homogeneous-Charge Compression Ignition (HCCI).

FIGURE 14 Relationship between pre-reaction heat release and inlet mixture temperature, from Pastell [92].

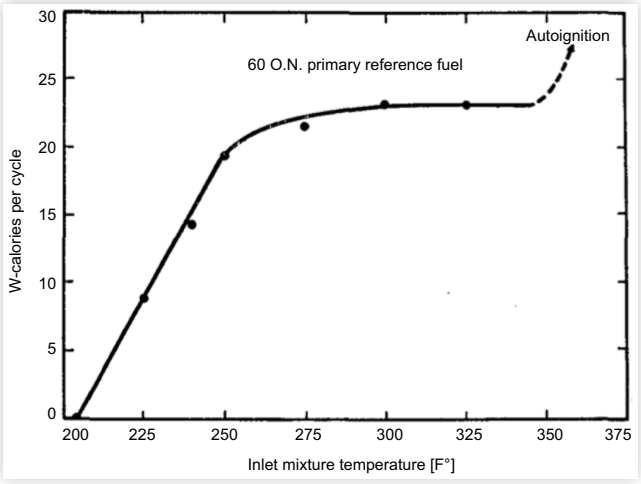

HC in a two-component mixture with normal paraffins also had an impact. It was noted that cyclopentane/n-heptane reduced pre-reaction heat release for a given octane number relative to iso-octane/n-heptane blends. Many years later cyclopentane would be discovered to be very effective in improving knock behavior when blended with iso-octane and aromatics [94]. The National Bureau of Standards investigated the nature of the cool-flame radiation using a spectroscope together with a photomultiplier tube in 1952, as described by Levedahl and Broida [95]. A CFR engine was run over a range of compression ratios to achieve either only pre-reactions or full autoignition with n-heptane fuel. Full autoignition was characterized by two peaks against time of emission intensity. The first peak, of lower intensity, was the cool-flame reaction. The second peak was the hot flame. Between the two peaks, emission intensity reduced. The spectrum of the cool-flame reactions was stated to be that of HCHO fluorescence. An interesting research activity also took place at Ethyl Corporation where a fueled motored CFR engine was used to generate partially reacted products, which were then sent to the intake of a fired engine. This was described by Mason and Hesselberg [96] in 1954. It was found that the knock limit of the fired engine depended on the compression ratio of the motored engine, and hence the extent of the preflame reactions. The highest compression ratios in the motored engine actually gave an improved knock rating in the fired engine, despite higher motored exhaust temperatures. A significant work by Sturgis [97], again of Du Pont, showed that radicals of hydrogen had perhaps the key role in the knock reaction chain: when running an engine on carbon monoxide (CO), the knocking tendency greatly reduced as humidity was lowered, and hence the engine was starved of hydrogen-containing molecules. In general, there was intense activity to understand the reaction chain resulting in knock and also the mechanism of antiknock substances. This field is known as chemical kinetics and is still a very

important part of knocking research today. The underlying theory is based on the concept of chain reactions. This was developed by Semenov [98] of the Institute of Chemical Physics of the USSR Academy of Sciences and Hinshelwood of Oxford University in the 1930s. They would share the Nobel prize in Chemistry in 1956 for their contribution to understanding chemical reactions.

The motored engine approach was an alternative to the Rapid Compression Machine technique, which was being used at MIT. The MIT apparatus was described in detail by Taylor et al. in 1950 [99]. The machine featured optical access to the combustion chamber. Various sensitivities were presented for a range of fuels including n-heptane, iso-octane, and benzene. It was not clear at the time how to compare data from such a machine with those of a running engine. A significant step forward was made in 1955 by Livengood and Wu [100] with their seminal paper "Correlation of Autoignition Phenomena in Internal Combustion Engines and Rapid Compression Machines." Equation 3 was presented.

$$\frac{d(x)}{dt} = \phi_1(p,T,t),\phi_2 \quad (F, \text{ chemical composition, etc.}) \qquad \text{Eq. (3)}$$

where

(x) is the concentration of pertinent reaction products
t is time
p is absolute pressure
T is absolute temperature
ϕ_1, ϕ_2 are the empirical functions
F is the fuel-air ratio

Equation 3 implies a fixed relationship between the rate of reaction and instantaneous state. It was assumed that there was a critical concentration of reactants, x_c, which would result in a sudden transition to a very rapid completion of combustion. The time required to reach x_c is known as the ignition delay, τ. Applying the concept of a critical concentration correlated with the ignition delay time, as shown in Equations 4 and 5,

$$\frac{d}{dt}\left[\frac{(x)}{(x_c)}\right] = \phi\left(\frac{t}{\tau}\right) \qquad \text{Eq. (4)}$$

$$\therefore \frac{(x)}{(x_c)} = \int_{t=0}^{t=t_c} \phi(t/\tau)\,dt = 1 \qquad \text{Eq. (5)}$$

Assuming the reaction rate does not change with time for a fixed state, we arrive at the final famous Livengood-Wu integral as shown in Equation 6:

$$\frac{(x)}{(x_c)} = \int_{t=0}^{t=t_c} \frac{1}{\tau}\,dt = 1 \qquad \text{Eq. (6)}$$

In order to apply Equation 6 to experimental data from an engine, the state/time history of the process must be known. The equation was shown to give good agreement between motored engine, fired engine, and RCM results. Some doubts were already raised in the paper that perhaps two separate integrations might be necessary to cover two-stage reactions. It was also noted that photographic evidence on the RCM devices available at the time showed evidence of inhomogeneity of the reactions and even flame-front propagation. Doubts were also raised by the authors concerning what would happen with mixtures of different HCs. Despite this, the Livengood-Wu approach is still used, with some refinements, to the present day. The work at MIT was sponsored by the Ethyl Corporation. A summary of some of the learning gained in this machine and its applicability to ICEs was given by Rifkin and Walcutt [101] of Ethyl Corporation in 1957. Notably, the dependence of the autoignition reaction rate on thermal gradients in the combustion chamber was commented upon, with small gradients hypothesized to result in autoignition of a large volume of unburnt charge in a small time—a volumetric ignition. It was thought that this could explain the appearance of supersonic reaction fronts in the optical measurements of Miller et al. from the previous decade. Miller himself attributed the supersonic reaction front to detonation waves. It is now known that both regimes are possible in a knocking engine and that this depends, among other things, on the thermal gradients around an exothermic center.

While numerous researchers were studying the impact of time on compressed reactants, the importance of flame propagation on knock was also being investigated, by Diggs [102] at Du Pont. He modified a CFR head to include 17 spark plugs that could be fired in any combination. The combustion duration was reduced to 60% of the standard value, which gives an improvement in the octane requirement of nine points at 900 rpm. The modified cylinder head is shown in Figure 15.

A new practical combustion problem also reared its head: "rumble." This was described in a paper by Meagher et al. [103] of Du Pont in 1955. This seemed to be brought about by the fact that compression ratios had increased by almost three points and octane numbers by nine units since the postwar

FIGURE 15 Modified cylinder head with 17 spark plug locations, from Diggs [102].

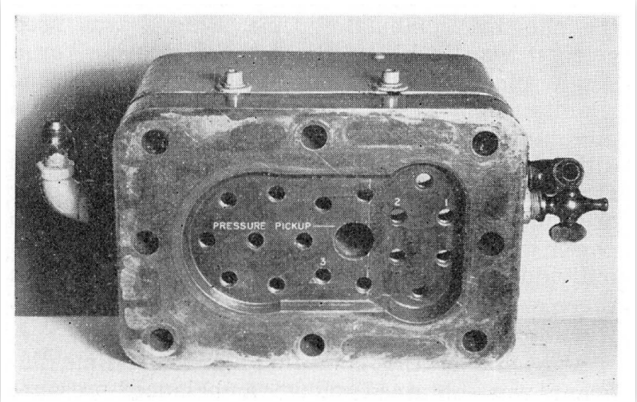

period, according to Perry et al. [104] of the Socony Mobil Oil. Indeed compression ratios were around 10:1 at this time, and fuels with a RON value of 102-108 were being used in research settings by Hostetler et al. [105] at Standard Oil Company of Ohio and Wiese [106] at GM. Rumble caused a low-frequency noise, distinct from knocking. It was believed to come from multiple ignition points resulting from hot combustion chamber deposits. It was found to correlate with surface ignition, and ion-current measurements were commonly used to diagnose it. A new crank-angle time recorder was also produced by Warren and Hinkamp [107] of Ethyl Corporation, which could keep track of cyclic variation in such events. Rumble was found to be worse with high aromatic content [105] and could be reduced by the use of additives and fuels with better tail-end volatility [106].

Some interesting historical papers were also published in this period. One was by Ricardo [108] and covered his early period including when he was an undergraduate under Hopkinson at Cambridge University in 1905. Hopkinson was possibly the first to suggest that knock was an explosion in the end gas. Ricardo proposed the concept of "highest useful compression ratio," and his early research work significantly informed the future CFR method of fuel testing. Pope [109] of Waukesha Motor Company also published a historical paper some years later, where he explained the background to what would go on to become the CFR engine. This was originally intended for testing at just 600 rpm, but improvements led to the 1948 version, which could run up to 4500 rpm. The Midgley/Dickinson Bouncing Pin indicator was used until 1954 when it was replaced by a new device. This was again based on a mechanical pin, but which now made contact with a magneto-restrictive pickup. It was in any case tuned to agree with audible knock.

The 1960s: Octane Rating Discussions and Computer Analysis

In the 1960s, there were renewed investigations on the representativeness of the RON and MON tests. Buerstetta et al. [110] of Ethyl Corporation and Esso Research and Engineering Co. described testing with four cars and a matrix of 51 fuels to investigate the impact of a range of key parameters. Uniontown and Borderline road methods were compared to RON, MON, and fuel composition information. A number of formulae were suggested to weigh RON and MON values to match the in-vehicle response. A common approach is shown in Equation 7. The Coefficient of Determination (R^2), value using Equation 7, was just 0.61. Adding a term of aromatics content, improved the R^2 value to 0.84. Adding further terms for TEL and sulfur content improved the correlation to an R^2 value of 0.96.

$$\text{Road Octane Number} = a \cdot RON + b \cdot MON + c \qquad \text{Eq. (7)}$$

Bartholomew [111] in 1961 described how engines, fuels, and vehicles had changed since the creation of the RON and MON tests. Engine cooling systems had improved, volumetric efficiency had increased giving better performance at higher speeds, and in the USA, automatic transmissions with high stall speeds had increased the engine speed of most relevance to knock. Compression ratios had more than doubled. Fuels had higher aromatic content than in the past and were of higher sensitivity. He commented that it was remarkable that the then-30-year-old RON and MON tests were still in use. Road testing was performed with a GM V8 engine at compression ratios from 8.5:1 to 12:1 on a range of fuels. A new laboratory test procedure was then created on the CFR engine with a high-speed crankcase and Removable Dome Head combustion chamber thought to be more representative of production engines of the time. A low-speed test point was rather similar to the standard RON condition. A 2400 rpm test point was also performed, again with low intake temperature. This was shown to give good correlation to results in-vehicle at 3500 rpm. Knock was detected by ear. The paper was intended to stimulate discussion to update the RON and MON tests for modern vehicles.

Brewster [112] of Ethyl Corp. gave a broad overview of combustion and fuel problems experienced in this period—not only knock but also preignition, rumble, excessive pressure rise rates,[8] deposit issues, and more. Gerard [113] of the Socony Mobil Oil published on an alternative octane formula that took into account mixture segregation in the intake manifold. This was said to be critical at low speeds and was confirmed by a comparison of the carburetor to fuel injection systems. A Distribution Octane Number (DON) was referred to. This was a modified RON test where fuel segregation in the intake system was provoked.

The number of cars on the road was increasing, particularly outside of the USA. While US consumers sought high performance and chose cars with automatic transmissions, in most other markets fuel economy was more important, and cars were sold mostly with manual transmissions [114]. Manual transmissions meant higher torque could be requested from the engine at low speeds than their automatic counterparts, and hence knock was more problematic in this operating region. A similar statement was made two paragraphs before. Maximum compression ratios in most markets were around 11:1, and premium gasoline was generally sold with a RON value of approximately 98 in 1967. This was a significant increase in comparison to the start of the decade and was mostly due to the use of catalytic reforming as a refinery technique.

Fundamental research continued in the laboratory, giving greater insight into what the RON and MON tests were really measuring. Gluckstein et al. [115] at Ethyl Corp. performed measurements of end-gas temperature in a modified CFR engine using an approach pioneered by MIT, based on the speed of sound in the unburnt medium. It was shown that

[8] Around 5 bar/°CA (Crank Angle) was the limit given—similar guideline values are still used today.

FIGURE 16 End-gas temperature measurements in a significantly modified CFR engine with iso-octane fuel and RON- and MON-like test conditions, from Gluckstein et al. [115].

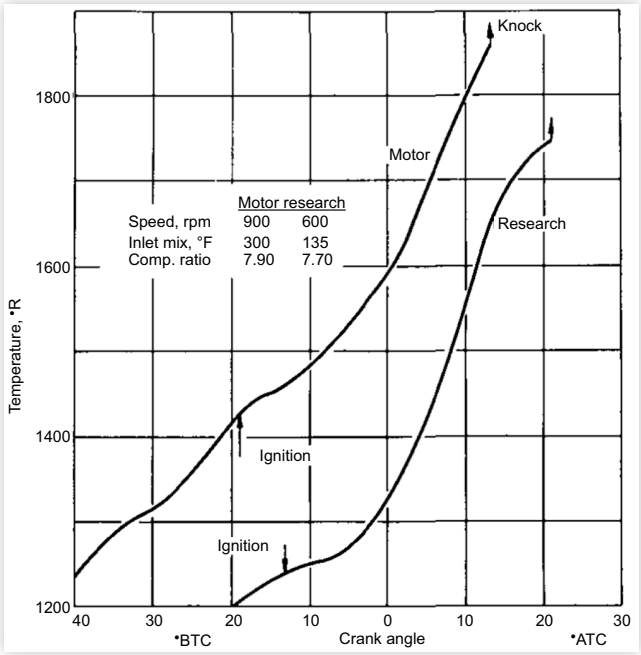

FIGURE 17 Erroneous knocking determination for benzene in comparison to its bracketing PRF, from Hoffman [117].

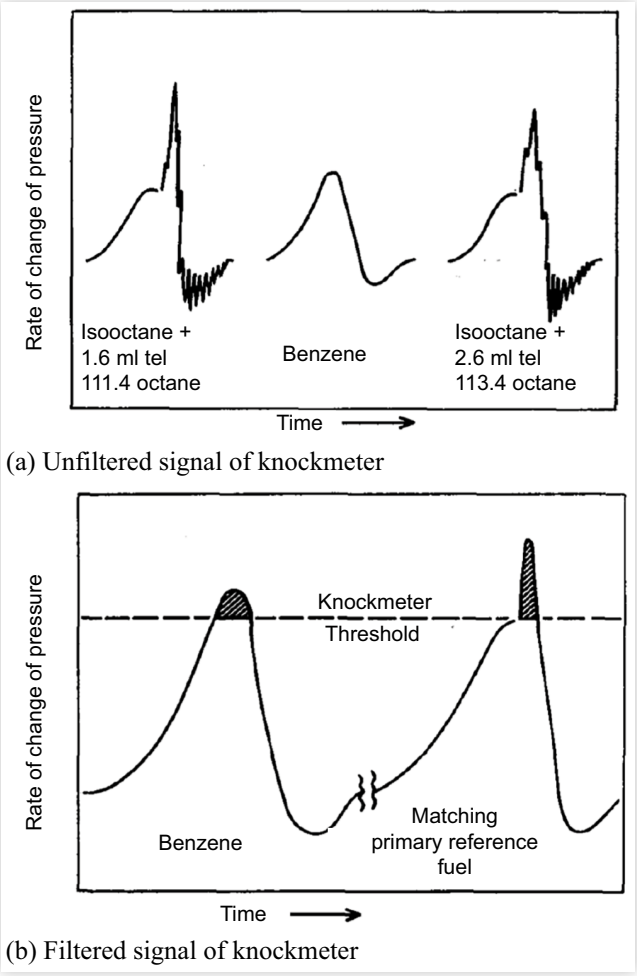

end-gas temperatures were significantly hotter for a MON-like test in comparison to RON-like conditions on iso-octane, while pressure conditions were relatively similar. Measured temperature histories for these two test conditions are shown in Figure 16. End-gas temperatures were evaluated using an alternative technique by Johnson [116] at the US Army Tank Automotive Center, in collaboration with Myers and Uyehara at the University of Wisconsin. Here an infrared pyrometer was employed. Measurements were complemented by calculations on an IBM computer running FORTRAN code. This was used to calculate the net rate of energy release from chemical reactions, based on Semenov's approach to reaction kinetics. The authors stated that as much as 10% of the energy of the fuel was released in pre-combustion reactions and, hence, neglecting these could lead to large errors.

The RON and MON tests used the Model 501 knockmeter at this stage, which had taken the place of the "bouncing pin." These meters apply a Low-Pass Filter (LPF) to the data from the pickup with a cutoff frequency of approximately 2500 Hz. This means they are not sensitive to the typical frequencies excited by knocking combustion in the CFR engine. The meter was shown by Hoffman [117] of Du Pont to respond to a maximum rate of pressure change, and this could lead to false knock detection for benzene, as illustrated in Figure 17. This issue had already been noted for the predecessor bouncing pin indicator in 1939 [62]. A Kistler piezoelectric sensor was mounted in the location of the knockmeter pickup, and characteristic resonant frequencies were measured for a range of fuels. It was confirmed that these were in the range 6000-7600 Hz. A knock index was defined where a High-Pass Filter (HPF) was used on the rate of change of pressure data. A threshold was defined based on background noise intensity and a counter system used to track threshold excursions over 1000 cycles. Knocking cycles were found to be random. Investigations were carried out on a range of fuels, using this system as the feedback instead of the knockmeter, for updated RON and MON ratings. The disadvantage of this approach was that it took longer than the standard method.

Taylor [118] at MIT studied the impact of engine size on knocking tendencies in 1962, citing previous activity in the German literature in 1939. He found that smaller cylinder sizes significantly improved the knock limit, both for matched piston speed and matched crankshaft angular velocity.

There was much debate at the time on the true nature of knock. Miller at NACA had claimed to have seen detonation waves during his activity in the previous decade, while other researchers thought that this was impossible. Curry [119] presented data in 1963 from an array of ion-current sensors in a split-head CFR engine. He said that this showed evidence of Flame-Front Acceleration (FFA) to 10-20 times the normal velocity. Strictly speaking, the experimental evidence

suggested much faster reaction rates in the end gas and an apparent reaction front in the same direction as the flame front. The approximately 10 mm spatial resolution and the fact that key zones of the OHV head could not be instrumented meant that strong assumptions were made to suggest a continuous combustion phenomenon and, hence, that the flame front had accelerated. An alternative explanation could have been autoignition occurring ahead of the flame front. The paper was also notable for a description of an Analog-to-Digital Converter (ADC) applied to the pressure signals to allow digital storage of experimental data on a magnetic tape unit. This could then be accessed by a computer and data plots from many cycles produced. Haskell [120], at Shell's Wood River Research Laboratory, measured knocking wavefront transit times, using two piezoelectric sensors and an oscilloscope triggered by an ion-current sensor. He observed only sonic velocities, and hence no detonation waves (which have supersonic propagation velocities) were detected. An optical window was also used with a photomultiplier to give a second measurement of the moment of autoignition at 8.5 mm distance from the ion probe. This showed a similar timing to the ion signal, and hence a volumetric explosion was implied, which suggests small temperature gradients in the end gas. The authors were confident that their work showed that autoignition was the "true" mechanism of knock, rather than FFA into developing detonation. Curry contested their claim. Haskell's colleague Graiff [121] published on the antiknock effect of TEL the following year. He used a fueled motored engine to study how TEL decomposed in an engine. Sweeping the compression ratio, various oxides of lead were obtained as confirmed by X-ray diffraction. There was a dependency of the oxide type on the fuel type used, and this was correlated with preflame reactions. For paraffinic fuels, pseudocubic oxide was formed, while, for benzene and toluene, only yellow orthorhombic oxide was observed. This could explain the different octane gains on different fuel types with the addition of TEL. TEL and the related compound Tetra Methyl Lead (TML) was once again coming under scrutiny as a potential health issue. Patterson [122] in the Journal *Archives of Environmental Health* in 1965 analyzed the amount of lead in human bodies in the USA in that period in comparison to natural levels. The level was estimated to be 100 times higher than that of preindustrial times. It was stated that lead alkyls (such as TEL) were the primary source of lead absorbed by the respiratory system in urban environments. Other sources with different pathways into the human body included lead piping, food can solder, and paints.

Air pollution was an increasingly public concern. Although the first version of the Clean Air Act had been passed in 1955 [123], this merely suggested that the Surgeon General should be involved in coordinating research. The 1963 Clean Air Act [124] gave the primary responsibility on reducing pollution to individual states but said that efforts should be made to reduce vehicle exhaust emissions. The 1965 Motor Vehicle Air Pollution Control Act [125] required the establishment of standards to reduce air pollution from motor vehicle emissions in order to protect the health and welfare of the public. NO_x, aldehydes, and evaporative HC emissions were the main concerns. Vehicles would be tested to demonstrate compliance. Funding was made available to realize these objectives.

Fundamental research on reactions was carried out by Burwell [126] of the United Aircraft Corporation using a steady flow reaction tube with iso-octane air mixtures. Ignition timing was mapped for a range of temperatures and pressures, although only up to twice atmospheric pressure. A measured 10% of the available oxygen was observed to have been consumed before autoignition and only 50% of the iso-octane remained at this point. A mass spectrometer was used to measure chemical species along the reaction tube. Propylene, ethylene, methane, hydrogen, CO, and CO_2 were observed. The first half of the preignition period was dominated by pyrolysis and then peroxidation reactions. Jost and Martinengo [127] of Göttingen University detailed studies on an RCM of n-octane-air and iso-octane-air mixtures. They discussed, in general, the history of the RCM method, which they traced back to Nernst in 1906, along with contributions by Ricardo's collaborators Tizard and Pye. The researchers at Göttingen used the rupture of a diaphragm at a predetermined stage of the reaction to rapidly expand and, hence, freeze the chemistry for further analysis using gas and paper chromatography. This allowed for the evaluation of species concentration against reaction time on a millisecond timescale, as shown in Figure 18. A two-stage reaction was seen for iso-octane, but not n-octane. Quader [128] at GM performed UV absorbance measurements in the end gas of a CFR engine in collaboration with Myers and Uyehara of the University of Wisconsin. Wavelengths from 250 nm to 500 nm were investigated with the highest absorbance seen at 260 nm. This was particularly the case for knocking cycles. It was not clear at

FIGURE 18 Species concentration against reaction time for n-octane-air and iso-octane-air mixtures, from Jost et al. [127].

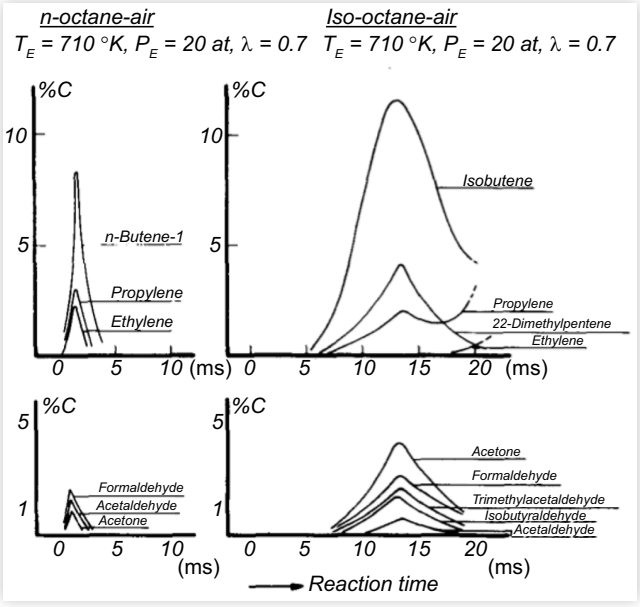

the time which species was absorbing at this wavelength. The absorption was strongly correlated with end-gas temperature and fuel type. No correlation was seen between the preflame reactions and flame-front velocity—contradicting the accelerating flame-front theory of knock, which as mentioned above still had some proponents at the time.

The 1970s: Oil Shortages, Emissions Control, and Unleaded Fuels

In 1970 the US Environmental Protection Agency (EPA) was founded. On the 31st of December of the same year, the Clean Air Act was significantly amended [129]. The EPA would set national standards of air quality, and its Administrator could bring civil action against those who did not comply. States would need to submit to the EPA plans of how they would achieve these standards. Vehicle emissions limits would be for Full Useful Life. Light-duty vehicle CO and HC emissions limits would be reduced by 90% from 1970 to 1975. This would result in the introduction of two-way oxidation catalysts. NO_x would need to be reduced by 90% of measured 1971 levels by 1976. Periodic inspection of motor vehicles for emissions compliance was implemented. The best emissions control technology that was technically and economically feasible should be applied. There was also a section on fuel additives that gave the Administrator of the EPA power to regulate such substances and to require manufacturers to conduct tests to demonstrate their safety in accordance with procedures of the EPA. However, a substance could only be regulated or banned after a cost-benefit analysis was performed, taking into account both scientific and economic data.

In the 1970s, the connection between leaded fuels, atmospheric lead, and health problems in the population was the object of detailed study. A series of reports from the newly formed EPA document this. In 1971 an EPA report by Engel et al. [130] of the Air Pollution Control Office stated that 97% of airborne lead was due to the combustion of leaded gasoline in vehicles. Atmospheric lead was correlated with traffic density and, hence, was a greater issue in urban areas. It was also noted that lead alkyl additives were incompatible with catalytic converter systems, which would shortly be introduced, and that this required the reintroduction of unleaded fuel from 1974 onwards. In 1972, the EPA published "Health Hazards of Lead" [131] and recommended that lead emissions from vehicles would need to reduce by at least 60% to achieve an air quality target of 2 μg/m^3. In 1972 the EPA also published their official position on the matter of health effects of airborne lead [132]. Lead from exhaust emissions could enter the human body both through the respiratory tract and through the ingestion of lead-contaminated dust. There was a correlation between neurological impairment in children and lead exposure. High lead concentrations were also found in the umbilical cord blood of pregnant women. It was stated that "Lead in the air as well as in street dirt and household dust are preventable exposures which can be readily decreased by regulating the use of lead as a gasoline additive." The previously proposed limit of 2 μg/m^3 was said to be too high, and in fact, a limit of 1.5 μg/m^3 was proposed in 1977 [133]. An EPA report in 1975 by Angle et al. [134] showed evidence of a link between blood lead levels in urban children and how close they lived to traffic. By 1979, numerous further studies had taken place suggesting a link between increased lead absorption and neurological problems in young children, as documented by Dage [135] of the EPA.

By the late 1970s, new regulations meant that unleaded gasoline accounted for a third of US sales, and this value was increasing, as shown in Figure 19, based on data from Dage. The proposed limit on average lead content for 1979 was 0.59 g/gal. As well as the introduction of unleaded gasoline, lead was also reduced in both regular and premium fuel types. The net result was a reduction in octane values of leaded gasoline, as documented by Shelton et al. [136] of the US Department Of Energy (DOE). The sales percentages from EPA data and the octane values compiled by the DOE, together with an assumed RON value of 91 for unleaded fuel in this period [137], have been combined in Figure 20. It can be seen that the average RON value reduced from 96.4 in 1970 to 93.1 in 1978. The average compression ratio of new cars sold in the USA was also documented by Shelton et al. This reduced from around 9.4 in 1970 to 8.2 already by 1974—manufacturers were designing their cars to tolerate the reduction in market octane values, and in particular, vehicles with catalytic converters would need to run on unleaded fuel with an EPA mandated minimum RON of 91 [137]. Lower compression ratios mean lower peak temperatures in the combustion chamber, and hence reduced NOx emisisons. Oxygenated components such as alcohols and ethers would eventually be used to improve the knock resistance of unleaded gasoline [13].

FIGURE 19 Leaded and unleaded gasoline US market share, average lead content, and proposed limit for 1979, data from Dage [135].

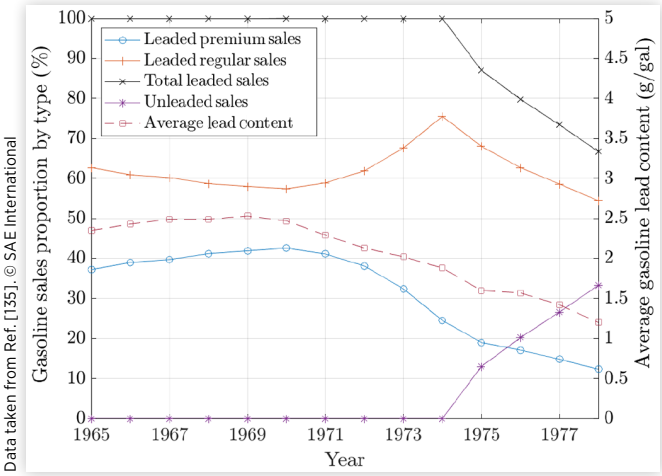

FIGURE 20 Octane number trends for US gasolines and compression ratio of US new car sales, based on data from Shelton et al. [136] and Dage [135].

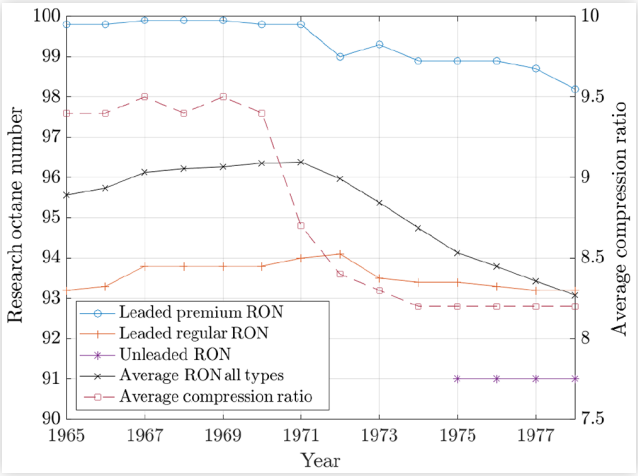

Data taken from Refs. [136] and [135]. © SAE International

Investigations were carried out to optimize engine-out emissions. Duke [138] of Pennsylvania State University showed that knock could reduce unburnt HC emissions due to reduced quenching on the cylinder walls. Advancing the engine into knock, however, increased NO_x emissions. Exhaust Gas Recirculation (EGR) was applied to reduce NO_x. An applied 10% EGR reduced NO_x emissions by 50% and 20% EGR by 75%. There was an upper limit though, dictated by combustion instability. With moderate levels of EGR (10-15%), the reduction in end-gas reactivity outweighed the slower flame-front propagation, and hence the compression ratio could be raised and Brake-Specific Fuel Consumption (BSFC) improved, as described by Hodges [139] of Rensselaer Polytechnic Institute. EGR in combination with lean AFRs was also being investigated by Morgan [140] of Mobil Research and Development Corp., but led to HC increases. Secondary air introduction into the exhaust system was found to be effective in reducing HC emissions, but only for stoichiometric or rich mixtures.

Oil shortages in the 1970s, due to the 1973 oil embargo of the USA and allies by the Organization of Arab Petroleum Exporting Countries, meant a new push to increase engine efficiency. Alternative fuels such as methanol were also investigated, by Gething [141] of Pennsylvania State University, to reduce the dependence on oil. The idea at the time, however, was to produce the methanol from coal rather than from biological sources. A number of manufacturers including Ford, GM, Honda, and Volkswagen were also working on lean-burn prechamber engines, as detailed in a large-scale review by Roessler and Muraszew [142] for the EPA in 1975. Such engines gave lower CO emission and a reduction in NO_x, along with potentially better fuel consumption, but similar HC emissions to a more conventional SI engine. Prechamber engines were not completely new: Honda's Compound Vortex Controlled Combustion prechamber engine had been in production in Japan since late 1973 and a Fairbanks opposed-piston heavy-duty stationary gas engine since 1952.[9] Detonation-like noise was observed for some prechamber concepts independently of fuel octane number. Some, but not all, concepts had a lower octane requirement—the Gussak active prechamber concept with a rich prechamber and lean main chamber permitted a compression ratio increase of 0.8 and could be run at an AFR of 30:1. The primary motivation at the time for most manufacturers, however, was to run lean for low pumping losses and with a view to meeting the 1977 Federal emissions standards without a three-way catalytic converter. It was thought that this would not be feasible if the NO_x limit was further reduced. There was a lot of variety with some systems featuring separate valves for the prechamber while others would be known today as passive systems, such as the Ford Torch Ignition engine. The majority of the described engines did not make it to market, largely as lean running was incompatible with three-way exhaust gas catalysts, which would become ubiquitous.

Research activity was also ongoing on better understanding the influence of turbulence in more conventional SI engines, again with the objective of improving combustion efficiency and emissions. Turbulence had been identified as key in accelerating flame-front propagation in the early days of the Otto engine by Clerk [5] but the quantitative relationship between turbulence and flame speed in ICEs was still not well understood at this stage. Blizard and Keck [143] of MIT made an important contribution to modeling the turbulent flame speed in engines in 1974. This was based on a characteristic turbulent eddy burn-up time $\tau = l_e/u_l$, where l_e is the eddy radius and u_l is the laminar flame speed. The rate of combustion depends on the eddy entrainment speed u_e, which itself was assumed to correlate with the inlet gas speed, l_e. Inlet gas speed was assumed to be a function of intake valve lift and compression ratio. The model was calibrated and compared against experimental data on a single-cylinder engine with good results. Lancaster [144] of GM measured turbulence in a motored CFR engine with both shrouded and non-shrouded intake valves in 1976. Measurements of turbulence intensity u' were made using a DISA 55F81 triaxial hot-wire anemometer with 10 μm elements. Data were analyzed from the engine shortly before end of compression at TDC. Turbulence intensity was defined as the Root Mean Square (RMS) of velocity fluctuation about a mean value. In a companion paper by Lancaster et al. [145], fired measurements were described. Gas was sampled through an electromagnetic valve prior to combustion, and pressure was measured with an AVL (Anstalt für Verbrennungskraftmaschinen List) piezoelectric transducer and a Kistler charge amplifier. Spherical flame-front propagation was assumed in the fired engine to calculate turbulent flame speed from heat release analysis. The turbulent flame speed was then compared to the expected laminar flame speed under these conditions giving a Flame-Speed Ratio (FSR). This was found to be linearly correlated with turbulence intensity from motored engine measurements over a range of

[9] Ricardo had already made a prechamber engine in 1918 [6].

FIGURE 21 Ratio of turbulent to laminar flame speed as determined by Lancaster et al. on a CFR engine and correlation with motored turbulence intensity u', from Lancaster et al. [145].

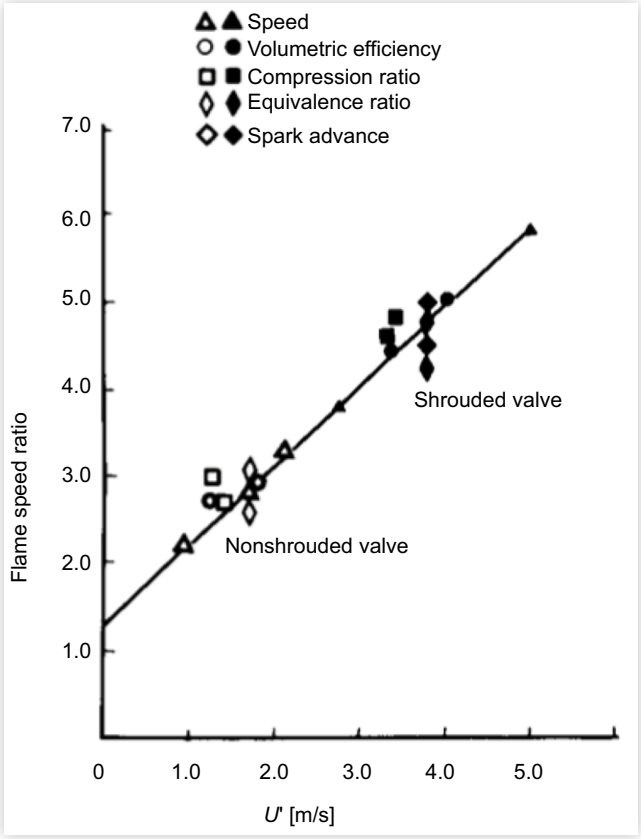

FIGURE 22 Extension of lean misfire limit with swirl and squish charge motions, from Nagayama et al. [146]. Std = Low Swirl and Squish, Sw = Increased Swirl, Sq = Increased Squish, Swq = Increased Swirl and Squish.

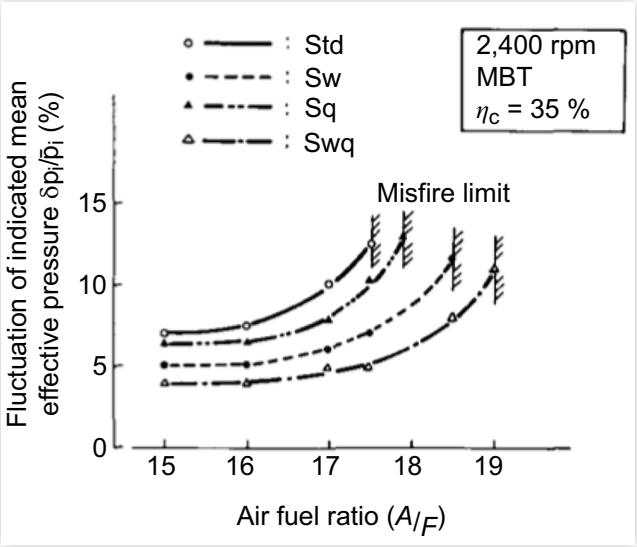

test conditions and both intake valve types, as shown in Figure 21. Nagayama et al. [146] published on the effect of swirl and squish the following year. Swirl generated by the cylinder head was measured with a paddle wheel in a flow rig and a motored engine using a spark discharge and ion-sensing technique. Squish was calculated based on bowl diameter and squish height. Swirl ratios were 0.7 and 1.4 for two different intake ports while maximum squish velocities at 2400 rpm were estimated as 4 m/s and 15 m/s for two different combustion chambers. Both swirl and squish improved the lean misfire limits, and the combined effect was better still, as shown in Figure 22. The motivation was to extend the dilution limit to improve fuel economy and engine-out emissions.

Electronic data acquisition systems were becoming more common, which permitted efficient evaluation of statistical phenomena. Allwood et al. [147] at Shell compared flame-front propagation, characterized by ion sensors, against cylinder pressure measurements on a statistical basis using a multi-channel electronic gating and counting system. Cyclic dispersion was compared for different fuels, residual gas content, and AFRs. It was seen that there was a tendency for knocking cycles at a given operating point to be those with faster burn rates. This implies that reducing cyclic variability would improve the knock limit—as KLSA is dictated by the faster burning cycles in the dataset rather than the mean cycle. Barton et al. [148] at Pennsylvania State University used an electronic system to target a given percentage of knocking cycles above a threshold. The feedback signal was based on a Band-Pass Filtered (BPF) rate of pressure rise measurement. The threshold was based on the RMS value of non-knocking cycles. Chiampo et al. [149] of FIAT also investigated the correlation between flame-front arrival time from ion sensors and knocking cylinder pressure measurements on a FIAT 125 engine and noted similar results to Allwood. An alternative "kinetic knock index" was proposed by Ferraro [150] of the Polytechnic University of Turin based on wave energy rather than the more typical amplitude or integral methods in use at the time, and indeed still today.

A greater number of papers in the SAE literature were being written in Europe. Here leaded fuel had not yet been removed from the market, although this was expected to take place in the future. Engines were therefore being prepared for RON 91 unleaded gasoline. It was noted by Arrigoni et al. [151] of Snamprogetti that the vast majority of literature to that date was on research engines, such as the CFR, rather than on production engines. Testing was therefore performed on the road to characterize knocking tendencies against engine speed, as had been done in the past. It was noted once again that high-speed knock was correlated with MON and low-speed knock with RON as had been observed in the prior decade. Engine damage was also studied in a disciplined manner with erosion seen on the head and piston. A later study by Cornetti et al. [152] at FIAT cited further failure modes such as ring sticking, head gasket failure, and piston holing. 100-hour knock damage accumulation tests were performed with temperature measurements in the combustion

chamber. Temperatures were seen to rise with engine speed, and so less knock intensity was required to cause the same damage at higher speeds. Ring sticking was the primary failure mode, driven by material transfer from the eroded piston.

Knock measurement was moving out of the laboratory and into production cars by the late 1970s.[10] Piezoelectric cylinder pressure sensors, typically manufactured by Kistler, connected to a charge amplifier had become the standard knock research tool. For on-road measurements or engine durability runs, accelerometers were popular according to Arrigoni et al. [153]. Microphones and load washers under the spark plug were also considered by Randall et al. [154] of Systems Control Inc., similar to an approach demonstrated by Kondo et al. [155] of Gakushuin University in 1975. A knock control system based on spark retard was described by Kraus et al. [156] of Exxon Research & Engineering Company in 1978, and in the same year, Buick introduced a closed-loop knock control system on its 1978 downsized turbocharged V6 engine, as detailed by Wallace [157]. A BPF accelerometer signal would retard the ignition angle in response to knock and then gradually return to the base settings. The base ignition management was through centrifugal and vacuum advance, and the electronics of the knock control system were analog rather than digital.

In terms of fundamental understanding, two papers stand out from the end of the decade. The first was by Douaud and Eyzat [158] at the L'Institut Français du Pétrole (IFP). They pointed out that RCM data allowed a good understanding of fuel knock tendencies, and the datasets thus generated could be applied to engines, but that it was rather difficult to implement such a methodology. They proposed a formula for the ignition delay with three unknowns. These unknowns could be obtained from engine testing at three conditions, although four were preferred to allow for error checking. They proposed a modified RON and MON test, together with the standard versions, to generate these data for each fuel. One of these constants was found to correlate with the octane number. This paper is famous and very frequently cited. The mathematical approach is as follows in Equations 8, 9, 10, and 11

$$\frac{d\alpha}{dt} = \alpha A' p^n e^{\frac{B}{T}} \qquad \text{Eq. (8)}$$

where

p is pressure
T is temperature
α is the concentration
A' is a constant
n is the pressure coefficient
B is the temperature coefficient

For constant pressure and temperature,

$$\tau = t_c - t_0 = A p^{-n} e^{\frac{B}{T}} \qquad \text{Eq. (9)}$$

[10]Although there had been some isolated examples in the late 1940s, it had not become a common technique.

where $\tau = t_c - t_0$ is usually referred to as the ignition delay. Assuming that the critical concentration α_c is independent of pressure and temperature,

$$1 = \int_{t_0}^{t_c} \frac{dt}{A p^{-n}(t) e^{\frac{B}{T(t)}}} \qquad \text{Eq. (10)}$$

There are, therefore, three unknowns A, n, and B to be determined experimentally from the engine data. For PRF with octane values "OCTN" between 80 and 100, with units of kilogram per square centimeter (kg/cm^2) for pressure and Kelvin for temperature, Douaud and Eyzat determined:

$$A = 0.01869\left(\frac{\text{OCTN}}{100}\right)^{3.4017} \qquad \text{Eq. (11)}$$

$$n = 1.7$$

$$B = 3800$$

Assuming a constant pressure of 22 kgf/cm^2 (21.6 bar), the predicted ignition delay response is as shown in Figure 23.

It should be underlined, however, that Equation 8 assumes a single-stage reaction. Such a simplification had also been employed by Livengood and Wu [100] in 1955. This is generally not the case for paraffinic HCs, which undergo a two-stage reaction. In 1975 Halstead, Kirsch, Prothero, and Quinn of Shell published "A mathematical model for hydrocarbon autoignition at high pressures" [159]. This was based on a degenerate branched-chain mechanism. The oxidation of a paraffinic fuel was described by eleven reactions as shown in Table 4. The rate coefficients for each reaction were assumed to follow Arrhenius-like behavior. The model initiates with

FIGURE 23 Ignition delay time τ as a function of PRF octane number and end-gas temperature with a pressure of 22 kgf/cm^2, as predicted by Douaud and Eyzat Approach [158]. It can be seen that higher octane numbers are correlated with longer ignition delay times.

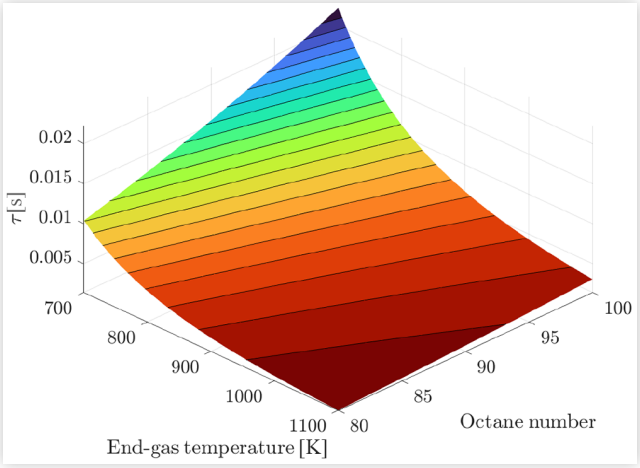

Data taken from Ref. [158]. © SAE International

TABLE 4 "Shell" reaction model of alkane oxidation by Halstead et al. [159].

Primary initiation	$RH + O_2 \rightarrow 2R\cdot$	1
Main propagation	$R\cdot + O_2 \rightarrow RO_2\cdot$	2
	$RO_2\cdot \rightarrow$ products + $OH\cdot$	3a
	$RO_2\cdot \rightarrow Q + OH\cdot$	3b
	$OH\cdot + RH \rightarrow R\cdot + H_2O$	4
Propagation forming degenerate branching agent	$RO_2\cdot + RH \rightarrow RO_2H + R\cdot$	5
	$RO_2\cdot Q \rightarrow RO_2H + R\cdot$	6
	$RO_2\cdot + RH \rightarrow H_2O_2$ + products + $R\cdot$	7
Branching	$RO_2H \rightarrow 2R\cdot$ + products	8
Decomposition	$H_2O_2 \rightarrow 2OH\cdot$	9
Termination	$R\cdot + R\cdot \rightarrow$ inert products	10
	$R\cdot + O_2 \rightarrow$ inert products	11

partial oxidation of the fuel "RH" resulting in chain propagating radicals "R" and combustion products. A number of further radical and reactive species are generated in the following steps, including an intermediate species "Q" produced by cool-flame chemistry, before the reaction terminates leaving only inert products. The model was compared with RCM data of iso-octane and was capable of reproducing similar two-stage ignition and NTC behavior. This model was applied by Kirsch and Quinn [160] at Shell in 1977. The chemical kinetics model was coupled to an engine simulation model of a CFR engine. PRF 90 and a Toluene Reference Fuel (TRF) also with RON of 90 were compared in the model at both RON and MON test conditions. The model prediction of knock and the relative behavior of the fuels between the test conditions were consistent with experimental data. The model suggested that temperature was the dominant cause of TRF fuels rating lower than PRF on the MON test if they have matched RON values. The approach of linking engine and chemical kinetics simulations has become standard practice today. The model became known as the "Shell model" and would be used frequently in the coming decades.

The 1980s: Electronic Ignition Control, Computerized Analysis, and Japanese Research

Closed-loop ignition control systems to protect production engines against knock had come to the market in the late 1970s [157] and would become ubiquitous during the 1980s. While the original Buick system was based on analog electronics and coupled to mechanical ignition timing adjustment, microprocessors would become standard during the 1980s, allowing greater precision and control. The most common reaction to detected knock was the reduction of ignition advance, as described by Boccadoro et al. [161] of Renault and Decker et al. [162] of Bosch.[11] Management of boost pressure was proposed as an alternative by Gillbrand [163] at Saab, and this system would also increase the boost pressure when a lower than expected knock was observed. This gave a performance increase, especially in transient maneuvers. An accelerometer was typically used as the feedback device, with the raw signal being BPF to highlight signal energy associated with the expected combustion chamber acoustic modes, as detailed by Nakamura et al. [164] of Toyota. Priede et al. [165] of the University of Cape Town explained how cylinder pressure oscillations transformed into structure-borne resonances in 1989 and studied experimentally the resonance modes of combustion chamber castings using a vibration generator and a local microphone. Alternatives to accelerometers were again considered: ion-current sensing using the spark plug electrodes was proposed by Collings et al. [166] at Cambridge University, and Sawamoto et al. [167] of Nissan again suggested the use of a piezoelectric ring fitted under the spark plug. Amann of GM published two detailed reviews of combustion analysis techniques in 1985 which are still frequently cited. The first of these [168] was a historical review of combustion analysis methods covering 100 years of progress. The second [169] covered the history of cylinder pressure measurement and gave guidelines on the information, which can be obtained from such an analysis, including knock. As knock had effectively become a closed loop in production vehicles, their octane appetite could be compared by evaluating acceleration times on a range of different fuels. McNally et al. [170] observed in a 1989 Coordinating Research Council (CRC) report that over a range of 15 cars, the Normally Aspirated (NA) models did not improve with a RON value higher than 87, while turbocharged models benefited from RON values as high as 100. Sutton et al. [171] stated that from 1945 to 1980 compression ratios had increased significantly. Fuels had also changed radically with higher RON and sensitivity (S) due to the implementation of catalytic cracking as a refinery technique. Despite this, typical vehicles at higher engine speeds still seemed to respond to MON values. It was expected that future engines would run lean, and it was shown that this engine type would have a knocking tendency more aligned with RON test conditions.

Computerized analysis in research labs meant it was much more convenient to perform statistical analysis on combustion data than in the past, and hence a number of statistical investigations were reported. By [172], the Northern Research and Engineering Co., together with Kempinski and Rife at MIT, published a large study on the CFR engine in 1981. The impact of fuels, compression ratio, equivalence ratio, ignition timing, EGR, inlet pressure, and inlet temperature were all studied experimentally, and results were compared to literature models. Leppard [173] at GM noted that the distribution of knock intensity characterized by the Maximum Amplitude of Pressure Oscillation (MAPO) was not normal, and skewness and kurtosis were described. In this same study,

[11] As has already been mentioned, WWII aircraft also had closed-loop control for knock, but the control parameter was AFR.

it was demonstrated that individual cylinders could have different octane requirements by up to four octane units. Chun and Heywood [174] at MIT also noted the statistical non-normality of knocking intensity with more cycles being observed at lower values. It was Iwata et al. [175] at Nippondenso in Japan who described the distribution as log-normal. This is still commonly stated today, although Iwata et al. actually wrote that both knocking and non-knocking cycles follow separate log-normal distributions of knock intensity. At borderline conditions, there exists a mixture of both, and hence two superimposed log-normal distributions are required to adequately describe the data. This was made clear using a diagram on log-normal probability paper as shown in Figure 24. In such a diagram, one axis is the logarithmic intensity and the other describes the Gaussian cumulative population. Such an analysis approach would appear to allow the number of knocking cycles in a dataset to be estimated without the need to manually select a threshold—a very useful feature.

The use of computerized analysis also meant it was possible to consider a wide range of different algorithms to describe knocking intensity on individual cycles. The MAPO was common [173, 176, 177, 178, 174] and indeed still is today. Integrating the pressure oscillations was an alternative [169]

FIGURE 24 Log-normal analysis by Iwata et al. showing separate distributions for knocking and non-knocking cycles in the same dataset [175].

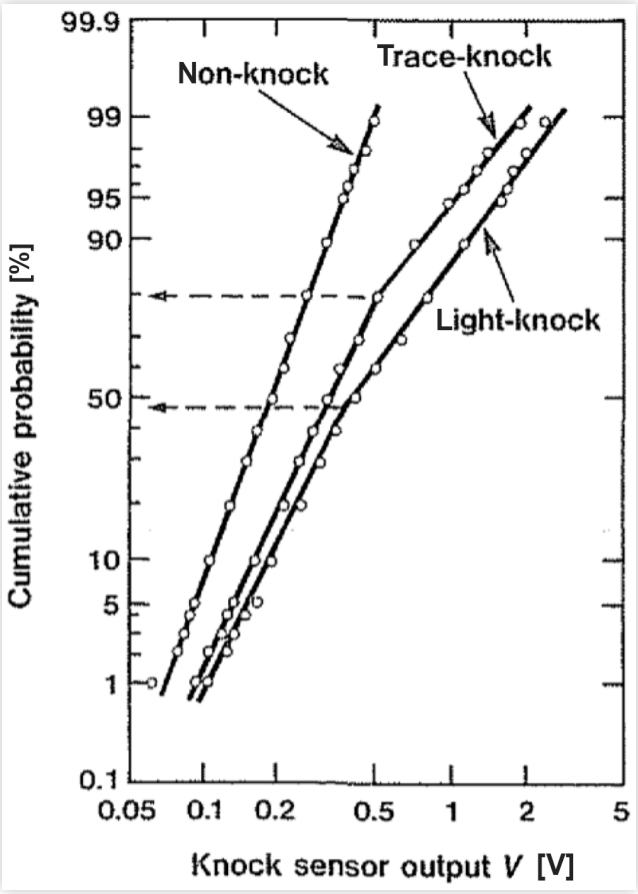

Reprinted with permission from Ref. [175]. © SAE International

FIGURE 25 Third derivative of cylinder pressure used by Checkel and Dale as a knock index [180].

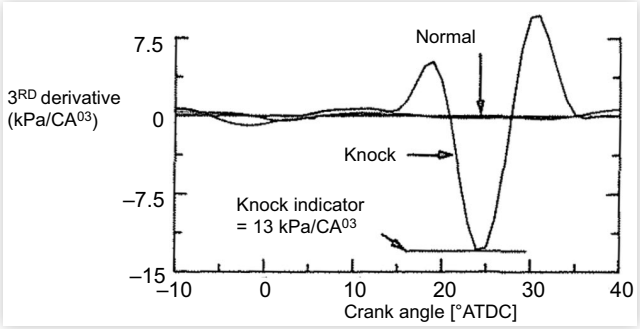

Reprinted with permission from Ref. [180]. © SAE International

as was the related technique of signal energy quantification used by Spicher and Kollmeier [179]. These methods relied on high-frequency acquisition and were also somewhat vulnerable to non-knock-related high-frequency noise sources. An alternative technique was proposed by Checkel and Dale [180] at the University of Alberta, based on the third derivative of the pressure trace. This did not require high sample rate data, as it was based on the idea that, when knock occurs, there is normally an abrupt increase followed by an abrupt decrease on the pressure curve.[12] This occurs before pressure oscillations are observed in the chamber. An example is shown in Figure 25. An index based on the second derivative of cylinder pressure was suggested by Hiromitsu Ando et al. [181] at Mitsubishi.

It was also becoming more straightforward to calculate the rate of heat release from pressure data. Harrington [182] of AMOCO (AMerican Oil Company) in 1982 showed plots of log pV^{γ}, which have a similar appearance to cumulative MFB plots, in a paper on the effects of both liquid and vapor phase water introduced in the intake system of a CFR engine. Slower combustion and increased HC emissions were noted with water introduction. Klimstra [183] of N.V. Nederlandse Gasunie applied Wiebe fits into the MFB data from cycles slightly retarded from the knock limit. He then used this profile to estimate the quantity of mixture remaining at the moment of autoignition for knocking cycles. The calculated isochoric pressure rise due to this mixture's ignition was used as a knock index. This assumes that knock intensity depends only on the unburnt gas quantity at the moment of autoignition, which would only be the case for an homogeneous end-gas thermal explosion.

The effects of knock on heat flux and engine damage were also investigated. Lee and Schaefer [176] at Volkswagen reported on a study where fast-response thermocouples on the cylinder head flame face showed that knocking cycles could have three times the heat losses of non-knocking cycles. Damage testing was performed that showed erosion on the

[12]This may be what causes the bouncing pin to lose contact with its diaphragm and, hence, bounce.

aluminum piston surface. Applying a 20 μm iron coating to the piston surface was enough to protect it.

While the prior decade had seen significant research on knock being reported in Europe, in the 1980s, there were a large number of high-quality studies originating in Japan. Some of these were on control topics with key contributions being the dual log-normal distribution already commented upon and a knock control ignition advancing (not only retarding) strategy, described by Ando et al. [181] of Mitsubishi. Here it was noted that up to 12° of ignition advance could be applied when combustion chambers were cool. The fundamental mechanisms of knock were also studied in Japan at that time. Iwashita and Saito [184] of Toyota described a high-speed camera and digitization system that permitted statistical analysis of flame-front propagation. Hayashi et al. [185], also of Toyota, used a Rapid Compression and Expansion Machine (RCEM) with transparent access and high-speed laser shadowgraph photography at 100,000 frames per second to study end-gas autoignition. The RCEM also featured a spark plug. This allowed fully premixed measurements to be made with very little flow or turbulence. It was shown that very strong autoignition events resulted in supersonic wave propagation (1600 m/s with a reference acoustic velocity of 1100 m/s). Only the incident wave exhibited this supersonic velocity, with the first reflected wave already traveling at normal acoustic speeds. Nakagawa et al. [177] of Nissan applied a similar technique in a fired engine with part optical access to study autoignition locations at 30,000 frames per second. Cylinder pressure data were also acquired. Multiple autoignition locations were seen, often close to the cylinder wall. Autoignition events just ahead of the flame front were also observed. It was confirmed that autoignition could occur without producing knocking cylinder pressure oscillations. His collaborator and co-author Takagi [186] was the lead of a study published in 1988, again using the laser shadowgraph technique, this time focusing on knocking heat release quantities. With heavy knock, up to 40% of the charge was consumed by autoignition, which was 90% of the remaining charge in the cylinder at the time. A squish piston was found to reduce the knocking tendency for a given spark timing due to faster combustion and increased end-gas cooling. In this study, it was also observed that a reflected pressure wave caused further autoignition events. In 1985 Hiroshi Sakai et al. [187] of the University of Tokyo published on an experimental supercharged Miller engine where effective EIVC was achieved through the use of a rotary valve in the intake system, together with a conventional poppet valve in the cylinder head. This was almost 40 years after the concept had first been proposed [79]. It was found that by advancing the effective intake valve closing, the end of compression temperature could be reduced by over 100 K. The system was shown to effectively mitigate knock, and a 15% power increase was achieved in boosted conditions, together with improved BSFC and lower exhaust gas temperatures.

Fundamental research was also taking place in Germany. An impressive study was described by Schäpertöns and Lee [188] of Volkswagen, where the Shell model of autoignition was coupled to a two-dimensional Computational Fluid Dynamics (2D CFD) simulation of a combustion chamber (Figure 26). The model was capable of simulating both the autoignition location and the ensuing pressure waves. This allowed, among other things, to show the sensitivity of pressure transducer location in the chamber.

FIGURE 26 2D CFD calculations with integrated shell kinetics model by Schäpertöns and Lee of Volkswagen in 1985 [188]. The simulation shows a hot spot on the left wall at knock onset.

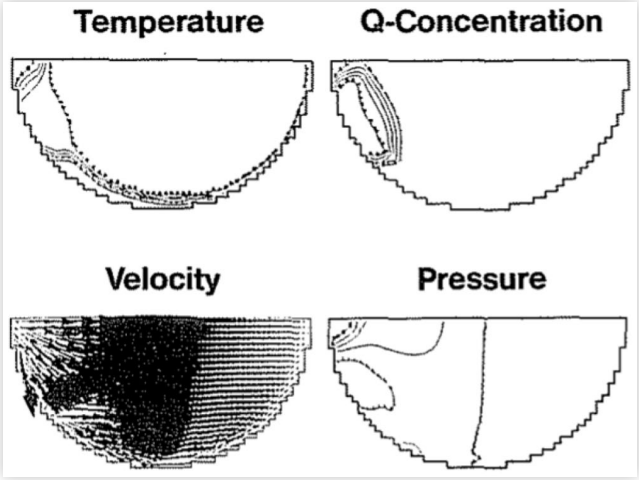

Spicher and Kollmeier [179] at Aachen Technical University in 1986, reported on a study where 51 optical fiber bundles were installed in a two-valve Rotax engine. Photomultiplier tubes were used to amplify the light in the range 250-650 nm. They observed supersonic wave velocities for strong autoignition events. Autoignition locations were distributed around the end gas with considerable variability. Interestingly, knock damage was observed in a different location to the preferred autoignition region. In the USA, the same Shell model implemented at Volkswagen in 2D CFD was used by Najt [178] of GM in a zero-dimensional (0D) model. Here the combustion chamber was described by three zones: burnt region, main unburnt region, and crevice. The model was compared to experimental data for both PRF 70 and PRF 90 fuels with good correlation observed. Lower octane PRF gave greater exothermic heat release from cool-flame chemistry.

When Kirsch et al. [160] first applied the Shell model to combustion engine modeling, they assumed homogeneous temperatures in the end gas. If the end-gas reactivity were truly homogeneous, autoignition would occur in the entire unburnt region simultaneously. In reality in practical systems, such as ICEs, reactivity gradients in the mixture exist. Zeldovich [189] of the Institute of Chemical Physics in Moscow explained in 1980 how such gradients can result in distinct reaction front "Spontaneous Propagation" velocities u_{sp} and pressures p.[13] This depends on the nature of the reactivity gradients in the unburnt mixture. The four different

[13]Zeldovich had been publishing on detonation since the 1940s, primarily in the Russian literature.

TABLE 5 Zeldovich spontaneous propagation reaction front classification [189].

Type	Reactivity gradient	Propagation velocity	Front pressure
1	Small	$u_{sp} > u_J$	$p_v < p < p_J$
2	Intermediate	$u_{sp} \leq u_J$	$p \approx p_J$
3	Large	$u_f < u_{sp} < < a < u_J$	$p \approx 0$
4	Very large	$u_{sp} = u_F$	$p \approx 0$

Data taken from Ref. [189]. © SAE International

possibilities are shown in Table 5. For Type 1, associated with small reactivity gradients (e.g., small temperature and species concentration gradients), the behavior is that of a thermal explosion. The reaction front velocity u_{sp} is above that of a classical detonation wave u_J, which means that the chemistry and the gas dynamics of the system cannot become coupled. Zeldovich referred to this as a weak detonation. The pressure rise is larger than that associated with constant volume combustion p_v, but no shock-wave behavior is present. Type 2 is potentially the most damaging. The reaction front velocity is less than or equal to the Jouguet velocity u_J. The chemical kinetics and gas dynamics are interacting, and the reaction is feeding energy into a shock wave. The pressure can approach that of a classical Chapman-Jouguet detonation. Type 3 could be described as benign autoignition. The reactivity gradient is large enough that when one element ignites, the surrounding medium has time to expand and hence equalize the pressure. This occurs for propagation velocities significantly less than the acoustic velocity but higher than that of the flame-front propagation. The pressure wave generated by the autoignition detaches before it can interact with the next element, which has yet to begin to autoignite. Type 4 is when reactivity gradients are so large that the next element ignites due to flame-front propagation before it has a chance to autoignite. Autoignition will therefore not occur.

The vast majority of activity was to understand knock and operate conventional engines close to their limit. Oppenheim [190], of the University of California, Berkeley, proposed that knock could be seen as a positive phenomenon if it were to be harnessed in a controlled manner. He performed a detailed literature review going back to the 1880s and then went on to describe measurements in optically accessible shock tubes to study the autoignition mechanism. He stated that a number of exothermic centers per unit mass are generally present, but their distribution is unknown. The temperature distribution, however, decides the character of the combustion. Autoignitions were characterized as strong or weak. As a means of eliminating knock, combustion by "a great multitude of miniscule, properly distributed in time, micro explosions" was proposed. This is effectively a Homogeneous-Charge Compression Ignition (HCCI) or CAI engine, although that terminology was not used. Oppenheim [191] also published "Dynamic Features of Combustion" in this period, describing the different combustion modes from flame propagation through to detonation. Examples of Deflagration to Detonation Transition (DDT) in constant cross-sectional tubular combustion bombs were shown. Here combustion begins at the closed end of the tube, and the burnt gases behind the flame front cause it to accelerate. Pressure waves coalesce forming shock waves that interact with the walls, thereby generating turbulence. Further pressure waves are created, and eventually, this positive feedback mechanism can accelerate the turbulent flame front until detonation occurs. This known phenomenon in tubular bombs was what led some researchers to suggest knock in an ICE resulted from FFA into detonation, notably Curry [119]. Maly and Ziegler [192] of the University of Stuttgart published a modeling study on this in 1982. A mechanism, whereby a positive feedback mechanism of flame-front turbulence in an ICE, was proposed and was said to explain some historical observations. Note that for DDT to occur, turbulent flame-front propagation needs to reach the Chapman-Jouguet detonation velocity, which is significantly higher than the acoustic velocity in the unburnt medium. This is more than an order of magnitude higher than typical turbulent flame velocities in an ICE, and hence a very strong positive feedback would be required. Cuttler [193] of Jaguar, together with Girgis of Coventry Polytechnic, described in 1988 three types of combustion that could theoretically result in knock-like noise: explosion (homogeneous autoignition), detonation (supersonic reaction front), and deflagration (subsonic flame-front propagation through rapid entrainment). Note that subsonic sequential autoignition is also possible. Optical measurements were carried out using a transparent "Bowditch" piston engine. On a disk-type combustion chamber, end-gas autoignition was observed. For a compact bowl in the piston chamber; on the other hand, rapid combustion in the squish region was hypothesized to be due to rapid entrainment and caused pressure rise rates of 8 bar/°CA. Pressure oscillations for this condition were rather weak. The window diameter was 60 mm with a bore diameter of 80 mm, and the frame rate of the camera was only 8000 frames per second; hence, the optical setup was not ideal for drawing firm conclusions. Reverse squish effects can accelerate a flame front into the squish zone as the piston descends, however, and this phenomenon, like knock, is also sensitive to ignition timing.

Swirl and squish had been used to improve turbulent flame speed for many years and had been quantitatively studied in the 1970s. In the 1980s, investigations on an alternative charge motion took place. In 1983, Witze et al. [194] of Sandia National Laboratories and the University of Michigan-Ann Arbor described experimental measurements of flow and turbulence in an optically accessible engine with an inlet valve in the side of the combustion chamber. Laser Doppler Velocimetry (LDV) was used to measure both mean and turbulent flow velocities. A shroud could be rotated on the intake valve generating different bulk fluid motions. It was discovered that by directing inlet flow towards the piston, a tumble motion was created in the charge. This large-scale motion was destroyed late in compression, which resulted in a peak in turbulence intensity at the center of the chamber at around 30°CA before firing TDC. Results were compared to a 0D turbulence model and fired engine data. The 0D model could not directly replicate the peak in turbulence during late

compression. In 1985, Gosman et al. [195] of Imperial College of Science and Technology again described flow and turbulence measurements using laser Doppler techniques. A transparent model engine was used with a single inlet valve in the head, once more with a shrouded section. A tumble motion was again produced, but this time experimental results were compared to a 3D CFD code.[14] A turbulence peak around firing TDC resulting from the tumble motion was once again observed, and it was commented that this would likely be beneficial in improving early combustion rates. Kent et al. [196] of Ford published on comparisons between swirl and tumble charge motions and their effect on burn rates on four-valve pent-roof engines in 1989. The charge motion of the engines was estimated in a flow rig with a moving piston and optical access, which used water as the test fluid rather than air. Reynolds numbers were matched to give dynamic similarity to the target low-speed engine condition. A tumble ratio of 1.4 was found to give a similar 0-90% burn duration to swirl ratios of a similar magnitude. It was suggested that a combined swirl and tumble charge motion may make sense—tumble results in a turbulence peak at around ignition timing whereas swirl survives later into the cycle and can improve burn rates at a later stage. Tumble was relatively easy to create with four-valve pent-roof heads, which were becoming more popular due to their improved volumetric efficiency, and hence power output. Of course, four-valve heads were not a new technology. They were widely used in WWII aircraft piston engines, as has already been described, and in racing applications.

In 1988, Heywood published his book *ICE Fundamentals* [197]. Knock was described as a "race between the advancing flame-front and the precombustion reactions in the unburned end-gas." Autoignition and accelerating flame-front theories of knock were both mentioned, although it was thought that autoignition theory was better supported by evidence, and hence the most widely accepted. The importance of cyclic variability was highlighted as fast-burning cycles have the highest knocking tendency, and so are those that limit the compression ratio. MAPO was suggested to be the most appropriate method of pressure sensor knock feedback. The road octane rating of vehicles at the time was said to be well aligned with an average of RON and MON values, the AntiKnock Index (AKI). This textbook would become one of the key references for university students of ICEs around the world and remains so to this day.

The 1980s was a period when high output turbocharged engines dominated Formula 1. Otobe et al. [198] of Honda published on their V6 1.5-liter (L) turbocharged engines in the last year of the relevant regulations—1989. The 1987 RA167E engine produced 1010 CV (1 CV = 0.7355 kW) at 4 bar absolute manifold pressure with a relatively low compression ratio of 7.4:1. A boost pressure limit of 2.5 bar for the 1988 season permitted an increase in compression ratio to 9.4:1. Power output was 685 CV and peak cylinder pressure 167 bar. IMEP was 38 bar. The maximum octane value of the fuel by regulation was a RON of 102. A study was performed using iso-octane, n-heptane, and toluene to perform a toluene sweep from 25% up to 84% at constant RON. It was possible to improve KLSA by more than 10°. As toluene was added, the MON dropped from 94 to 90, and hence it could be interpreted that this engine had a negative "K-factor," as will be explained in a subsequent section.

[14]Gosman would later become one of the key figures behind STAR-CD 3D CFD software—one of the most popular CFD packages used in engine development in the 1990s and still today.

The 1990s: Chemical Kinetics, Exothermic Centers, and Time-Frequency Analysis

In 1990, Maly and Konig of Daimler-Benz together with Klein of Princeton and Peters [199] of RWTH (Rheinisch-Westfälische Technische Hochschule) Aachen University published a very detailed study on the impact of shock waves in an L-shaped combustion chamber, intended to represent the piston top-land crevice zone. The experiments were at atmospheric pressure but used an ethylene/oxygen mixture. The device is shown in Figure 27. The initial section resembles a tubular bomb. A spark plug was sufficient to generate the incident shock wave. The initial shock traveled at up to 2000 m/s whereas the reflections were at around one-third of this speed. However, the reflected shocks gave higher pressures

FIGURE 27 Bomb used to study detonation waves entering piston crevice area by Maly et al. [199].

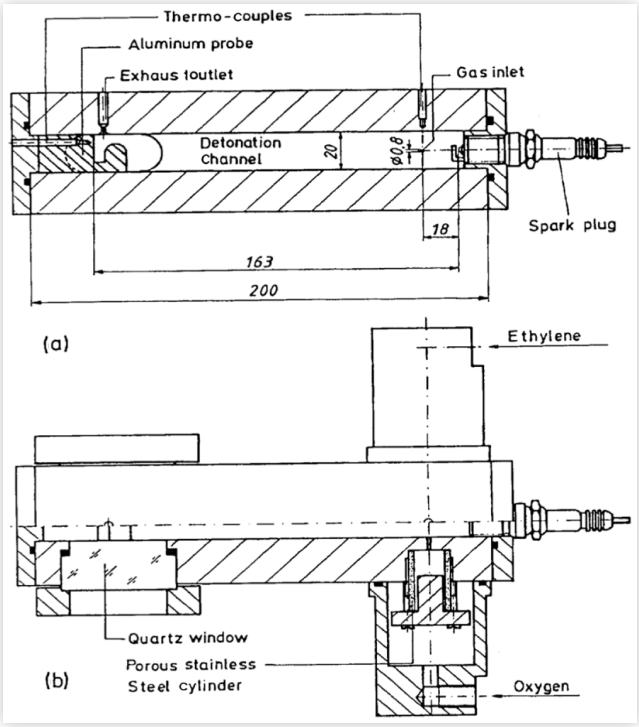

and temperatures than the incident wavefront. Duration runs were carried out on this bomb, and erosion damage was seen, which resembled that typically observed on the piston of a knocking engine. One of the co-authors, König, published two other key works the same year in collaboration, firstly, with Sheppard [200] of the University of Leeds and, secondly, with Maly, Sheppard, Bradley, and Lau [201]. Here the importance of temperature gradients around exothermic centers was discussed based on the theory of Zeldovich. Developing detonation was promoted through the introduction of metal particles in the engine in an effort to generate appropriate exothermic centers and gradients. Maly also co-authored a paper with Herweg [202] in this period on flame kernel modeling in SI engines. The model accounted for electrical parameters of the ignition system, heat loss to the electrodes, mixture properties, and turbulence. It was shown to correlate well with optical measurements of flame kernel growth taken in a specially adapted engine. Understanding properly early flame kernel growth is key for extending the dilution limit of engines, which also improves the knock limit. Later in the decade, Pan [203], of the University of Leeds, published on computer code that could reproduce the three autoignition modes of Zeldovich. In 1991, Spicher [204], now of FEV (Forschungsgesellschaft für Energietechnik und Verbrennungsmotoren) together with Kröger and Ganser of the Technical University of Aachen, published schlieren photography at 200,000 frames per second together with optical fiber measurements at 500 kHz. Here supersonic reaction fronts were seen.

Almost homogeneous autoignition was also observed. The highest knocking intensities were correlated with the fastest reaction front propagation and were thought to likely be developing detonations. It was highlighted in this work that accelerating flame fronts were never observed, and hence the autoignition theory of knock appeared to be the correct one. It was also remarked that it was not obvious why in the 50 films examined, autoignition never began next to the advancing flame front, given that this region could be expected to be the hottest and, hence, most reactive.

Chemical kinetics calculations were coming of age in engine development, and more complex models were being published. Westbrook [205] and Pitz of Lawrence Livermore National Laboratory (LLNL), together with Leppard of GM, applied a mechanism with 500 species and 2500 elementary reactions to CFR engine data. Analysis of the reaction mechanism showed the importance of the production of hydroxyl (OH) radicals from isomerization reactions on octane values. A detailed model was also used by Ronney et al. [206] of Princeton University, again together with LLNL, where the knock-limited intake temperature for a range of different fuels with enleanment was compared. Those that featured an NTC region benefited the most from enleanment. It was suggested that this was due to a reduced alkylperoxy radical isomerization with greater presence of oxygen, based on the reaction mechanisms. A much simpler model was used by Brussovansky et al. [207] at MIT with just 17 species and 19 reactions. This work also studied the effects of heat transfer. A similar kinetics model was used by Nakano et al. [208] of Toyota. Simpler models had the advantage of shorter calculation times, particularly if implemented in multidimensional CFD. The Shell model was integrated in 3D CFD code at Loughborough University by Blunsdon and Dent [209]. This model was capable of simulating knock and the resulting pressure waves. The expected acoustic modes of the combustion chamber were excited in the model.

Chemical kinetics models require accurate descriptions of temperature in the end gas to produce reliable results. They are generally calibrated using rapid compression machines and shock tubes, where conditions are better known and more conveniently measured than in an engine. Researchers in the 1990s applied Coherent Anti-Stokes Raman Spectroscopy (CARS) techniques to measure end-gas temperature in a running engine. These are based on the overlaying of two laser beams of different wavelengths to excite nitrogen molecules. The resulting spectrum corresponds to the temperature. This can be calibrated in a simple bomb. CARS gives a point measurement based on where the beams are focused. Kalghatgi et al. [210] of Shell applied CARS on a Ricardo E6 engine for a range of different fuels and compared measured temperatures to those predicted by polytropic compression. For all fuels except propane, which does not exhibit cool-flame chemistry, measured temperatures indicated Low-Temperature Heat Release (LTHR) was taking place. Knocking cycles were also seen to exhibit higher end-gas temperatures shortly before autoignition. Nakano et al. [208] of Toyota compared CARS measurements with chemical kinetics calculations. Direct sampling of residual gases was also performed. The calibrated engine model that resulted was then used to see the relative impact of faster burn rates on knock-limited torque—rapid combustion was confirmed to be an advantage for a given temperature during late compression, and trade-offs between these two parameters were presented. An alternative approach to chemical kinetics modeling is to measure chemical activity directly. Direct measurements of OH, CH, and C_2 radicals, using absorption and emission spectroscopy on a running engine, were performed by Shoji and Saima of Nihon University together with Shiino of Mazda [211]. The engine was run with PRF 50 fuel and a compression ratio of just 6.4:1 at a speed of 1800 rpm. The level of activity in the blue flame interval, characterized by dips in CH and C_2 absorption, correlated to subsequent autoignition intensity. An example is shown in Figure 28. Golombok et al. [212] of Shell published on the differences in knocking heat release rate between paraffinic (such as iso-octane and n-heptane) and aromatic fuels.

The maximum heat release rate for aromatics when knocking was seen to be much lower than for PRF blends—coherent with empirical knowledge that aromatics knock "more quietly." This may be due to the lack of an NTC region encouraging more progressive sequential autoignition. The benefits of N-Methyl Aniline (NMA) as a knock suppressor were also demonstrated, and the mechanism was shown to be through modification of only the low-temperature chemistry.

FIGURE 28 Absorption and emission spectroscopy measurements in a knocking engine by Shoji et al. [211].

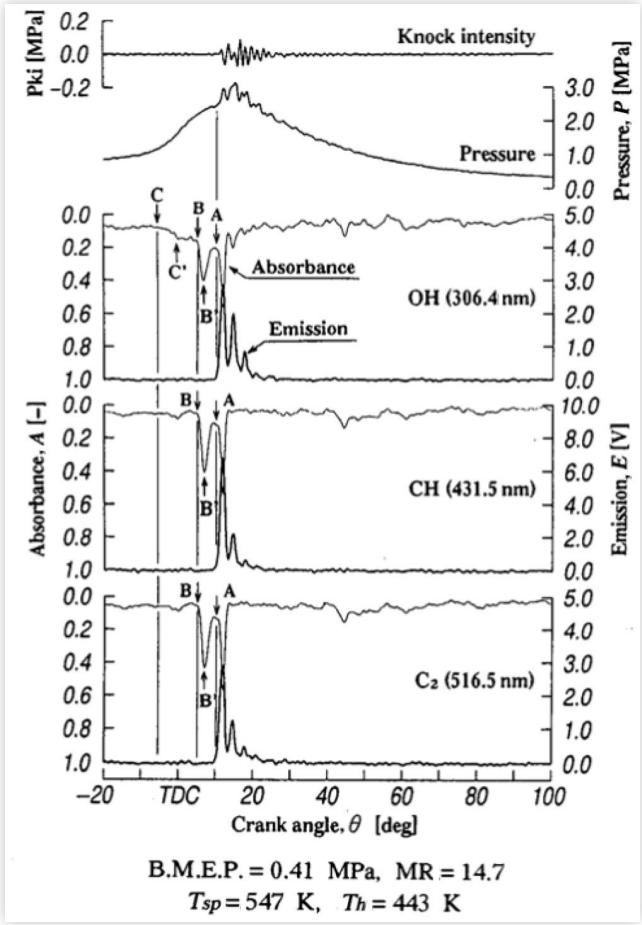

More complex techniques were also being applied to interpret knocking cylinder pressure signals. Kaneyasu et al. [213] of Hitachi used the Signal-to-Noise Ratio (SNR) in multiple frequency bands to separate knocking from non-knocking cycles. Samimy et al. [214] of Ohio State University applied the Wigner-Ville Distribution to create time-frequency plots of knocking data. The same technique was also applied by Scholl et al. [215] of Ford. Burgdorf et al. [216] of Chalmers University of Technology applied Wavelet Transforms. They took advantage of their flexible time-frequency windows and reduced computational intensity in comparison to windowed Fast Fourier Transform (FFT) analysis. They were also able to show multiple autoignition events in the same cycle using this approach. Burgdorf and Denbratt [217] would also compare eight different pressure-based knock detection methods in a separate publication, but no method was thought to have a significant advantage over the conventional MAPO approach. The same authors [218] also published the following year on knock statistics, including giving advice on minimum population sizes. More than 1000 cycles were required to meet their criterion for a pent-roof geometry. That same year, Burgdorf and Chomiak [219] presented a study that seeks to understand why sometimes pressure oscillations increase after the initial knock event, even for low amplitude knock. A micro shock tube was used to fire into the end gas of a combustion chamber. At idle-like conditions, this gave a knock-like signal but no autoignition. The flame front was seen to act as a sort of LPF. It was hypothesized that shock waves may reflect in crevice zones and eject crevice gases into the main charge and, thereby, ignite them.

Some new optical measurements were also being performed. Stiebels et al. [220], of the Lehrstuhl für Technische Thermodynamik of RWTH Aachen University, used two Intensified Charge-Coupled Device (ICCD) cameras, 15 µs out of phase, triggered by autoignition. This allowed autoignition location and reaction spatial velocity to be studied. Velocities ranged from subsonic to sonic. As seen by other researchers, autoignition frequently originated close to the wall. This was believed to be due to NTC behavior. Once again it was observed that autoignition did not always produce knocking cylinder pressure oscillations (three pressure transducers were used simultaneously to measure these). A representative image from this work is shown in Figure 29.

Knock location could also be calculated from cylinder pressure data if there were at least three transducers opportunely arranged in the combustion chamber. This was demonstrated by Liiva et al. [221] of Texaco. Four transducers were used on a CFR engine, mounted on a spacer plate between the head and the cylinder. This allowed checking of errors between groups of three sensors. The knock location generally agreed to within 6 mm between the groups. Such a calculation assumes that the incident knock wavefront travels spherically at reference acoustic velocities. In engine development environments, combustion and knock calculations from cylinder pressure data could now be performed in real time, and hence

FIGURE 29 Two superimposed images of autoignition region in an engine end gas with 15 µs time difference used by Stiebels et al. to calculate autoignition front velocity [220].

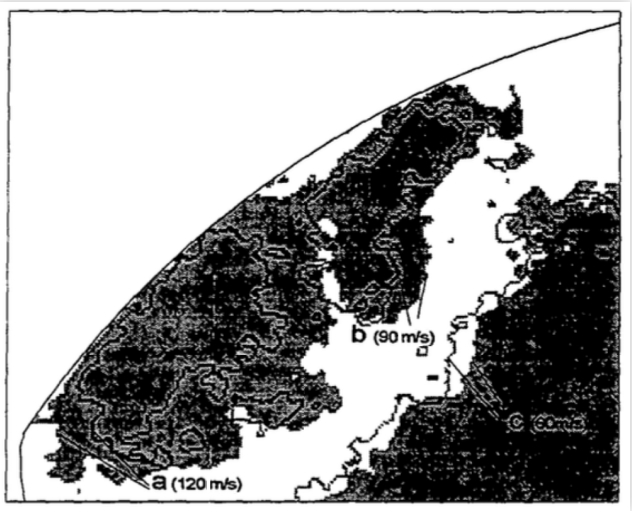

used for automatic mapping and calibration, as demonstrated by Gschweitl et al. [222] of AVL.

Cooled EGR was being investigated as a replacement for enrichment fueling to avoid knock and/or high temperatures. Grandin et al. [223] of the Royal Institute of Technology in Stockholm and Saab Automobile tested cooled EGR in the range 0-21% on a four-cylinder 2.3 L turbocharged engine. The highest load was achieved with 13% EGR, but combustion stability was poor. A 10% EGR gave the same maximum load as 10% enrichment at fixed boost pressure.

Another approach to reduce knock, suggested by Ueda et al. [224] of Toyota, was to increase squish effects on a pent-roof engine through the use of a slanted squish area. A 5° gain in knock-limited ignition timing was found. Goto [225], together with collaborators at Mazda and the Kanesaka Technical Institute, described a downsized V6 supercharged engine with a Late Intake Valve Closing (LIVC) strategy. This had the expansion ratio of an NA engine and the effective compression ratio of a turbocharged engine. A Lysholm compressor was used to avoid turbo lag. The 2.3 L supercharged Miller engine had an equivalent performance to a 3.3 L NA but with 13% improved cycle fuel consumption. The following year, Hitomi [226] and researchers at Mazda presented an analysis of the Miller cycle as an effective approach to improve CO_2 emissions. LIVC was thought to be superior to EIVC as less heat transfer to the charge in the cylinder was expected. The boost pressure characteristic against engine speed was also more favorable. Despite this, 1 year later Ueda [227] of the University of Tokyo, together with colleagues and collaborators at Mazda, published on an effective EIVC engine where a rotary valve in the intake system was applied, such as had been studied by the same University a decade before. This time the engine in question was naturally aspirated and intended to take the place of a diesel engine. The expansion ratio was increased from 8.4:1 to 11:1. Problems with long burn durations at low load were observed, although it was suggested that these could be reduced through the use of a high-energy ignition system.

GDI engines were also reintroduced to the automotive market in the late 1990s. GDI had been used on fighter aircraft in WWII and subsequently in 1954 on the Mercedes-Benz 300SL, but most production cars in the 1990s used Port Fuel Injection (PFI) systems. Mitsubishi's GDI engine went on sale in Japan in 1996 and that of Toyota one year later. Iwamoto et al. [228] of Mitsubishi described their concept in 1997. Electronic control of the injection timing meant these modern concepts could adopt different strategies over the engine speed and load range. Late injection timing at low speed and low load permitted lean stratified operation, with an ignitable AFR still guaranteed at the spark plug. At high speed and high load, early injection timing produced a homogeneous mixture. The Mitsubishi engine featured an unusual reverse tumble intake port that produced a tumble ratio of 1.8. The injector was mounted underneath this. The piston featured an offset spherical bowl and high squish on the exhaust side. The injection pressure was rather low by current standards (50 bar), both to reduce fuel pump work and for reliability concerns. AFRs greater than 30:1 could be run in the stratified mode together with EGR. Maximum EGR quantities were as high as 40%, despite a coil energy of just 60 mJ and a narrow-gap plug. EGR was used to reduce engine-out NO_x emissions, but the exhaust aftertreatment also included a NO_x abatement system. The use of homogeneous GDI in full load gave a 5% improvement in volumetric efficiency and an estimated reduction in the end of compression temperature of 30 K. Harada et al. [229] described the Toyota Direct Injection gasoline engine in the same year. In contrast to the Mitsubishi system, a swirl control valve was used to generate charge motion in the piston bowl. Low speed and load were again partnered with a late injection strategy while high speed and load were with early injection. The transition zone used two injections per cycle. The injection pressure was 120 bar. Like the Mitsubishi engine, a combination of enleanment and up to 35% EGR was used, and a NO_x aftertreatment system was required. Claimed fuel consumption reductions for these two engine types were in the range 20-30%.

Not all engine manufacturers were convinced that stratified lean systems would comply with future emissions limits. Anderson et al. [231] of Ford published a research activity on a GDI engine designed for homogeneous operation in 1996. The engine featured an open combustion chamber. Both the injector and the spark plug were mounted centrally. This compromised the valve sizes, and hence a high volumetric efficiency, low tumble intake port was applied to compensate. Comparisons between PFI and GDI injection on the same research engine at full-load and knock-limited conditions were presented. GDI fueling allowed a 10% increase in Wide-Open Throttle (WOT) IMEP. Around 2% of this was from improved volumetric efficiency while the rest was from knock mitigation. The knock limit improved as injection time was retarded, up until the point where combustion became unstable due to inadequate mixing time. Volumetric efficiency peaked at earlier injection timings where the intake valve was still open. The knock limit improvement was attributed to the more effective charge cooling of DI—the vaporization of the fuel cools the air directly, rather than cooling the intake port and valve, as in a PFI system. This is shown schematically in Figure 30 from Yang et al. [230] of the same research group in 1998. In this publication, a split injection strategy was used to achieve

FIGURE 30 Potential of improved charge cooling with a Direct-Injection Spark-Ignition (DISI) system in comparison to PFI, from Yang et al. [230].

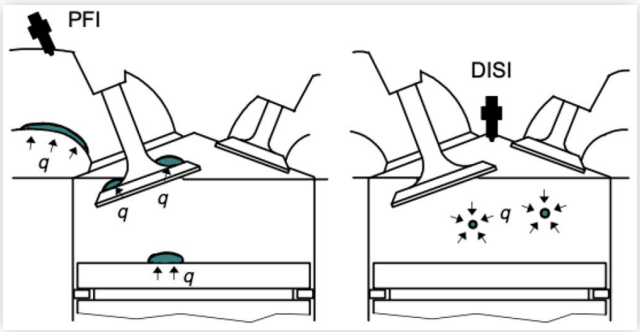

Reprinted with permission from Ref. [230]. © SAE International

a better trade-off between volumetric efficiency and knock. GDI systems are ubiquitous now, and generally modern GDI engines run at stoichiometric conditions to fulfill significantly more stringent emissions limits with the use of a three-way catalytic converter and without lean aftertreatment systems. They take advantage of the knock mitigation effect of DI to run higher compression ratios than their PFI predecessors.

DI of gasoline was also seen as a potential enabling technology for CAI. A collaborative venture between Daimler-Benz, IFP, Ford, and Peugeot to study CAI was described by Willand et al. [232] of Daimler-Benz in the same period. It was thought that negative valve overlap could be applied to promote autoignition and stratified charge, through DI strategies, used to control it.

The 2000s: Optical Measurements in Engine Development and Developing Detonation Theory

In the early 2000s, optical measurements began to come out of the research lab and into the standard development environment. Spicher [179] had already published on optical fibers in a cylinder head in 1986. His collaborators Töpfer et al. [233] described the installation of optical fibers into a spark plug in 2000, as shown in Figure 31. This was used on a production Mitsubishi GDI engine. A similar approach was taken by Philipp et al. [234] of AVL in their work published the following year. These systems meant that optical measurements could be conveniently applied even on production engines, with no modifications required. They could be used for autoignition location determination, early flame-front propagation measurement, and to identify diffusive combustion.

Fundamental research on knock continued in the lab, with a number of interesting studies being published by Swedish universities, in a collaborative research project. Westin et al. [235] of the Royal Institute of Technology applied direct sampling on a 2.3 L four-cylinder turbocharged engine and tested the effect of residuals concentration on KLSA. A 2% increase in residuals corresponded to a 5° retard requirement. This was at least partly temperature driven, and indeed the effect on charge temperatures was estimated at 30 K, although it was remarked that the NO concentration of the residual gases may also have a significant effect. Stenlåås et al. [236] of Lund University of Technology investigated the impact of NO by adding it to the intake system on the same engine type used by Westin. In this study, NO was found to worsen the KLSA with 400 ppm corresponding to almost 4° of retard. Burluka et al. [237] of the University of Leeds found that the effects of NO depended on the fuel used: with pure iso-octane the knock limit actually improved as NO was added. For unleaded gasoline, it worsened. Both Westin and Stenlåås had used unleaded gasoline in their activities. A series of investigations took place at Swedish universities on a modified Volvo cylinder head, with a horseshoe-shaped combustion chamber and dual side-spark locations to allow optical access to the end gas. CARS was applied by Grandin et al. [238] of Chalmers University of Technology, together with thin-film resistance temperature measurement, to measure heat flux for knocking and non-knocking cycles. Peak heat flux was three times higher when knock occurred—a similar value had been found by Lee et al. [176] in the 1980s. The thermal boundary layer was also measured and found to be just 0.5 mm thick. The experimental setup is shown in Figure 32. In the same year, the same authors [239], together

FIGURE 31 Spark plug with optical fibers used by Töpfer et al. for knock location determination on a production GDI engine [233].

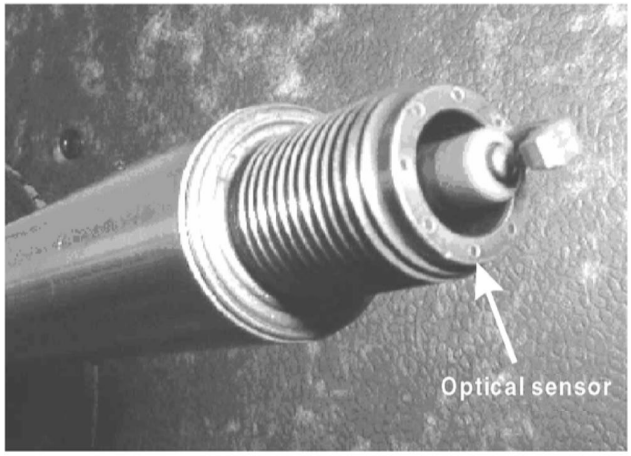

FIGURE 32 Modified Volvo cylinder head with horseshoe combustion chamber and twin side spark plugs used by Grandin and a series of researchers in Sweden. CARS beams shown [238].

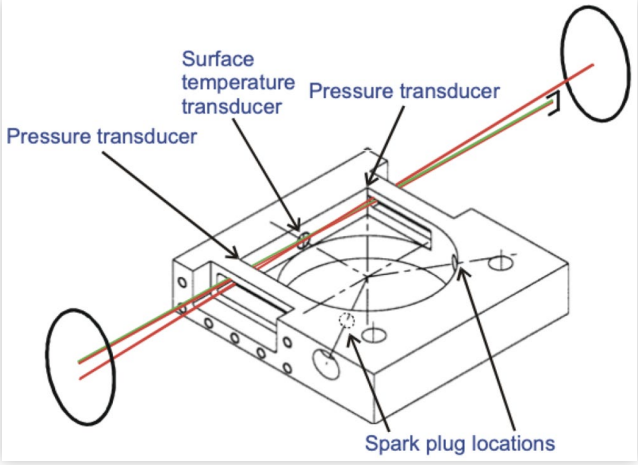

with researchers at Lund University, also published on heat release in the end gas with PRF 75 fuel for a range of AFRs and EGR concentrations. Significant end-gas heating was found for all conditions due to preflame reactions—temperatures were typically 50 K hotter than that predicted by isentropic compression. A 60 species, 232 reaction chemical kinetics model was also used in the study. Two-zone combustion models were popular, as they were computationally efficient, and chemical kinetics calculations could be implemented in them without necessitating excessively high calculation times. A simple two-zone model assumes homogeneous end gas, however, which is rarely the case in reality, and exothermic centers had been highlighted as key in the previous decades. Gogan et al. [240] of Lund University combined a two-zone model with stochastic particles based on a Probability Density Function (PDF). Particles gradually move from the unburnt to the burnt zone in this approach, and random variations of temperature and mass can be described. Turbulence mixing governs how the original variations converge to the mean bulk conditions over time. This methodology gave more realistic autoignition pressure peaks than simple two-zone models. An alternative was presented by Sjöberg et al. [241] of Sandia in 2005. They applied a five-zone approach to model HCCI combustion. One zone was dedicated to the crevice region, and others could be used to describe temperature stratification.

More lean-burn engines were coming to market, and hence understanding cyclic variability was crucial. Aleiferis et al. [242] of Imperial College of Science, Technology, and Medicine, in collaboration with Honda, published on the subject in 2000. Particular emphasis was placed on early flame kernel growth. Optical measurements of flame kernel volume were found to be strongly correlated with burn rates later in the cycle. Cross-flow spark plug ground electrode orientations were found to perform best, and sensitivity to ignition energy and spark duration was also demonstrated. Extended spark durations were thought to be particularly effective if AFRs varied strongly with crank angle near the spark plug location at ignition timing.

GDI engines were increasingly popular, as summarized in a book by Zhao et al. [243] in 2002. Already at this stage production and near-production systems existed at Nissan, Renault, Adam Opel, Audi, FIAT, Ford, Honda, Isuzu, Mazda, Mercedes-Benz, Peugeot Société Anonyme (PSA), Saab, Subaru, and Volkswagen. While the first DI engines to market in the 1990s ran at part load in stratified lean conditions, some manufacturers were now using the technology with engines that only ran at stoichiometric AFR. This meant a conventional three-way catalyst was the only aftertreatment required to meet emissions limits. The knock mitigation benefits of DI were of increased importance when it became popular to combine GDI with turbocharging and downsizing later in the decade. One example of this is the Ford EcoBoost engine, described by Yi et al. [244] in 2009. A turbocharged DI 3.5 L engine took the place of an NA PFI engine of 5.4 L capacity. The combustion system was optimized through a combination of CFD, optical measurements, and conventional dynamometer testing,

FIGURE 33 Integrated combustion system development methodology combining CFD, optical engine, and dyno testing, as applied at Ford in EcoBoost engine development, from Yi et al. [244].

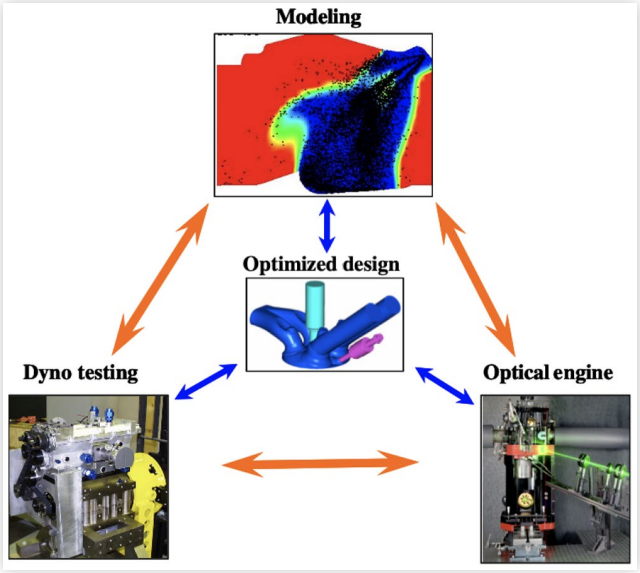

as illustrated in Figure 33. CFD was now well established in engine development environments and allowed a wide range of potential hardware designs to be screened in software. This meant a reduced number of prototype parts needed to be produced and is now the standard approach of most engine manufacturers. The engine ran in a homogeneous mode for all operating conditions except for cold start and catalyst heating. A dedicated stratified injection strategy was used to improve stability during catalyst warm-up. This is particularly challenging for turbocharged engines as some of the exhaust enthalpy required for catalyst light-off is lost in warming up the turbocharger. A modified piston crown was also implemented to improve stability in this operating point. Careful work on optimizing the combustion system for knock allowed a compression ratio of 10:1 to be used, despite the downsizing. A drive cycle fuel economy improvement of 12% was achieved for similar power and torque to the larger engine.

Research continued on alternative combustion concepts, some of these with direct relevance to conventional SI knock. A significant paper on CAI engines was published by Bradley and Morley [245] of the University of Leeds and Shell in 2002 together with Gu and Emerson of CLRC Daresbury Laboratory. Hot spots inevitably exist in the end gas of both CAI and SI engines. There tends to be a reaction gradient around them, and Zeldovich [189] had shown in 1980 that if an autoignition front develops, its velocity relative to acoustic and Chapman-Jouguet detonation velocities is key in determining if a developing detonation occurs. A resonance parameter was defined as $\xi = \frac{a}{u_a}$, where a is the acoustic velocity and u_a is the autoignition front velocity. The authors showed that a second term

FIGURE 34 Diagram proposed by Bradley et al. to explain conditions necessary for developing detonation in an engine. $\xi = \frac{a}{u_a}$ is the resonance parameter. $\varepsilon = \frac{r_0/a}{\tau_e}$ defines the hot spot reactivity and depends on the hot spot dimensions [245].

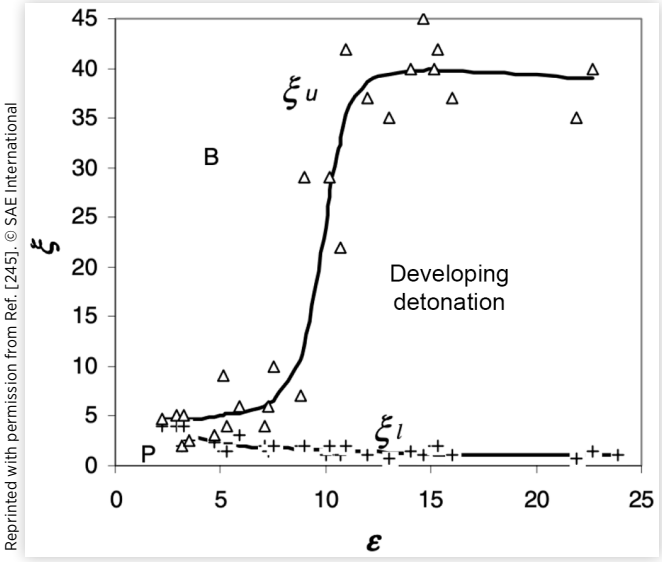

is also required to ascertain if developing detonation can occur in practical systems: $\varepsilon = \frac{r_0/a}{\tau_e}$, where r_0 is the hot spot radius and τ_e is the excitation time (time from 5% to maximum chemical power). When ξ and ε are plotted against each other, developing detonations only occur in a given range, as shown in Figure 34. The hot spot size is key, with very small hot spots not resulting in developing detonation. In the same year, Eng [246] published an analysis on the differences between pressure waves resulting from HCCI combustion and knock. It was shown that HCCI combustion generally leads to high signal energy at around 5-6 kHz—in this sense, similarly to knocking combustion. For HCCI however, around 90% of the energy from 4 kHz to 22 kHz is for this mode while, for knocking combustion, it is just 65%. It was suggested that objectionable engine noise from knock was a result of more effective transmission of these higher frequencies through the block structure, and hence to the ambient air. A formula for Ringing Intensity of HCCI combustion was derived based on wave intensity I. Wave intensity is described by Equation 12 and has units of watt per square meter (W/m^2). It was assumed that pressure pulsation amplitude Δp should scale with maximum pressure rise rate $\frac{dP}{dt}$. The Ringing Intensity was then as shown in Equation 13 [246]. β was a constant to be tuned with experimental data and was found to have a value of 0.05 for the described experiment. This formula was frequently cited by HCCI researchers in the coming years.

$$I = \frac{1}{2\gamma}\frac{\Delta p^2}{p}\sqrt{\gamma RT} \qquad \text{Eq. (12)}$$

$$\text{Ringing Intensity} \approx \frac{1}{2\gamma}\frac{\left(\beta \frac{dP}{dt}_{max}\right)^2}{P_{max}}\sqrt{\gamma RT_{max}} \qquad \text{Eq. (13)}$$

Bradley and Kalghatgi [247] published a further work in 2009 linking pressure oscillations Δp to the rate of autoignition-driven combustion. This was based on the rate of an autoignition hot spot expansion in comparison to local acoustic velocity. For non-detonative autoignition in engines, the resulting pressure oscillation behavior is approximated by Equation 14, where p is the undisturbed cylinder pressure.

$$\frac{\Delta p_{max}}{p} \approx \xi^{-2} \qquad \text{Eq. (14)}$$

A new CAI control mode for four-stroke applications was also researched—SACI. Two notable papers were published on the topic in 2005. Hyvönen [248] of Fiat-GM Powertrain Sweden, together with Haraldsson and Johansson of Lund Institute of Technology, performed testing on a Saab variable compression ratio five-cylinder engine with PFI fueling. The compression ratio could be controlled from 10 to 30:1, and an inlet air heater was also present. Cylinder pressure analysis showed an initial heat release primarily from SI before a transition to autoignition, as shown in Figure 35. Ringing on the pressure trace can be seen, and hence this is effectively similar to a knocking cycle in a conventional SI engine, although the transition to autoignition may occur at much lower MFB percentages—around 36% for the example shown. The amount of heat release from flame-front propagation was just 5% at high compression ratios with a relative AFR $\lambda > 2$. The spark-assisted mode was seen as a means of transferring in a controlled manner from extremely lean HCCI with high compression ratios to stoichiometric conventional SI at low compression ratios. Urushihara et al. [249] of Nissan published

FIGURE 35 Spark-assisted HCCI pressure trace and heat release analysis, from Hyvönen et al. [248].

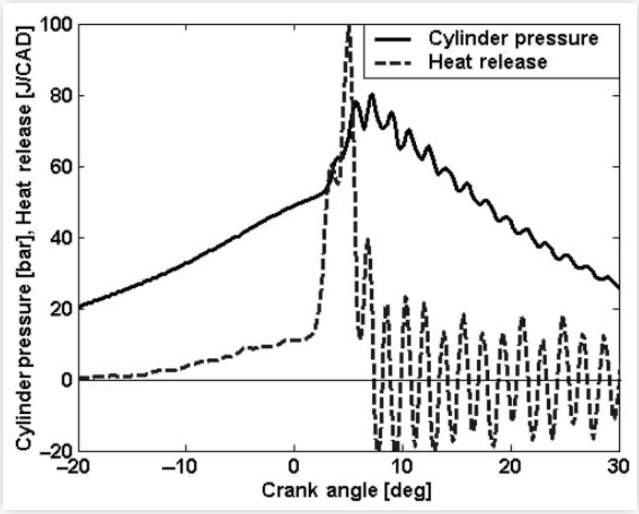

FIGURE 36 Nissan spark-assisted gasoline compression ignition research engine, from Urushihara et al. [249].

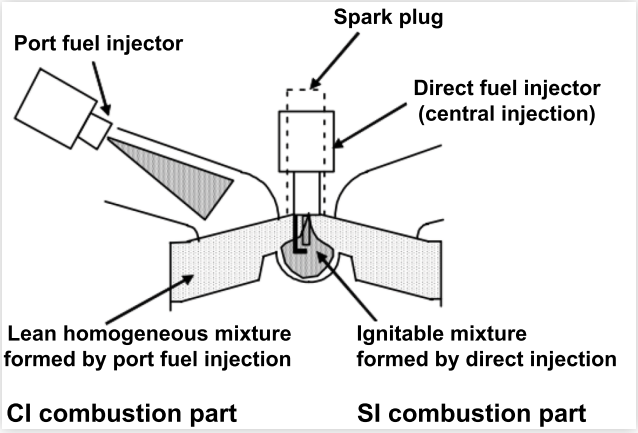

Reprinted with permission from Ref. [249]. © SAE International

their study on spark-assisted gasoline compression ignition engines the same year. Here the compression ratio was fixed at 15:1. The engine featured PFI fueling to create an overall lean homogeneous mixture, and a direct injector was used to produce a locally rich cloud near the spark plug. A small bowl was created in the piston for the same reason. The concept is shown in Figure 36. The pressure rise from flame-front propagation was said to function similarly to increasing the compression ratio. Variable valve overlap to control internal residuals allowed the use of SACI from IMEP values of around 3.5-6.5 bar without knocking. Airflow was fixed at WOT conditions and PFI fueling was used to adjust the load. Knocking limited the richest AFR, and hence the load that could be achieved. At still lower loads, pure HCCI was run.

Fundamental knocking research also continued in Japan. Suzuki et al. [250], of Nihon University, used light emission spectroscopy to study HCHO (cool flames, 395 nm) and HCO (formyl radical—blue flames, 330 nm) in the end-gas region of a single-cylinder engine. Ion-current sensors were also utilized. It was found that the duration of HCHO formation before knock was sensitive to combustion chamber temperature for PRF 30 and PRF 60, but not for pure n-heptane. The duration of HCO light emission decreased for all blends as combustion chamber wall temperature increased. Hirooka et al. [251] of Toyota studied the impact of turbulence on burn rates and knock using DI of high-pressure air and of hydrogen. Various patterns of high-pressure air could increase turbulence near the spark plug or in the periphery of the combustion chamber. Combustion duration could be halved. Best results were found when accelerating the late part of combustion, with a 13° improvement in KLSA. Note that turbulence generated by tumble tends to primarily accelerate the early phase of combustion. Fast burn rates also led to combustion noise, however, between 800 Hz and 2000 Hz. Although the gain in performance was as much as 10%, when compressor work to generate the high-pressure air was factored in, the overall efficiency gain dropped to 4%. The hydrogen study documented by Shinagawa et al. [252] gave similar burn rates to that of the compressed air research, and again it was possible to improve conditions close to the plug or in the end gas. At similar burn rates to the high-pressure air injection study, the knock limit was further improved. Chemical kinetics calculations suggested this was due to the consumption of the OH radical by hydrogen.

A great number of papers were published on signal processing techniques. Part of the reason was to improve the SNR of production accelerometers, but noise was also an issue for cylinder pressure transducers. Zhang [253] of the Industrial Technology Center of Okayama Prefecture and Tomota of Okayama University used wavelet transforms with multiple voices per octave to identify knock in noisy signals. Wavelet pattern matching was applied to compare actual and reference signals. Carstens-Behrens [254] of Ruhr University Bochum, together with collaborators at Bosch, performed time-frequency analysis using the Wigner-Ville transform and compared this to Finite Element Method (FEM) acoustic mode calculations of a pent-roof combustion chamber for various piston heights, as shown in Figure 37. Noubari and Dumont [255] of the University of Tehran and the University of British Columbia, respectively, employed wavelet methods to reduce both white and colored noise in accelerometer signals. The entropy of the de-noised accelerometer signal could be used to quantify knock: knocking cycles showed lower entropy. Borg et al. [256], of Hitachi America and Oakland University, Michigan, also used wavelet transforms. Correlation was studied between accelerometers and pressure transducers. The best correlation in this study was found between 4 kHz and 8 kHz. Borg et al. [257] characterized autoignition using heat release analysis in the same year. The maximum heat release rate of knocking as opposed to non-knocking cycles was compared. Worret et al. [258], of the University of Karlsruhe, reviewed a number of pressure-based knock algorithms and also proposed a variant based on Rate Of Heat Release (ROHR) 3 years prior to this. One of the issues in using ROHR as a knock index is that the data becomes very noisy when knock occurs. Corti et al. [259] of the University of Bologna suggested to use a combination of three Wiebe functions, with one being dedicated for the knocking heat release. Hettinger et al. [260] of Bosch suggested dealing with

FIGURE 37 First ten acoustic modes for pent-roof combustion chamber as calculated by Carstens-Behrens et al. [254].

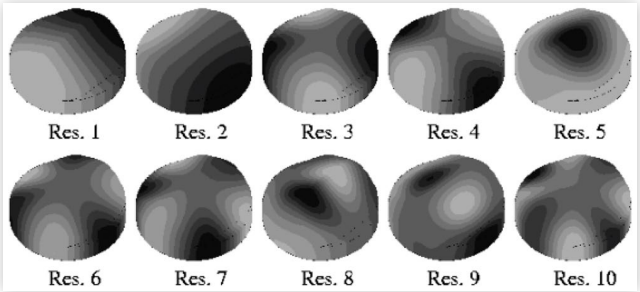

Reprinted with permission from Ref. [254]. © SAE International

FIGURE 38 Comparison of cylinder pressure transducer and accelerometer time-frequency data by Naber et al. [262].

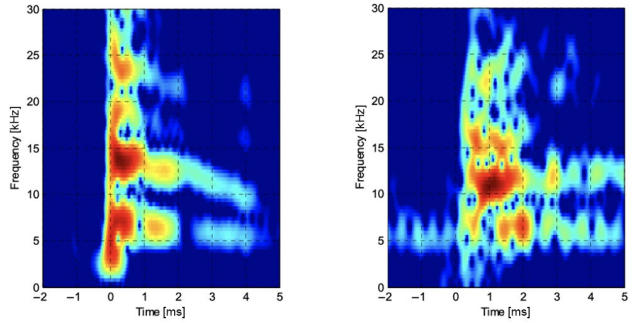

Reprinted with permission from Ref. [262]. © SAE International

the problem by fitting a single Wiebe function only up to the moment of knock onset and then comparing this to the measured heat release post-knock. In general, noise on the pressure transducer and accelerometer signals becomes more problematic at higher engine speeds and loads. Cavina et al. [261] of the University of Bologna proposed methods to deal with this and examined the susceptibility of different indices to windowing and filtering effects. Naber et al. [262] of Michigan Technological University and Motorola compared time-frequency spectrograms of cylinder pressure and accelerometer signals, as shown in Figure 38. They also considered the knock intensity from both sensors to be well fitted by a single log-normal distribution.[15]

Cylinder pressure transducers and accelerometers were the standard tools, but Mittal et al. [263] of MIT found in their study that a microphone could also identify knocking peaks at around 6 kHz. Higher amplitudes were seen on the cylinder pressure signal in the 15-22 kHz range, but the microphone signal was BPF from 6 kHz to 12 kHz to correspond to audible knock. Abhijit and Naber [264], of Michigan Technological University, compared cylinder pressure and ion-current signals using a range of techniques. It was stressed that both are local measurements, and hence, for single cycles the correlation may be poor. It was also noted that only two peaks were visible on an FFT of the ion-current signal while four could be seen for the pressure transducer. Correlation was best between the highest frequency common peak. This was partly because, at high speed, noise extended above 6 kHz on the ion-current signal. Although cyclic correlation was poor, statistically the two sensors responded in a coherent manner to changing spark advance. Knock statistics were also studied by Zhu et al. [265] of Visteon. A stochastic knock controller was proposed, based on a nonlinearly modified Gaussian PDF. This was updated cyclically by an online buffer. It allowed a more stable ignition control than for conventional "count-up/down" knock controllers and hence a lower COV (Coefficient Of Variation) of IMEP.

[15]The dual log-normal work of Iwata et al. [175] was not referenced.

Knock localization could be performed with optical techniques, but a number of researchers developed the multiple pressure sensor method as well. One of the main issues is to reliably estimate the time difference between the signals, to allow triangulation of the incident knock wave source. Castagné et al. [266] of IFP and Metravib RDS used an intercorrelation calculation rather than relying on the simple wave arrival time. For 5 mm geometric accuracy, the time difference needs to be precise to within 5 µs. It was seen that piezoelectric pressure sensors were reliable in bench testing to within 1 µs. The methodology was tested also in CFD to check the influence of engine geometry and inhomogeneous acoustic speeds and was found to still be valid. Both four standard Kistler 6052 piezoelectric sensors and an instrumented head gasket with twelve pressure-sensitive elements were tried. Rothe et al. [267] of the University of Karlsruhe used data from five cylinder pressure transducers to ascertain the location of autoignition and combined this with flame-front measurements from 17 optical fibers. Knock was seen to occur in regions of the end gas where the flame front arrives late. Hettinger et al. [260] of Bosch, used six sensors, one of which was in the spark plug. Modal analysis with FEM was used to identify knocking frequencies and the pressure distribution in the chamber. The effect on the accuracy of considering acoustic velocity stratification was quantified and found to be nonnegligible. Knock was also seen in this study to primarily occur in the last region where the flame front arrived, as measured by OH visualization.

In 2001 Kalghatgi [268, 269] of Shell published two papers on how RON and MON values could be used, together with a "K-factor," to match road octane requirements of modern vehicles. The first paper dealt with testing on a single-cylinder engine with a pent-roof head and two different compression ratios. A fuel matrix of thirteen blends with decorrelated RON and S was used. It was found that KLSA was weakly correlated with MON, quite well correlated with RON, and strongly correlated with a new octane index, as shown in Equation 15. The K-factor was found to become less negative as engine speed increased, but more negative as octane requirement increased. Acceleration testing on 23 European and Japanese cars with knock control systems, over a range of fuels, showed that most cars had a negative K-factor and, hence, responded best to fuels with high RON and low MON. Mittal and Heywood [270] of MIT applied the K-factor concept in the analysis of historical data from 70 years of CRC vehicle octane sensitivity studies. While, in 1951, only 10% of vehicles exhibited a negative K-factor; by 1991, this had increased to 50%. It was suggested and demonstrated by one-dimensional (1D) simulations that modern engines with higher volumetric efficiency, faster burn rates, and better cooling meant that conditions in the combustion chamber were at higher pressures and lower temperatures than for older vehicles. This meant that the relevant temperature regime had moved away from MON towards RON. For boosted DI engines, the calculations suggested a negative K-factor as described by Kalghatgi or "beyond RON" conditions.

$$OI = RON - KS \qquad \text{Eq. (15)}$$

Milpied [271] of IFP together with collaborators from Renault, Ademe, Total, and PSA attempted to separate the effects of latent Heat Of Vaporization (HOV) from RON and MON by exchanging Ethyl Tert-Butyl Ether (ETBE) for ethanol in a fuel matrix at matched RON. It was estimated that 30-60% of the knock-limited load gain benefit of ethanol blends at matched RON was from their increased latent HOV, which reduces charge temperatures. These studies were performed on a downsized boosted single-cylinder engine with DI. Nakama [272] of Suzuki Motor Corporation, together with Kusaka and Daisho of Waseda University, showed that splash blends of ethanol in a ternary mixture of iso-octane, n-heptane, and toluene gave significant knock benefits: 20% of ethanol allowed a 5-10° KLSA improvement on a 0.33 L engine with compression ratios ranging from 9:1 to 15:1. An alternative approach to knock mitigation with conventional gasoline was through the addition of fuel reformate (CO and H_2). This was being studied by Topinka et al. [273] at MIT with a 15% simulated reformate giving an 8° improvement in KLSA on a single-cylinder pent-roof engine.

Swarts et al. [274] at the University of Cape Town and Sasol Technology Research and Development investigated what the RON and MON tests actually measured by instrumenting a CFR engine with a cylinder pressure transducer and an exhaust gas oxygen sensor. Testing was performed in RON-like conditions but with a fixed relative AFR $\lambda = 0.9$. It was noted that changes in the burn rate could be seen on pressure and MFB curves before knocking oscillations were observed. It was suggested that the standard knockmeter responds to these burn rate variations. This problem had also been noted in the 1960s by Hoffman [117].

Chemical kinetics were frequently employed in simulation environments. Some employed simple techniques, such as that used by Elmqvist et al. [275] of Fiat-GM Powertrain, the Royal Institute of Technology, and Shell. Their approach was based on Livengood-Wu/Douaud-Eyzat methods to enable a closed-loop controller on knock in a 1D simulation environment. Noda et al. [276] of Nissan used a reduced mechanism from LLNL, with 99 species and 462 reactions, to study the cause of knock at the beginning of vehicle accelerations. This was found to be due to a spike in temperatures in the intake system. The mechanism was for PRF fuels, and it was stated that a chemical kinetic model for real gasoline was not available. Yates et al. [277] of the University of Cape Town and Sasol Advanced Fuels Laboratory fitted chemical kinetics calculations with thousands of reactions using a three-stage Arrhenius model. The total ignition delay is expressed as shown in Equation 16.

$$\tau_{overall} = \left[\left(\tau_1 + \tau_2 \right)^{-1} + \left(\tau_3 \right)^{-1} \right]^{-1} \qquad \text{Eq. (16)}$$

Figure 39 compares the ignition delay map for iso-octane based on the fit terms of Yates et al. to that which results from Douaud and Eyzat's CFR-based approach using the same fuel. The single-Arrhenius fit of Douaud and Eyzat, of course, cannot describe the NTC region, which is clear in the correlation of Yates et al. In the high-temperature region, the models

FIGURE 39 Stoichiometric ignition delay for iso-octane based on triple-Arrhenius approach of Yates et al. [277] compared with Douaud and Eyzat's [158] single-Arrhenius method recalculated from CFR data at maximum knock AFR.

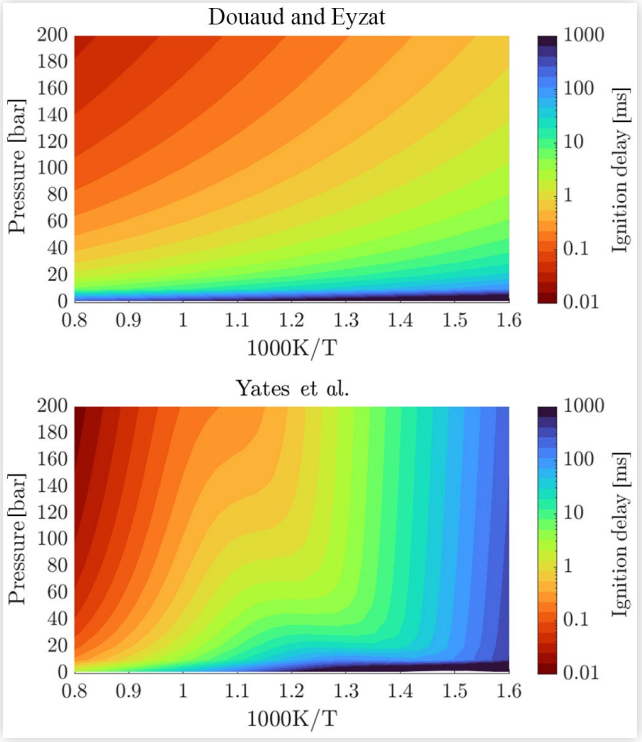

Data taken from Refs. [277] and [158]. © SAE International

give more similar results. For example, using a temperature of 1010 K and a pressure of 22 kgf/cm^2 (a reference point from Douaud and Eyzat's original paper), their formula gives 2.9 ms while that of Yates et al. results in 1.6 ms. Commercial gasolines tend to have a smaller NTC region than iso-octane, but care should, in any case, be taken in describing their characteristics by a single Arrhenius fit. Of course, many more data points would be required to fit three Arrhenius functions to the engine data in comparison to the Douaud and Eyzat approach. Fitting to the engine data also requires significant assumptions to be made regarding end-gas temperature and homogeneity. Two papers were published by Polytechnic University of Milan on detailed kinetic models in this period. The first paper by Mehl et al. [278] was with 250 species and 5000 reactions. This was implemented in a two-zone model, but it was possible to account for temperature stratification in the crevices. The model was correlated against data of critical compression ratios in PRF testing on CFR engines. A successive activity described by D'Errico et al. [279] used a quasi-dimensional approach with 300 species and 6000 reactions. A transparent piston engine was tested with UV optical measurements for OH and HCO. HCO was shown to precede OH and was a result of HCHO decomposition. A simpler kinetic scheme with 32 species and 55 reactions was used by Bozza et al. [280] at the University of Naples "Federico II," again in a quasi-dimensional model. Here cyclic variability was introduced through random variations of flame kernel duration and radius, AFR,

residuals concentration, and intensity. The quasi-dimensional simulation of combustion was also performed by Hattrell et al. [281] at the University of Leeds and Mahle Powertrain. This was used to evaluate burn rates for various knock reduction strategies. While 30% enleanment and 15% EGR gave similar BSFC benefits, the combustion stability was poorer for the lean case. It was calculated that lean running results in a lower Damkohler number than the use of EGR, and hence a greater risk of local quenching and poor combustion stability. Liang et al. [282] at the University of Wisconsin-Madison used the so-called "G-equation" model in KIVA-3 3D CFD code to model turbulent combustion, combined with a chemical kinetics mechanism in CHEMKIN software for iso-octane with 22 species and 42 reactions. This was benchmarked against experimental activity on a 12:1 compression ratio GDI SI engine with excellent agreement observed. Eckert et al. [283] of the same research group had published on knock simulation using the Shell kinetics model, again in KIVA-3, some years earlier. A "discrete particle ignition kernel" model was used. Good agreement was found in comparison to engine data and pressure oscillations were also reproduced. Corti and Forte [284], of the University of Bologna, also used KIVA-3 but with the alternative Extended Coherent Flamelet Model (ECFM) for turbulent flame-front propagation and a simpler kinetic approach based on the Shell mechanism. Experimental activity on the same FIAT 1.2 L engine then showed that knocking cycles could be identified based on their net heat release, which was lower due to the increase in heat transfer due to knock.

Coupled 3D simulations were also being applied to water jacket optimization in an effort to improve knock limits. Kleeman et al. [285] at IFP and Renault used FLUENT for water jacket simulation coupled with KIVA-2 combustion modeling using the Douaud knock model. The influence of local cooling on knock could therefore be investigated. It was noted that cooling of the exhaust valves did not result in a change in autoignition location in comparison to cooling of the liner—knock remained under the exhaust valves in both cases. In the same year, Shih et al. [286] of Honda Research and Development (R&D) performed simulations of the water jacket of a V6 engine using STAR-CD software. An experimental approach with thermocouples and knock limit measurements was used to confirm the simulated improvements in knock from increased cooling of the central cylinder of each bank.

There was renewed activity on prechamber engines in a number of countries. Couet et al. [287] of the University of Orleans presented the so-called APIR concept, meaning "Self-ignition Triggered by Radical Injection." A rich prechamber was used together with small holes, which caused quenching of the reaction products and, hence, seeded radicals into the main combustion chamber. This resulted in distributed ignition sites in the main chamber, far from the prechamber itself, as evidenced by combined laser sheet tomography and direct visualization. Kettner et al. [288] at the University of Karlsruhe with Kuhnert and Latsch of Multitorch published on a passive prechamber spark plug where a rich mixture was introduced from a small bowl in the piston into the prechamber late in the compression stroke. This was known as the BPI concept. Full-load combustion phasing could be improved by 5°CA in comparison to the same engine with a conventional spark plug. Kuhnert and Latsch [289] also published a paper, together with Getzlaff and colleagues at Ingenieurgesellschaft Auto und Verkehr (IAV), on a prechamber with pilot injection. A single-stroke engine with optical access was used together with a filtered ICCD camera to capture OH radiation. It should be noted that prechambers were already common on large gas engines, as documented by Kawabata and Mori [290] of Tokyo Gas Company and Winter et al. [291] of Graz University of Technology. Prechamber research was also undertaken at the University of Melbourne by Toulson, Watson, and Attard [292]. A fueled prechamber was added to a CFR engine in the side of the chamber (the normal spark plug location). Various fuels were compared both for the prechamber and the main chamber. Chemical kinetics calculations were integrated in 3D CFD and compared to optical results. The main chamber and prechamber lambda were also varied. Best results were obtained with a rich prechamber mixture and H_2 as the prechamber fuel. It was possible to run to a relative AFR as lean as $\lambda = 5$. Interest in prechambers for both lean limit and knock limit extension would increase in the following decade.

The 2010s: Aggressive CO_2 Targets, Electrification, and Downsizing

The number of publications on knock has increased significantly in the last 10 years. This is largely driven by greater pressure on manufacturers to reduce fleet average CO_2 emissions. While for a period diesel was seen as an appropriate means to achieve this, at least in Europe, the Volkswagen diesel emissions scandal of 2015 [4] led to a crash of the diesel engine car market and, hence, manufacturers having to make significant improvements in gasoline-powered vehicle CO_2 in order to meet their targets. Downsizing enables the reduction of pumping losses and friction on emissions drive cycles by increasing engine load for a given vehicle power requirement. This higher load increases the risk of knocking, however, particularly at high output.

Cooled EGR was widely studied once again. It gives efficiency gains through lower peak cylinder temperatures and hence lower heat losses and dissociation, an increase in specific heat ratio, and a knock limit improvement. It also reduces flame speeds, however, and so the quantity of EGR that can be tolerated is limited by combustion stability. Hoepke et al. [293] of MIT proposed a modification of the Douaud and Eyzat ignition delay expression to account for EGR and to calculate an equivalence of EGR and octane number. Every 10% of EGR was found to have a similar effect to a 3% improvement in octane. Alger et al. [294], at Southwest Research Institute, evaluated EGR and octane interactions with fuels

of RON 91 up to RON 109. As much as 30% of EGR could be tolerated on an engine with a tumble ratio of 1.5 and fine electrode spark plugs with a large gap. A somewhat higher sensitivity was found in comparison to the MIT work. Every 1% of EGR was equivalent to a 0.5-0.75 improvement in octane number. EGR from stoichiometric combustion is largely composed of CO_2, N_2, and H_2O, but will also contain traces of other substances, particularly if taken upstream of a catalytic converter. Of these, NO is of particular interest as it may worsen the knock limit as had already been shown in the previous decade. Investigations on its effect continued at the University of Leeds where Roberts et al. [295] compared synthetic EGR with and without NO for PRF, TRF, and full boiling range blends. The results implied that NO was detrimental to knock for fuels with little NTC region, but could give an improvement on PRF 90. Of course, EGR does not necessarily have to come from stoichiometric combustion, and researchers at Southwest Research Institute demonstrated a "Direct-EGR" engine, where one cylinder ran rich and is exhausted to the inlet manifold of the other three cylinders of a four-cylinder engine. This meant that the EGR was high in CO and H_2, and therefore the normal issues of reduced flame speed and poor combustion stability were mitigated. Every 10% of enrichment in the EGR producing cylinder gave an octane improvement of 1.8 units. The EGR cylinder began to run into rich stability issues, however, at equivalence ratios $\phi > 1.3$ as described by Algers et al. [296]. Szybist et al. [297] of Oak Ridge National Laboratory commented that turbocharged engines were increasingly popular in the USA, with the market having increased from 3% in 2006 to 25% in 2016. The effectiveness of EGR at high loads (up to 19 bar IMEP) was studied, and it was found that, at high pressures and low temperatures, EGR did not significantly improve ignition delay time. In 2019, Sjöberg et al. [298] of Sandia National Laboratories performed a further investigation on the effect of NO in EGR gas. Skip firing was used to clean the test engine of residual NO, and then synthetic EGR and bottled NO were added in a range of concentrations on different fuel types. The NO response curve in terms of knock-limited combustion phasing was confirmed to be significantly different for different fuel types. While for alkylate fuel (low Sensitivity) knock strongly worsened in the range 0-40 ppm, and then the effect gradually diminished; for all other fuels, NO had a smaller detrimental effect up to 500 ppm. With aromatic fuel, the effect was slight. Interestingly, a correlation was found between the peak pressure of the preceding cycle and NO concentration in residuals—this gives a prior-cycle effect in terms of knock, even though the cyclic variation in knock is normally considered to be random. Cooled EGR was used together with twin-stage boosting, a high tumble intake port, and DI on the heavily downsized "Ultra Boost" engine. This was a collaboration between Jaguar Land Rover, GE Precision Engineering, Lotus Engineering, Shell Global Solutions, CD-adapco, the University of Bath, Imperial College London, and the University of Leeds as described by Turner et al. [299]. The target was to replace a 5.0 L V8 engine with a 2.0 L unit, achieving the same torque curve but with a reduction in drive

FIGURE 40 Knock implications of PFI and GDI fueling strategies at 2000 rpm on "Ultra Boost" project engine [299].

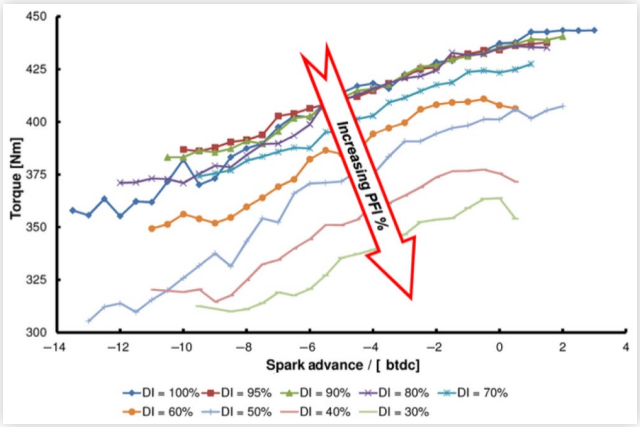

Reprinted with permission from Ref. [299]. © SAE International

cycle fuel consumption of 35%. The engine had a compression ratio of 9:1 but could run at over 32 bar BMEP at 3500 rpm in stoichiometric conditions, even without EGR, with RON 97 E5 gasoline. EGR and enrichment were used at higher speeds. The engine featured both PFI and GDI fueling systems, and testing showed that the knock limit improved as the proportion of fuel injected directly into the cylinder increased, as shown in Figure 40.

Dilution has a detrimental impact on combustion speed and stability as it reduces laminar flame speed. One of the main ways of compensating for this is with increased turbulence. The intake port design is key in achieving this. It had already been demonstrated in the 1980s that high tumble ports resulted in improved turbulence and higher flame speeds. A high tumble port may, however, also generate strong secondary motions, such as cross tumble, omega tumble, and swirl. Cyclic variability in the flow structures may have a detrimental impact on combustion stability and knock. This was examined using high-speed Particle Image Velocimetry (PIV) by Adomeit et al. [300] of FEV in 2011. Testing was performed on a motored engine rig with a transparent liner. Peak tumble ratios from 2.4 to 5.8 were investigated. A solid-state Nd:YLF laser and a high-speed CMOS (Complementary Metal Oxide Semiconductor) camera allowed a frame rate of 6000 Hz at a resolution of 1024 × 992 pixels. Imaging was in both the tumble and cross-tumble planes. It was found that ports that gave higher tumble intensities also gave higher cyclic variability in the cross-tumble plane. This would also likely lead to higher cyclic variability in combustion. The optimum port design is therefore a trade-off. Flow measurements in engines had generally been either point based (such as hot-wire anemometry) or planar (such as PIV) up until this point. Baum et al. [301] of the Technical University of Darmstadt, together with LaVision, published on tomographic PIV in 2012. This allowed the 3D flow field in an engine to be interrogated directly for the first time. The technique required the use of four CCD cameras simultaneously. The measurement volume in the region of the tumble plane had dimensions of 47 × 35 × 4 mm.

Such tools can be used to calibrate 3D CFD models of charge motion, which can then be used to screen intake port geometries in a software environment. One of the main inlet port trade-offs studied in CFD is the relationship between tumble and volumetric efficiency. Tumble is normally generated by biasing more flow over the upper edge of the valve and less over the lower side. This is generally achieved by having a large included angle between the intake valve axis and that of the inlet port and/or through shrouding of the lower part of the intake valve. This reduces the effective valve curtain area and, hence, is detrimental to filling efficiency. This is particularly important for NA engines where volumetric efficiency cannot be compensated with increased manifold pressure. The optimization of the tumble/flow trade-off was described by Yoshihara et al. [302] of Toyota in 2016. Both the inlet port-to-inlet valve angle and the inlet port-to-exhaust valve angle were found to be important in order to generate efficient tumble. Tumble efficiency was defined as energy transformed into generating tumble normalized by extra pumping work due to intake flow restriction. Stroke-to-bore ratio is also a key design decision to be made when designing a new engine and was shown to be a trade-off by Itabashi et al. [303] of Toyota in 2017. Low stroke-to-bore ratios mean large valves can be fitted, which improves volumetric efficiency and hence specific output for a given manifold pressure. Mean piston speed is reduced, which helps limit friction. Large stroke-to-bore ratios, on the other hand, mean small flame travel distances and high mean piston velocities (driving turbulence), and hence fast combustion. EGR tolerance, knock, and thermal efficiency are therefore improved. The trade-off in intake port design is shown in Figure 41 and that of stroke-to-bore ratio is shown in Figure 42. The optimized NA engine achieved a maximum thermal efficiency of 40% with a compression ratio of 13:1 and 61 kW/L specific output.

While tumble can help improve early burn rates in dilute mixtures, the ignition system may also require development. High tumble ports can promote significant residual charge motion at ignition timing. This may result in excessive velocities across the spark plug. It is generally desirable to mount the spark plug ground electrode in a cross-flow orientation in comparison to the residual flow. This promotes the extension of the discharge channel out of the plug gap, which therefore increases the discharge channel surface area and reduces the heat losses to the electrodes. Suzuki et al. [304] in 2016 described how flow velocities in excess of 30 m/s could however lead to misfire. The discharge channel is overly extended, leading to a short-circuiting or blow-off behavior. This may mean inadequate time for the discharge channel to produce a self-sustaining flame kernel in the surrounding mixture. Small flame kernels with low laminar flame speeds also may not survive in highly turbulent environments. Suzuki was the co-author of a subsequent paper on the theme by Hayashi et al. [305] of Denso and Toyota the following year. Here discharge current sensitivities were further examined. Examples of blow-off and short-circuiting were shown with optical analysis as can be seen in Figure 43 [305]. Restriking can be reduced and the flame kernel encouraged to grow by

FIGURE 41 Tumble efficiency sensitivity to exhaust valve/inlet valve included angle θ_1 and inlet port/inlet valve included angle θ_2 from Itabashi et al. [303].

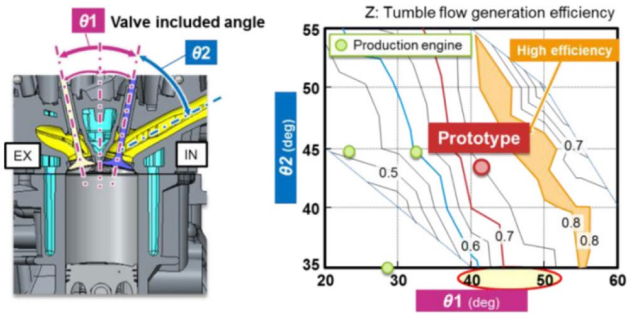

Reprinted with permission from Ref. [303]. © SAE International

FIGURE 42 Stroke-to-bore ratio trade-offs, from Itabashi et al. [303].

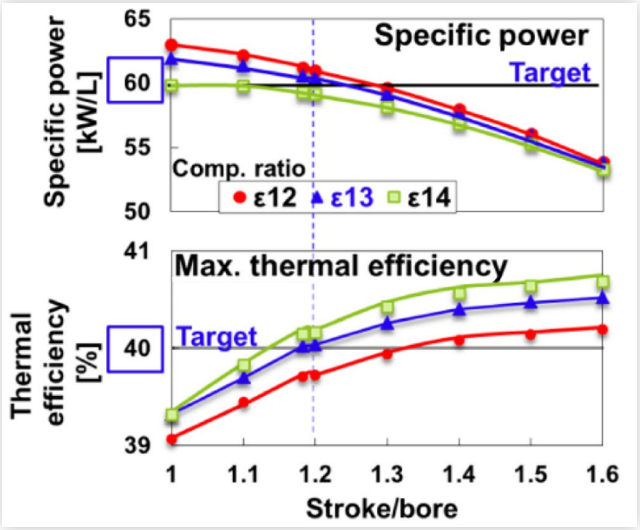

Reprinted with permission from Ref. [303]. © SAE International

FIGURE 43 Blow-off and short-circuiting of SI discharges in a high-velocity flow field, from Hayashi et al. [305].

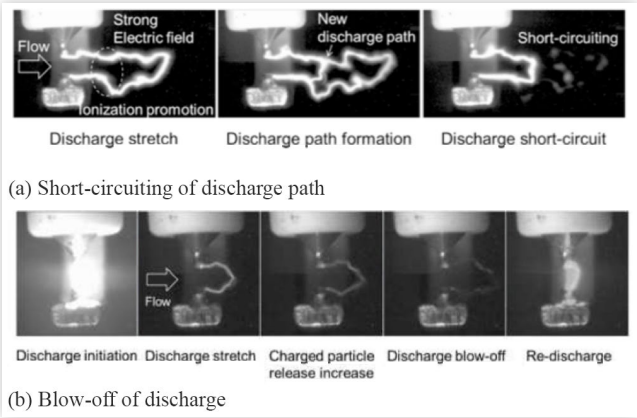

Reprinted with permission from Ref. [305]. © SAE International

maintaining adequate discharge current for an extended period. A conventional ignition coil produces a descending discharge current profile following breakdown. A constant current profile, realized by closed-loop control, allowed blow-offs to be suppressed and the lean limit to be extended by 15% at lower energy expenditure than for a conventional high energy system. While large spark gaps may help to improve ignitability through extension of the discharge channel length and reduced heat loss from the early flame kernel to the electrodes, on highly boosted engines gap size may be limited by maximum sustainable breakdown voltages. A limit of around 36 kV for M10 size spark plugs was identified by Corrigan et al. [306] of Ferrari in the testing of a highly boosted single-cylinder engine for Formula 1 research. A gap size of 0.8 mm allowed sparking at up to 50-60 bar cylinder pressure while a gap of 0.6 mm permitted sparking up to almost 80 bar. This came with a combustion stability penalty however. Alternative ignition systems have been demonstrated to improve dilution tolerance. One of these is the Corona Ignition System, which has been shown by a number of researchers to give benefits, including Idicheria et al. [307] of GM. This allowed halving of the COV of IMEP at an AFR of 26:1 when tested against a conventional coil and plug ignition setup. Nonthermal transient plasma ignition systems have also been described by Singleton et al. [308] of Transient Plasma Systems, together with collaborators at Sandia and Argonne National Laboratories. The EGR limit could be improved by 3-6% in comparison to a conventional ignition system. Neither of these systems has yet to come to market, however, with primary focus remaining on the development of ignition coil and spark plug-based systems to improve dilution limits.

EGR may be an effective solution on vehicles of low to medium power output, but for a high-performance vehicle, it is not considered appropriate, as the heat rejection requirements of an EGR cooler in this horsepower range are difficult to manage in terms of vehicle packaging. Water injection is seen as an interesting alternative. A pioneering rediscovery of the potential of water injection to mitigate knock was proposed by d'Adamo et al. [309] of the University of Modena in 2015. A number of papers were presented on the subject at the Fifth International Conference on Knocking Combustion in Berlin in 2017. Hermann et al. [310] of Opel gave an overview of the possibilities, which include plenum water injection, Port Water Injection (PWI), mixed Gasoline/Water Direct Injection (GWDI), and Direct Water Injection (DWI). The primary motivation is to increase stoichiometric power on downsized engines. The DI systems gave the best performance, but would be most costly to introduce in production. Plenum injection performed poorly whereas PWI was seen as a good compromise. Heinrich et al. [311] of Trier University of Applied Sciences performed a number of comparisons of PWI and GWDI systems. The GWDI system was shown to give significant reductions in preignitions. Hunger et al. [312] of IAV, together with collaborators at Daimler, showed the benefits of the DWI system, including the possibility of phasing the water injection timing to maximize the end of compression temperature reduction. Both Ferrari and Porsche

FIGURE 44 Combustion stability limitations of combining early intake valve timing and high water injection quantities, from Paltrinieri et al. [313].

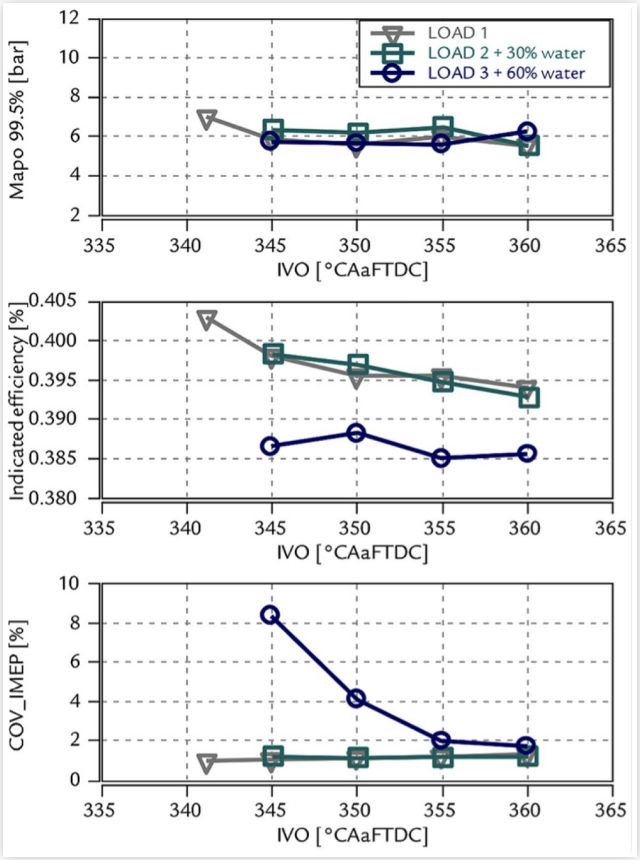

presented an activity on water injection at the 2019 SAENA ICE conference in Capri. Paltrinieri et al. [313] of Ferrari presented experimental activity with PWI on a boosted single-cylinder research engine, complemented by CFD and chemical kinetics calculations. Limits to knock mitigation synergies of EIVC and water injection were evidenced, with combustion stability eventually suffering, as shown in Figure 44. Vacca and Bargende [314] of the University of Stuttgart, together with collaborators at Brandenburg University of Technology and Porsche, presented a simulation approach to validate various water injection strategies. Chemical kinetics were included in CONVERGE 3D CFD software, and the Bradley detonation diagram was used to interpret results. CFD was supported by experimental activity on a transparent research engine where both PWI and DWI strategies were trialed. It was found that although the DWI system gives a better knock-limited combustion phasing, exhaust temperatures were lower for the PWI system due in part to more homogeneous water distribution. Other researchers have employed a purely simulation-based approach. Franken et al. [315] in 2020 used detailed chemistry in a quasi-dimensional Stochastic Reactor Model (SRM), together with a Bradley diagram interpretation, to investigate the efficacy of water on knock suppression for

a range of fuels. A RON 90 fuel with a 50-80% water-to-fuel ratio was calculated to be similar in terms of knock resistance to RON 100 gasoline.

Chemical kinetics is now routinely applied in CFD. Whereas, in the past, dedicated chemistry solvers, notably CHEMKIN [316], needed to be coupled with 3D CFD code; modern CFD packages such as CONVERGE [317] and STAR-CCM+ [318] have integrated chemistry solvers. While many surrogate reaction mechanisms have been widely applied over an extended period in ICE research, with perhaps the most obvious example being the historic Shell mechanism, updated mechanisms for even the most basic surrogate of gasoline—pure iso-octane—are still being published. Atef et al. [319] documented an improved iso-octane mechanism as recently as 2017. This was a large-scale collaborative effort with authors from King Abdullah University of Science and Technology, the University of Connecticut, National University of Ireland Galway, and LLNL. Primary validation data from rapid compression machines and shock tubes was in the range of 20-40 bar pressure and 632-1060 K temperature. Pressure conditions in the engine end gas will routinely be significantly higher than this in a full-load operation of modern downsized engines. One approach is to extrapolate trends to cover ranges beyond that of the rig experiments. Another is to apply a theoretically based ab initio approach. A review of the current status of "theory-informed chemical kinetics models" was given by Miller et al. [320] in 2020. Once again this was a large-scale collaborative study with researchers from Argonne National Laboratory, Brown University, Columbia University, Sandia National Laboratories, the University of Colorado Boulder, the Technical University of Denmark, and Southeast University, Nanjing. More theoretically based reaction modeling will undoubtedly have an impact on knocking analysis in ICEs in the coming years.

The Miller cycle allows improvements in the knock limit without the necessity for additional cooling circuits or fluid systems. However, it is detrimental to volumetric efficiency. It has been a key area of research and application in the last 10 years. While the original Miller concept is based on EIVC [79], a similar effect can be achieved with LIVC, as applied by Mazda in the 1990s [225]. A comparison of these two strategies was carried out by Luisi et al. [321] of Centro Ricerche FIAT (CRF) and Polytechnic University of Turin in 2015. EIVC has the disadvantage of reducing in-cylinder turbulence both for the early closing angle and the fact that a reduced lift is also frequently necessary to avoid excessive valve accelerations. In fact, on the 1.4 L PFI test engine with a "MultiAir" Variable Valve Actuation (VVA) system, better knock-limited combustion phasing at 2500 rpm for a given turbine inlet temperature was recorded for the LIVC strategy, as shown in Figure 45. This gain also translated into a relative reduction in component protection overfueling. Such results depend somewhat on the base combustion system of the engine where testing is performed. A large-scale project was undertaken by Ketterer et al. [322] of GM studying EIVC and LIVC strategies with dedicated combustion systems for each. Here it was found that at peak power, the EIVC system had an advantage in terms of end of compression temperatures, and hence knock-limited combustion phasing, as it was more difficult to control the backflow of the LIVC concept at higher speeds.

FIGURE 45 Comparison of EIVC and LIVC Miller strategies on a 1.4 L VVA engine at 2500 rpm and 19 bar BMEP by Luisi et al. [321].

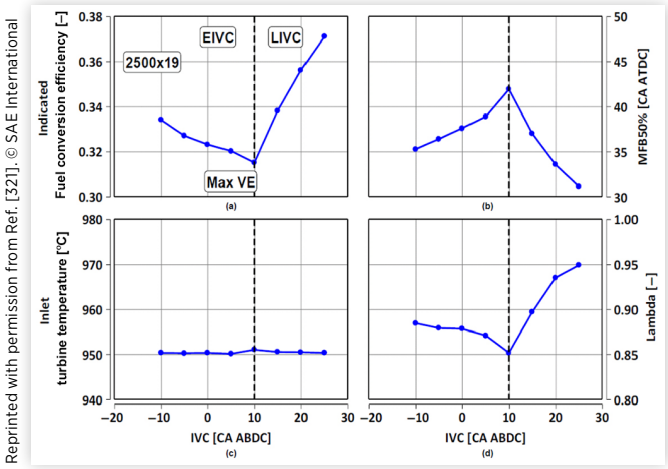

Reprinted with permission from Ref. [321]. © SAE International

Gas dynamics tuning has long been known as a method of increasing the volumetric efficiency of high-performance NA engines, and a detailed discussion was given by Blair of Queen's University Belfast in his book published in 1999 [323]. Finite amplitude wave reflections are harnessed in order to increase mass flow in the intake system and pressure at the intake valve, in particular in the intake ramming period between Bottom Dead Center (BDC) and IVC.[16] The increased pressure before IVC, however, also means increased temperature with respect to plenum conditions. This hot charge is ingested by the cylinder, and of course, this increases the risk of knock. Such "positive" tuning is normally reserved for high-speed, high-performance NA engines where knock is unlikely to occur. In 2012, Taylor and collaborators at Mahle investigated tuning effects on a downsized turbocharged gasoline engine [324]. The standard turbocharged engine method "inert tuning"—use of very short intake runners to avoid wave action—was compared to conventional intake tuning for increasing volumetric efficiency and "anti-tuning," where the goal was to have low pressure at IVC. This last option means

[16]While filling/emptying isentropic models are frequently applied at the intake valve, flow in the intake ducts depends on the pressure of oppositely moving waves in the intake system, each contributing to particle flow. The basic equation is shown in Equation 17, where c is the particle velocity, a_0 is the acoustic velocity for undisturbed conditions, p_0 is the pressure at undisturbed conditions, p is the pressure of the wave, and γ is the ratio of specific heats. This needs to be applied separately for superimposed waves in opposite directions calculated in unsteady gas dynamics code while only the superposition pressure can be measured experimentally [323].

$$c = \pm \frac{2a_0}{\gamma - 1}\left[\left(\frac{p}{p_0}\right)^{\frac{\gamma-1}{\gamma}} - 1\right] \qquad \text{Eq. (17)}$$

that the intake valve is open during an expansion in the intake system, and hence local gas temperature will also be lower than plenum conditions. It can therefore be considered a sort of gas-dynamics Miller cycle, and in fact, a 5% improvement in BSFC was obtained at high speed and load. The disadvantage is that volumetric efficiency decreases, as per an EIVC or LIVC Miller approach, and also that intake lengths of over one meter would be required for effective anti-tuning at 5000 rpm.

Prechamber research for automotive applications has increased in recent years. A large-scale literature survey was performed in 2010 by Toulson and Schock of Michigan State University, together with Attard of Mahle Powertrain [325]. Toulson and Attard had previously researched prechambers at Melbourne University. In the review, prechambers were classified based on the presence of auxiliary fueling and volume as a percentage of clearance volume. The survey went back to 1918, and the Ricardo Dolphin engine mentioned in his 1921 paper and already cited in the present work [6]. Attard published extensively on prechambers in the following years, with colleagues at Mahle Powertrain, both on lean combustion with an actively fueled prechamber [326, 327, 328, 329] and highlighting the knock gains even for stoichiometric conditions and passive prechamber technology [330]. In this last work, testing was performed on a modern PFI engine with a pent-roof combustion chamber based on a GM Ecotec LE5 design. At Maximum Brake Torque (MBT) ignition timing, a PRF 96 blend with conventional SI corresponded to PRF 86 with the prechamber igniter, as shown in Figure 46. While there has been a lot of activity since then by a large number of universities, research organizations, and car companies, it was not until 2020 that a manufacturer would once again prepare to go into production with a prechamber engine. The manufacturer was Maserati. Its engine also features an additional spark plug in the main chamber as described in the patent by Mazzoni et al. [331]. It produces 210 CV/L (154 kW/L) and has a compression ratio of 11:1 [332]. The secondary plug is shown mounted laterally in the combustion chamber in the patent application. An alternative layout with a secondary spark plug arranged in a manner to guarantee that "spark-coupled" injection strategies can still be used in catalyst heating was patented by Corrigan et al. [333] of Ferrari later the same year.

Research of CAI continued with increasing interest in Spark-Assisted CAI techniques. Yun et al. [334] of GM used spark assistance to extend the maximum load limit of a stoichiometric EGR CAI engine. This relied on both external EGR and adjustable negative valve overlap for adequate dilution and charge temperature management. As had been observed by previous researchers, consuming part of the charge by flame-front propagation resulted in an extended overall burn duration, and hence lower ringing noise. Manofsky et al. [335] also used a negative valve overlap strategy combined with external EGR and spark assistance to study stoichiometric load extension on an HCCI engine. The engine had a compression ratio of 12.5:1 and DI. 7.5 bar IMEP was reached before knock began to occur. Up until that point, the ringing intensity was well below the limit value. The operating map achieved is shown in Figure 47. Alternative techniques exist to extend HCCI load limits without

FIGURE 46 Knock limit benefits in terms of combustion phasing (CA50) and octane for a passive prechamber system, from Attard et al. [330].

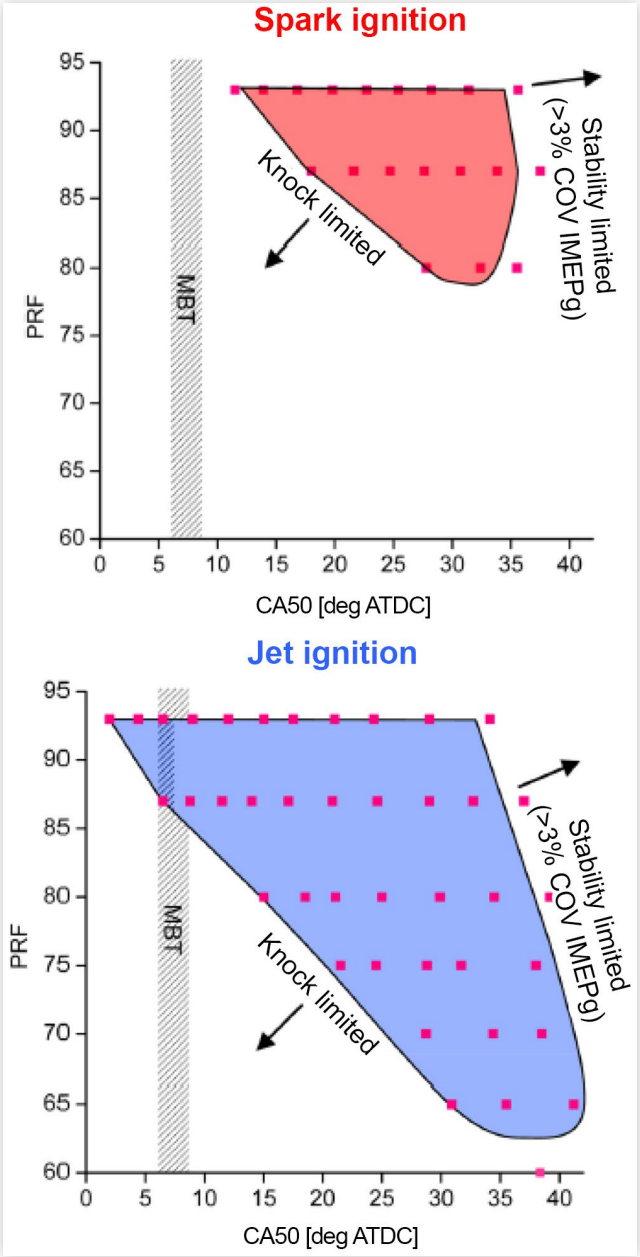

knocking. A combination of boost and 60% EGR allowed Dec et al. [336] of Sandia to demonstrate 16 bar IMEP. Even if knock does not occur, ringing combustion is a problem with HCCI, and hence, much activity was carried out to connect pressure waves to heat release. Maria et al. [337] of MIT used cylinder pressure measurements and microphone analysis to correlate acoustic and combustion data. A correlation between pressure oscillation amplitude Δp and maximum pressure rise rate $\frac{dp}{dt}$, originally demonstrated by Eng [246], was modified to account

FIGURE 47 HCCI and SACI operating ranges from Manofsky et al. [335].

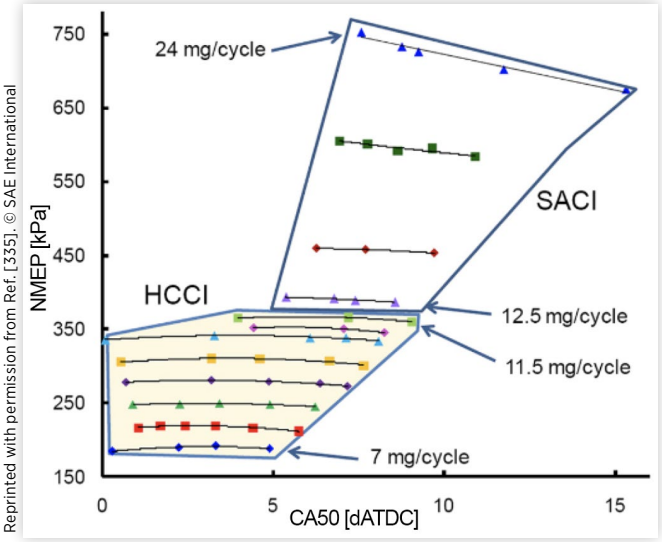

for expansion work from the initial autoignition event. This gave a consistent proportionality constant $\beta = \Delta p / \frac{dp}{dt}$ over a wider range of operating conditions than the original Eng correlation. The transition from controlled HCCI to knock was studied by Iijima et al. [338] of Nihon University. It was found that knocking intensity was correlated with time-based maximum pressure rise rate in experiments on an optical access HCCI engine. For non-knocking combustion, multiple autoignition events took place over around 5°CA at 1200 rpm. For knocking combustion, a large end-gas region was seen to ignite with a reaction front at around 540 m/s. In further measurements the following year [339], autoignition fronts at up to 1200 m/s were seen. Strong light emission from the CO-O reaction was observed at maximum pressure rise rate. A very strong knock resulted in higher excitation of the second transversal acoustic mode of the combustion chamber.

In 2019, a CAI engine finally made production. This was the Mazda Skyactiv-X engine that was described at the *28th Aachen Colloquium on Automobile and Engine Technology* by Nakai et al. [340]. It has a compression ratio of 16.3:1 and is supercharged. The engine appears to function in a manner similar to that described by Urishihara et al. of Nissan in 2005, although it features only GDI fueling rather than a combined PFI/GDI setup. The engine transitions from HCCI to SACI to conventional SI as load is increased. A piezoelectric cylinder pressure transducer is used as the feedback device to manage the combustion process. The model-based control system predicts both flame propagation and end-gas conditions. A 700 bar centrally mounted GDI system together with controllable swirl can be used to control mixture distribution, and hence end-gas cooling. Depending on the operating regime, the engine can run stoichiometric, lean, or lean with EGR. In some operating points, it has a better BSFC than the company's diesel engine.

Ethanol, which had been shown to be effective against knock by Ricardo in the 1920s [6], has again been investigated by a number of researchers in recent years. Ethanol from biological sources is potentially carbon neutral, and a further impetus for its use on the US market was with a view to greater US energy independence, as described by Kasseris and Heywood [341] of MIT. Ethanol also has a much higher latent HOV in comparison to typical non-oxygenated HCs used in gasoline blends. For stoichiometric mixture with air, it is four times higher than gasoline. This gives improved charge cooling, particularly on DI engines. Kasseris et al. showed that with a DI engine, this charge-cooling benefit was almost linear as ethanol was added to premium gasoline, with a RON of 97, up to the maximum concentration tested of 85%. The chemical octane benefit may saturate at 30-40%. Ethanol as fuel was also being tested by Steurs et al. [342] at the Swiss Federal Institute of Technology at the time, and comparisons were made to a number of ignition delay models in the literature [343]. A large-scale investigation was carried out by Leone [344] and colleagues at Ford, in collaboration with AVL, on a modern 3.5 L turbocharged GDI engine. Both "splash blends" (where ethanol was added to an existing gasoline in various concentrations) and "matched blends" (same RON and similar MON) were tested for E10, E20, and E30 fuels. Testing was performed both at the standard compression ratio of 10:1 and at increased compression ratios. Only marginal gains were observed for matched E20 and E30 blends and only for high load and retarded conditions. Adding 10% of ethanol to the existing E10 fuel gives an improvement in RON of six units, however, together with higher sensitivity, allowing a two-point increase in compression ratio. The Lower Heating Value (LHV) of ethanol is significantly less than that of non-oxygenated gasolines, and hence, the compression ratio needs to be increased together with RON in order to arrive at a similar or better fuel economy in terms of Miles Per Gallon (MPG). Chupka et al. [345] at the National Renewable Energy Laboratory performed HOV measurements on gasoline/ethanol blends using two different methodologies. HOV is a function of temperature and reduces to zero as this becomes critical. This is strongly the case for ethanol whose HOV halves from 50°C to 200°C. E20 fuel at 50°C has an adiabatic temperature drop of 28°C in comparison to 21°C for E10. It is not clear how much of this HOV increase is included in the RON result on a CFR engine, where the air temperature is controlled before fuel addition to the intake.

Using methane as a fuel could assist in reducing CO_2 from ICE vehicles, as described by Binder et al. [346] of IAV. Methane can be produced from fossil fuels but also from biological sources or methanation of hydrogen. If hydrogen is generated by electrolysis making use of carbon-neutral electricity, a so-called Power-to-Gas (PtG) "e-Fuel" results. Energy is lost in each step going from electricity to an e-Fuel, and hence, such an approach makes the most sense as a method of storing energy when there is excess grid capacity. Exhaust gas aftertreatment of methane engines is also difficult at low load and cold start. Hybridization and an electrically heated catalyst were suggested to combat this. Methane has better knock resistance than conventional gasoline, however, and

hence, the compression ratio can be increased by around two units by switching fuels. An active prechamber, with an integrated air-assisted fuel injector, was also used in this study to further improve the knock limit, giving the possibility to raise the compression ratio a further two units. A final compression ratio of 17:1 was used with a specific power output of 58 kW/L. The potential of a methane-based ICE was also demonstrated by Stoffels et al. [347] of Ford in collaboration with Continental Powertrain, Luk, and Schaeffler Technologies. Here a strong downsizing approach was taken. A three-cylinder engine of just 1 L capacity achieved 112 kW/L specific output with a compression ratio of 13:1. A 48 V electrically assisted compressor in series with a turbocharger with variable intake geometry was used to give adequate low-end torque and transient response. Similar performance was demonstrated to a 1.5 L turbocharged GDI engine. 5% efficiency was gained from downsizing (largely enabled by methane's improved knock resistance) and a further 12% from the use of a 48V mild hybrid system. Considering the lower carbon density of methane in comparison to gasoline, CO_2 on a WLTC could be reduced by 35% even if the fuel was fossil derived.

Hydrogen can also be used as a fuel, as tested by Ricardo [6] 100 years ago. Its high laminar flame speed allows significant dilution increases in comparison to gasoline, as already demonstrated in that period. Hydrogen also has good knock resistance. The main obstacle to its use is the low density of the gas. This necessitates high-pressure storage or cryogenic solutions, as described by Johnson et al. [348]. Despite tank pressures of 700 bar and the increased efficiency of fuel cells in comparison to ICE, particularly in part-load conditions, hydrogen tank volumes are typically four times larger for a Fuel Cell Electric Vehicle (FCEV) in comparison to gasoline fuel tanks of an ICE vehicle of a similar range. If the hydrogen refueling network is developed in the coming years primarily for fuel-cell vehicles, it may make sense to further evaluate hydrogen also as an ICE fuel, particularly for applications where the engine operates consistently at high loads and/or peak efficiency. An estimated 45% Brake Thermal Efficiency (BTE) was exceeded at 2000 rpm and 13.5 bar BMEP by Matthias et al. [349] of Argonne National Laboratory in 2012. This result was based on measurements on a single-cylinder engine with turbocharger simulation and multicylinder friction estimation. The engine ran at around $\lambda = 3$ for most of the operating range with a compression ratio of 13:1. The engine efficiency map is shown in Figure 48.

Methanol is an alternative energy carrier that has the advantage of being liquid at ambient conditions. It can be created through a number of routes including notably the Fischer-Tropsch process [350]. Another method is the co-electrolysis of H_2 and CO_2. This is a Power-to-Liquid (PtL) e-fuel. Biological pathways are also available. Methanol is a very interesting fuel from a knock point of view with a blending RON value[17] in the range 115-130 [13] and has been used in racing series in the past, notably Indycar. It can be further processed to produce a synthetic gasoline. This gives a so-called "drop-in" solution to reduce CO_2 output from the existing SI vehicle fleet. This approach is being studied by the C3 (Closed Carbon Cycle) Mobility consortium. Over 30 companies are involved including vehicle and engine manufacturers, universities, research organizations, and a major energy company [351].

FIGURE 48 Hydrogen ICE efficiency map, from Matthias et al. [349].

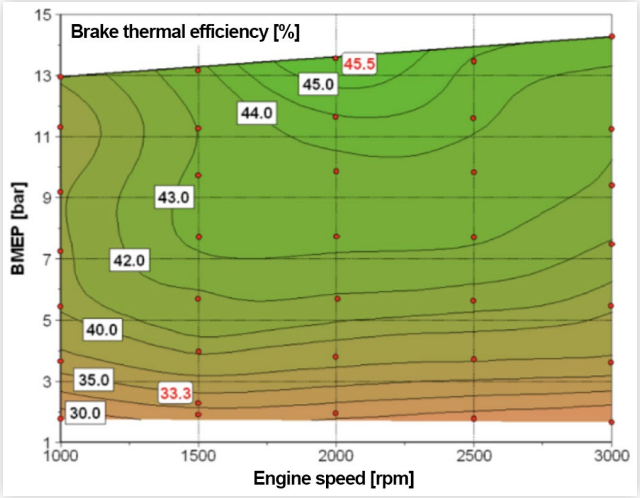

Conventional gasoline is also likely to further evolve in the near future as well. Concawe, a research consortium of many major European energy companies, published two reports in 2020 on the benefits of moving to higher octane fuel. The first of these, by Williams et al. [352], studied the impact of increasing RON on a downsized three-cylinder engine with a compression ratio of 12.2:1 and a maximum BMEP of 30 bar. RON was swept in steps from 95 up to 102. The combustion phasing was improved by around 5°CA of MFB50 (50% MFB) with the highest octane variant, widening the high-efficiency region of the BSFC map. In Real Driving Emissions (RDE) type cycles, fuel efficiency was improved by as much as 4% at the tested compression ratio. Including the gain from compression ratio increases, the estimated benefit was a reduction in CO_2 of around 5% in both emissions cycles and real driving conditions. The additional CO_2 emitted by refineries to produce higher octane fuel must also be taken into account for a Well-to-Wheel (WtW) analysis. A follow-on report by Valdenaire et al. [353] suggested a significant saving in total CO_2 WtW emissions could be achieved if 50% of gasoline sales became RON 102, and engines were adapted to the use of the fuel. This would likely require the greater use of oxygenated fuel components and, in particular, MTBE.

Kalghatgi had introduced his "K-factor" concept in the previous decade. His collaborator, Amer [354] at Saudi Aramco, investigated the K-factor for a matrix of 15 fuels with decorrelated RON and S at up to 3.4 bar absolute manifold pressure on a DI single-cylinder engine with compression ratios of 8.5:1 and 10:1. As boost pressure increased, the

[17]Octane values "blend non-linearly" by volume fraction and individual components often behave differently in combination with others from a knock resistance point of view. Blending of hydrocarbons to achieve a certain octane quality is therefore complex and generally supported by a combination of modeling and trial and error [13].

K-factor was found to decrease as far as −0.93. The temperature at 15 bar compression pressure was suggested as an index to compare to RON and MON conditions. Kalghatgi [355] in 2014 commented that PRF fuels were fundamentally not representative of modern gasolines, and hence, it would make sense to move to an n-heptane/toluene rating scale [355].[18] Kalghatgi showed that typical modern gasolines could be much better matched in terms of RON and S and, as a consequence, in terms of knock-limited performance on a modern boosted engine, with binary toluene/n-heptane blends. A perfect match of RON and S is possible with a three-component surrogate (iso-octane, n-heptane, and toluene). Kalghatgi presented simple formulae to allow calculation of RON and S of such ternary mixtures based on toluene mole fraction [356]. Fitting of such blends was carried out to the Andrae kinetics mechanism, and subsequent quasi-dimensional engine calculations showed good agreement with testing on a PFI single-cylinder engine at 1.6 bar manifold pressure. In 2020, Gail of Shell together with colleagues and collaborators at RWTH Aachen University and Ferrari compared an alternative surrogate formulation to premium RON 98 gasoline in an RCM and a high-performance GDI engine [357]. The surrogate was based on Toluene, n-Heptane, and Iso-Pentane (THIP). It is easier to match fuel vapor pressure using these components than with a traditional TRF blend. Good agreement with the target gasoline was found both in RCM testing and in terms of the knock limit on the engine. A number of chemical kinetics mechanisms were compared to the experimental data including the 2012 LLNL model of Mehl et al. [358]. A simpler model was that of Tsurushima. This was applied by Kitada of Mitsubishi and compared to measurements of a 1.2 L three-cylinder engine with a compression ratio of 13:1 on PRF 95 fuel [359]. In order to match the experimental pressure curve, LTHR had to be taken into account. This was shown to increase the end of compression temperature by almost 100 K. A modified version of the Douaud equation was proposed including a term for equivalence ratio ϕ as shown in Equation 18.

$$\tau = 0.01869\left(\frac{OCN}{100}\right)^{3.4017}\left(\frac{P}{P_0}\right)^{-1.7}\phi^{-1.7}\exp\left(\frac{3800}{T}\right) \qquad \text{Eq. (18)}$$

The Douaud and Eyzat method is based on Arrhenius-like behavior, which can be prone to significant error for fuels with NTC regions. Yates had suggested a method to fit into the ignition delay data of such a fuel using three ignition delay terms instead of one in 2005, as shown in Equation 16 [277]. Fandakov of the University of Stuttgart proposed an alternative approach based on a two-stage ignition with a triple-Arrhenius fit for high temperature and double-Arrhenius fit for low-temperature conditions [360]. This was applied to ethanol containing surrogate blends based on chemical kinetics calculations with 500 species. A larger mechanism was used by Kim of Sandia in 2019 for ethanol-containing blends. This LLNL mechanism featured 2871 species and 12,804 reactions [361]. Surrogates using nine base HCs were used to model alkylate, aromatic, and ethanol blends with a matched RON of 98. It was shown that at high temperatures, E30 had shorter ignition delay times than an aromatic blend, even allowing for charge cooling. LTHR was shown to be most significant for alkylates and least for ethanol. The alkylate fuel was the only one with a true NTC region, although regions of reduced temperature sensitivity were also visible for aromatic and to, a lesser extent, ethanol blends. The effect is that thermal stratification tends to decrease during compression and early combustion for alkylate blends, meaning a more likelihood of autoignition in a cool zone and a greater probability of fast sequential autoignition. This study also compared lean running with EGR in comparison to experimental results. It was shown that lean running did not improve the knock limit, and this was traced to an increase in LTHR and NO, both of which are significantly reduced by N_2 and CO_2 dilution.

Chemical kinetics is now routinely used either directly or in a look-up table form in 3D CFD. In a real engine with cyclic variability, the combustion phasing is generally managed such that knocking cycles are rare. They will typically be faster burning than the average cycle. Reynolds-Averaged Navier-Stokes (RANS) is still the most common 3D CFD approach but results in a prediction of an average combustion cycle. Large Eddy Simulations (LES) fundamentally calculate cyclic variability and, hence, are ideal for knocking investigations but are more computationally intensive. In 2013 Fontanesi et al. [362] of the University of Modena applied LES calculations with detailed chemistry to a high-performance Ferrari road car engine. Ignition delay was taken from pre-calculated look-up tables as a function of pressure, temperature, mixture strength, and residuals. Both the Andrae (138 species) and an LLNL mechanism with 1389 species were applied. A knock margin was defined for each cell in the unburnt range of a number of spark advance angles. Three example cycles are shown in Figure 49. LES was also used to study knock in an ICE by Robert et al. [363] of Institut Français du Pétrole Energies Nouvelles (IFPEN) in 2015 with a particular emphasis on the DDT. Three different spark timings with different corresponding knock amplitudes were simulated. Tabulated kinetics were once again employed. A total of 15 LES cycles were compared to an experimental

FIGURE 49 Three LES cycles showing flame-front progress and autoignition, from Fontanesi et al. [362].

Reprinted with permission from Ref. [362]. © SAE International

[18]Ricardo had suggested in 1922 to use another aromatic, benzene, as the knock-resistant hydrocarbon in the rating scale [6], but in the end, iso-octane became the knock-resistant reference for RON and MON testing as already discussed. At the time typical octane values were in the range 40-60 and fuel sensitivity was also lower [30].

dataset of 500 cycles. A BPF MAPO calculation was performed from 5 kHz to 9 kHz on both experimental and simulation data. A nonlinearity of MAPO against mass burnt by autoignition was observed suggesting a mode transition. Realistic single-cycle reactivity gradients also permitted calculating ξ in order to perform the Bradley correlation. Assumptions had to be made to estimate ε, which depends on local length scales. The analysis, in any case, suggested that many cells were in the developing detonation region for the most advanced cycles simulated. A mathematical function was created to indicate if individual cycles were in the detonation peninsula. This agreed well with direct analysis of the LES data where coupling of autoignition and pressure fronts was observed. Often the DDT did not occur from the first autoignition location of each cycle, meaning that reacting flows must be simulated to evaluate detonation risk.

LES can also be applied to the optimization of in-cylinder flow. As with any other computational technique, it is important to validate the methodology. Ritter et al. [364] of IFPEN compared LES simulations of charge motion and mixture formation in CONVERGE software to high-speed PIV and Laser-Induced Fluorescence (LIF) measurements of an optically accessible DI engine in 2020. A total of 40 PIV cycles were compared to ten cycles in LES. It was remarked that ten LES cycles give a reliable average result, although it was spatially somewhat "noisier" than the average PIV results, as can be seen in Figure 50. In-cylinder equivalence ratio distributions calculated with LES were also well aligned on average to LIF mixture measurements. Here 12 cycles were thought insufficient however to fully capture the real cyclic variability of the process. LES techniques are expected to become increasingly common in industrial environments, driven by improvements in processing power and software. This will enable optimization of cyclic variation in a much more direct manner in CFD than was possible in the past. As knocking cycles are generally the most advanced combustion cycles in a given population, understanding and reducing cyclic variability is key in improving the knock-limited compression ratio that can be used.

A computationally less intensive alternative to LES is to approximate cyclic variability using RANS CFD. Corti et al. [365] of the University of Bologna used calculated variability in equivalence ratio and turbulence in a sphere around the spark plugs of a 599 cm^3 two-cylinder motorcycle engine, taken from RANS CFD, to perturb laminar flame speed and turbulence parameters in the model. D'Adamo et al. [366] of the University of Modena applied PDF of temperature and equivalence ratio in individual cells of a RANS simulation to estimate knocking probability in CFD. This was further developed in a subsequent publication [367]. Breda et al. [368], again of the University of Modena, would tune RANS calculations in STAR-CD software to match the statistically fast-burning combustion profile of knocking cycles obtained on an optically accessible GDI engine.

3D CFD is now a standard combustion development tool, but researchers have continued to work on 0D models due to their computational simplicity, and hence rapid speed.

FIGURE 50 Comparison of average PIV and LES data of in-cylinder flow, from Ritter et al. [364].

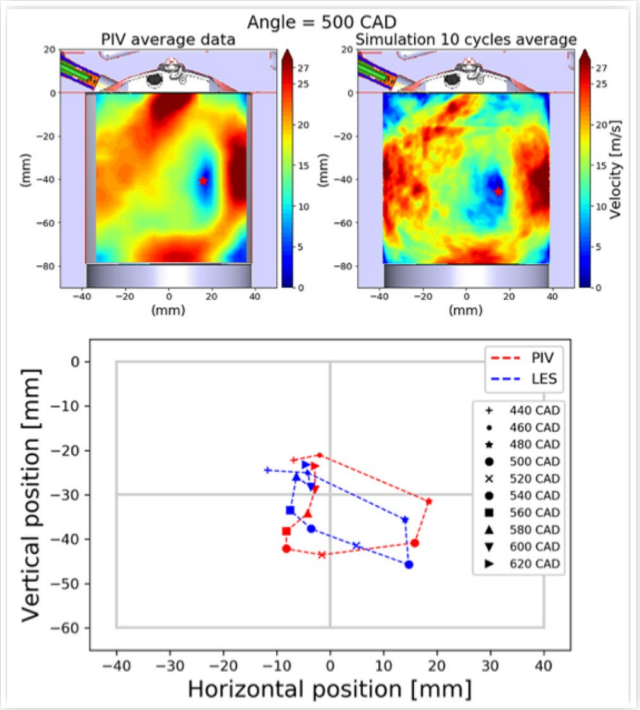

Turbulence and engine geometry effects can still be included, albeit indirectly. Bjerkborn et al. [369] of LOGE AB applied Monte Carlo techniques to a two-zone SRM. Here the mass of each zone is divided into a number of particles. The particles change from unburnt to burnt as the calculation progresses. Flame volume is assumed to be spherical but interacts with the combustion chamber walls. Detailed chemistry from a 200-species PRF mechanism was used both for ignition delay times and laminar flame speed. Kozarac et al. [370] of the University of Zagreb divided the unburnt region of a 0D model into around 20 bins covering a range of thermal stratification of 200 K at each timestep. LTHR was included. A fractal model was used in a 1D code for cyclic variation. Both LLNL and Andrae mechanisms were applied. Good agreement was demonstrated with KLSA of a CFR engine. Bozza et al. [280], of the University of Naples, also applied fractal combustion models in a 1D engine simulation environment in the same year. A starting MFB curve was modified for cyclic variation based on experimental analysis. De Bellis et al. [371], also of the University of Naples, showed how it could be correlated to combustion phasing and duration on a given engine. A three-component surrogate reaction mechanism was employed, and good agreement in terms of knock was seen when comparing the fast-burning cycles from the simulation with that those of high performance naturally aspirated V12 Lamborghini engine [372]. The fractal approach was also used by Fontanesi et al. [373] in knock tendency analysis of a small VVA engine with turbulence in the 1D model being calibrated from 3D CFD results. Kikusato et al. [374], at Waseda

University, used a two-zone combustion model where chemical kinetics, in this case, the original Shell model, were coupled to thermal calculations of the combustion chamber walls. Transient maneuvers showed that such temperatures may not stabilize for up to 20 seconds after a sudden load change. The model was then used to evaluate the application of coatings to reduce heat losses, ideally without worsening the knock limit. The concept is to have a very dynamic wall temperature with variations of several hundred Kelvin in the cycle to avoid heating up the charge from the walls during compression and to avoid excess heat transfer during regular combustion. It was subsequently shown that this was possible through careful application of coatings with low thermal inertia and thicknesses of the order of 0.1 mm, although it became more difficult to achieve a knocking gain as load increased [375].

The concept of developing detonation, explained by Bradley in 2002 as depending both on the resonance factor ξ and ε, the rate at which heat release is loaded into the acoustic wave, was applied by a number of researchers to the SI engine "super-knock" phenomenon. Super-knock occurs when an LSPI event turns into developing detonation. The LSPI itself is typically driven by particles or droplets of fuel/oil mixture. Peters et al. [376] of RWTH Aachen used dissipation elements in Direct Numerical Simulations (DNS) to estimate the dimension of the thermal gradient around exothermic centers in 2013. This depends on the integral timescale, which is large when mean velocity gradients are low. Excitation times were calculated in chemical kinetics simulation. The outcome was then used in RANS 3D CFD simulations of a GDI engine over a range of conditions. Developing detonation was seen to be more likely at low speed and high load as expected. Lauer et al. [377], of the Technical University of Vienna, used Lagrangian tracking of droplets to infer tendency towards LSPI in a CFD model of a GDI engine in STAR-CD software in 2014. Liu [378] of Tsinghau University, together with collaborators there and at the University of Michigan and Chery Automobile, studied super-knock both on a 1.6 L four-cylinder turbocharged GDI engine and an optical RCM. On the engine, super-knock was found to take place only over a range of spark advance at low temperatures and high charge densities. In RCM testing, sequential autoignition was interpreted as normal knock and developing detonation as a super-knock mode. Starting in the super-knock mode in the RCM, while increasing the temperature, the combustion mode was seen to transition back to sequential autoignition. The difference in appearance of the various autoignition modes could be clearly seen in the optical access RCM, as shown in Figure 51. In 2017, Liu together with Wang [9] of Tsinghau University, along with Reitz of the University of Wisconsin-Madison, published an extremely detailed review of the current status of the literature on knock and preignition. Particular emphasis was placed on transitions from deflagration to detonation modes and the importance of shock wave reflections near the combustion chamber walls. Over 300 papers were reviewed with more emphasis on recent activity than in the current work.

FIGURE 51 Flame-front propagation, sequential autoignition, and detonation in a rapid compression machine, from Liu et al. [378].

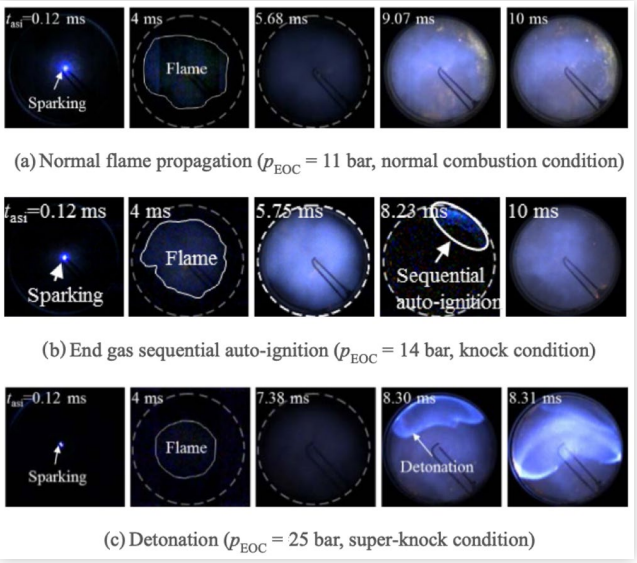

Kalghatgi, who is acknowledged by Bradley as having contributed to discussions in his 2002 paper [245], published on super-knock in 2017. He showed that the resonance parameter ξ could be calculated from engine pressure data. Some assumptions were required to calculate the reactivity parameter ε. He used this theory to explain the conditions necessary to obtain super-knock from preignition in modern downsized engines [379]. In 2018, Ohtomo et al. [380] of Toyota Central R&D Labs studied how to achieve autoignition without knock both in an RCM and in an engine through dilution. H_2 was mixed with gasoline in the engine intake to allow dilution levels up to 50%. A band was shown on a load/dilution diagram where autoignition was possible without knock. Cho et al. [381], of Seoul National University, separated the ξ term into equivalence ratio and temperature gradients. The RON test condition on iso-octane was simulated in a multi-zone 0D model using initial size and equivalence ratio gradients of rich and lean spots from Planar Laser-Induced Fluorescence (PLIF) measurements at a higher engine speed. An RCM replicated pressure-temperature history that was expected in the engine. Local temperature was correlated with local equivalence ratio due to specific heats and evaporative cooling. Lean spots are therefore more likely to be autoignition centers and lead to knock.

Optical measurements of conventional SI combustion have continued of course. Catapano et al. [382], of Consiglio Nazionale delle Ricerche (CNR, National Research Center), showed testing on a GDI engine with a Bowditch piston and that autoignition generally occurred in regions of negative flame curvature. This could also be captured in CFD. The Shell model was also used in CFD, and key reactive species concentrations from the model were correlated with experimental autoignition locations. The same researcher published a paper

FIGURE 52 Flame centroid movement during knocking combustion as measured by Catapano [383].

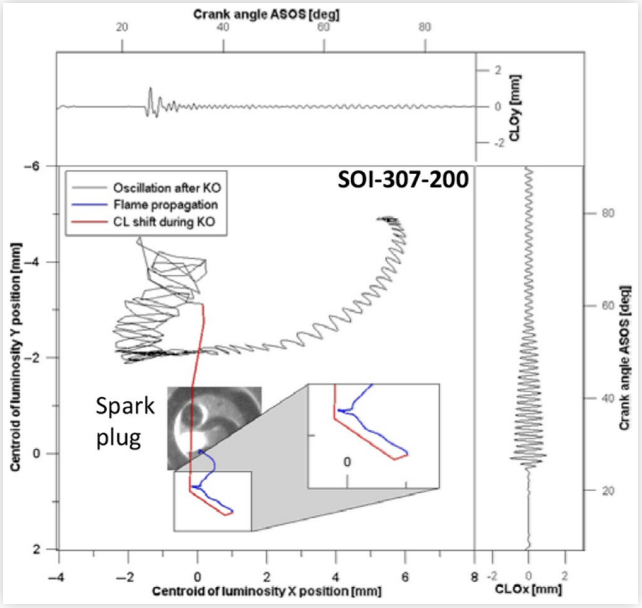

Reprinted with permission from Ref. [383]. © SAE International

FIGURE 53 Supersonic reaction front identified by Iijima [385].

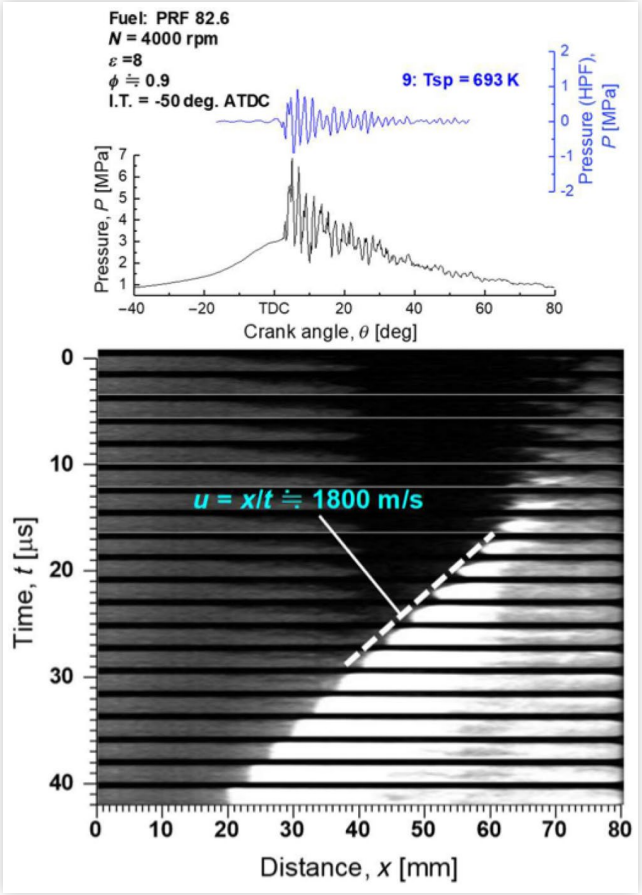

Reprinted with permission from Ref. [385]. © SAE International

a few years later on split injection with a four-cylinder 1.75 L engine with DI. Again a Bowditch piston was employed, and optical measurements of the flame front were taken at 50,000 frames per second. A new optically based knock index was described: MACLO (Maximum Amplitude of Centroid Luminosity Oscillation). When knock occurred, the flame centroid could be seen to oscillate at 6 kHz. Examination of centroid movement could also evidence multiple autoignitions, even if they were outside the field of view of the optical window [383]. An example is shown in Figure 52. Imaoka et al. [384], of Nissan, used laser-induced phosphorescence thermography to measure piston crown temperatures on a 2 L NA GDI engine and a single-cylinder equivalent. Despite using a piston bowl with a sharp edge, no hot spots were seen in this region. The study was notable also for using five separate cooling jackets—head inlet, center and exhaust sides, and upper and lower liner. Lowering the head intake side coolant temperature gave the greatest improvement in the knock limit. CFD suggested that 40% of the heat transfer to the charge was from the intake port. A plastic port liner improved the knock limit by 2°CA MFB50. Iijima et al. [385] of Nihon University performed optical measurements on a side spark and side-valve engine at 500,000 frames per second. The engine had no cooling system and, hence, transitioned progressively into knock as it warmed up. Frequently, the first autoignition event led to further in the vicinity allowing optical identification of a reaction front. It was seen that such a front could propagate at a range of velocities from subsonic to supersonic, as shown in Figure 53. The knocking intensity as judged by cylinder pressure measurements was correlated with the reaction front velocity—strong pressure oscillations were correlated with detonation waves.

It is interesting that despite the fact that the CFR engine is almost 90 years old, and is the basis of fuel RON and MON measurements, it is still not fully understood today. Huber et al. [386] of Ingolstadt University of Applied Sciences performed investigations on modernizing the test procedure and engine using an Electronic Control Unit (ECU), PFI, lambda control, and pressure indication in 2013. Pal et al. [387], at Argonne National Laboratory, created what they suspected to be the first 3D CFD model of a Waukesha CFR engine in 2018. Multicycle RANS with detailed chemistry was implemented in CONVERGE software. The G-equation was used for turbulence modeling with laminar flame speeds from chemical kinetics. The engine was X-rayed to obtain the geometry of the head and water jacket to parameterize a 1D model. The engine was instrumented with an intake cylinder and exhaust dynamic pressure sensors, a lambda sensor, and thermocouples. It was calculated that running iso-octane in the RON test condition, residuals were around 6%. Simulations suggested knock occurred towards the exhaust side due to flame bias towards the intake, driven by asymmetric flow from the shrouded intake valve. Rockstroh et al. [388], also of Argonne National Laboratory, compared a wide range of cylinder pressure-based knock metrics to the standard CFR

501-C knockmeter. Correlation between the knockmeter and common modern indices such as MAPO was very poor. There was some correlation between peak pressure and rate of pressure rise. The knockmeter features an LPF and, hence, is not sensitive to information in the 6 kHz range, which is the lowest acoustic mode commonly excited in this engine by knock. RON testing, according to ASTM D2699, is performed at maximum knocking lambda (and fixed ignition timing). The effects of these two variables had been investigated in 1931, just before the RON method was made official, by Campbell and collaborators [37]. The impact of this was revisited by the Argonne team in 2019 and described in a paper by Hoth [389]. It was found that peak knock lambda was generally slightly rich for all blends, but was around 0.88 for PRF fuels and as lean as 0.95 for aromatic and ethanol-containing mixtures. This means that such fuels are not compared at the same lambda in standard RON tests. Paraffinic fuels were found to have a steeper gradient of knock with lambda, but also to give higher MAPO values for a given knockmeter reading in the standard "peak knock lambda" test condition. These two effects somewhat compensate each other and mean that MAPO-based RON values at stoichiometry are not dissimilar for fuels of different chemistry, but similar RON. The MFB50 for a given spark timing was found to be within 1.5°CA for all fuels, with only a slight reduction for those containing high ethanol concentration.

Knock control understanding has also increased in the last 10 years. With modern ECUs, it has become possible to introduce basic simulation models into real-time control systems. Xiao et al. [390] of Clemson University demonstrated the feasibility of a real-time capable model, which could suggest knock-limited ignition timing, using a Douaud and Eyzat ignition delay model for knock and a Blizard and Keck turbulent entrainment model for flame-front propagation. It was suggested that such a model could be used for fuel adaptation, but would likely require cylinder pressure sensors. A similar system would appear to now be in production on the Mazda Skyactiv-X engine [340]. Corti et al. [391], of the University of Bologna, suggested a somewhat similar approach in 2017. A triple Arrhenius function was used for ignition delay times, based on the output of chemical kinetics calculations. A combustion progress variable was based on a linear fit through 10% and 50% MFB points and then extrapolation to zero and 100%. Both 10% and 50% MFB were assumed to be normally distributed. A further simplification was that when knock occurs, the entire mixture was assumed to autoignite. A normal distribution of unburnt gas temperature was considered and a calibrated temperature at intake valve closing initially imposed and then adjusted based on measured feedback. A 99th percentile MAPO was predicted by the model, and it corresponded closely to experimental data when tested on a Ducati motorcycle engine.

A number of papers on knock statistics and control were published by Peyton Jones and collaborators at Villanova University. Spelina et al. [392] gave an overview of knock simulation and control in 2014, and she suggested that, although most production knock controllers aim for around 1% of strong knocking cycles, controller stability would be greatly improved by targeting around 20% of weak knocking events. Peyton Jones et al. [393] elaborated on this concept the following year and described a weighted error function to enable threshold optimization to correctly weight false-positive and false-negative errors. Further details on control-oriented simulation techniques were published one year later with the importance of considering the stochastic element highlighted [394]. MAPO remains the most common knock index, but Siano [395] of the Istituto Motori CNR compared knock detection based on autoregressive models, a normalization of knock pressure oscillations and online calculated discrete wavelet transforms. The autoregressive model appeared to have an advantage in terms of sensitivity over the conventional MAPO approach.

Some of the highest efficiency knock-limited engines are currently found in Formula 1. Turbocharged engines returned to the sport in 2014 together with a fuel mass flow limit of 100 kg/h. This effectively turned Formula 1 into a BSFC competition, and hence development principally focuses on reducing knock to allow increasing of the compression ratio. As such, both EIVC and anti-tuning are applied to minimize the end of compression temperature for a given geometric compression ratio, as documented by Rosetti et al. [396] of Ferrari and shown in Figure 54. The engines also run lean in full load, which gives a further knock limit improvement. A comparison of how volumetric efficiency and relative AFR have changed as the formula moved from NA to fuel-flow limited turbocharged engines was documented by Sassi et al. [397] of Ferrari and Shell and is repeated in Figure 55. Homogeneous lean SI combustion at high loads is rarely documented in the literature. A recent paper by Clasen et al. [398] did explore this topic, although only at loads up to 17 bar IMEP and speeds in the range 1500-2500 rpm. In this operating area, the knock limit was actually found to worsen in combustion phasing terms moving from stoichiometric conditions to relative AFRs

FIGURE 54 Influence of intake runner length and intake valve closing angle on the end of compression temperature for a Formula 1 powertrain, from Rosetti et al. [396].

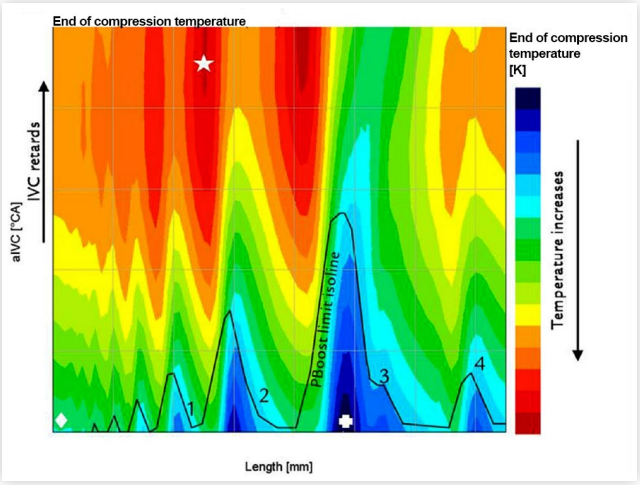

Reprinted with permission from Ref. [396].

FIGURE 55 Changes in relative AFR and volumetric efficiency as Formula 1 regulations changed from NA V10 and V8 engines to knock-limited turbocharged units, from Sassi et al. [397].

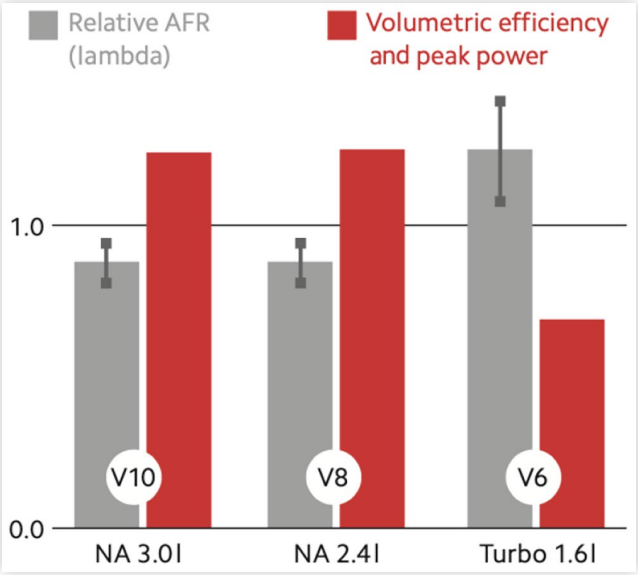

of around 1.3. This is not a speed and load range of interest to racing applications, and it would appear that this trend does not hold at much higher speeds and loads. The combination of anti-tuning, EIVC, and enleanment leads to long burn delays, and hence significant activity was carried out to optimize the ignition system as documented by Corrigan et al. [306] of Ferrari with collaborators at MOT (Motorentechnik, Optik und Thermodynamik). While conventional SI was used in early development, all manufacturers now use passive prechambers to further improve knocking performance, as confirmed by Symonds [399], Chief Technical Officer of Formula 1, in 2020. Formula 1 also features a deep technical collaboration between engine and fuel suppliers. Fuels and engines are developed together, historically bringing evolutions of both engine hardware and fuel to the track on multiple occasions in a single season. Some of this activity has been published in the literature. These engines are quite far away from the CFR type in terms of design and operating conditions; hence, rapid compression machines and shock tubes are used to support development, as documented by Dauphin et al. [94] of Total, together with collaborators at IFP and the University of Lille. The use of an RCM to characterize the antiknock performance of high octane fuels was also presented by Burke [400] of RWTH Aachen, together with collaborators at Shell and Ferrari. A Chemical Ignition Number (CIN) was proposed based on an iso-octane/ethanol scale where temperature, pressure, and AFR were tailored to the target engine. These results can be used to calibrate chemical kinetics models to generate new fuel blends that are optimized for the pressure/temperature regime of these engines. The intention of the regulations [401] is to ensure that road-relevant components

TABLE 6 Comparison between current road-car and Formula 1 engine technology.

	Production road car	Formula 1
Swept volume	1.5 L	1.6L
Compression ratio	13:1	16-18:1
Specific output	75 kW/L at 5500 rpm	360-400 kW/L at 11,000 rpm
Thermal efficiency	42.5%	>50%
Dilution	$\lambda = 1$ with ≈20% EGR	20-40% enleanment
Intake strategy	Miller and detuning	Miller and anti-tuning
Ignition system	120 mJ coil, spark plugs	Prechamber
Fuel system	350 bar GDI	500 bar GDI
Fuel type	Commercial RON 95	Tailored 100 < RON < 110
Waste heat recovery	None	From turbine
Aftertreatment	TWC and GPF	None

are used in the specific blends, and hence fuel development is constrained.

Mercedes published in 2018 that their Formula 1 engine had exceeded 50% thermal efficiency [402]. This is achieved at >40 bar IMEP at 11,000 rpm with peak cylinder pressures of the order of 250 bar. The current best road car technology is the Geely Hybrid engine, which reaches 42.5% peak thermal efficiency and has a specific output of 75 kW/L as described by Zhang et al. [403]. A comparison between the engine types is given in Table 6 and will now be described with comments on the applicability of racing knock mitigation techniques to road-car use. Where Formula 1 data in the literature is incomplete, estimated ranges are given.

The Formula 1 engine achieves very high BTE due to its high compression ratio and waste heat recovery—effectively a form of turbocompounding. Such a high compression ratio at the extreme specific output can only be tolerated due to very effective knock mitigation. The combination of Miller and anti-tuning gives very strong reductions in the end of compression temperature. The anti-tuning system would require inlet runner lengths of the order of 1 m for road-car engine speeds and would be difficult to package. Variable runner length is also required to have effective anti-tuning over a reasonable speed range. The combination of strong Millerization and lean running requires a robust ignition system, and prechambers are used to this effect. These also give good knock mitigation at high loads and generate turbulence in the main chamber, increasing combustion speed. Extremely retarded conditions, such as catalyst heating, are difficult to achieve with prechambers, but need not be run for a racing application. However, prechamber engine layouts with secondary spark plugs have recently been proposed for road-car applications. The possibility of designing a fuel to match the engine, albeit within regulatory limits, is of course a significant benefit. A number of new road-car fuels are currently under consideration, however, including ethanol,

methanol, methane, hydrogen, and synthetic gasolines. Many of these have improved knock resistance in comparison to today's market gasolines. The Formula 1 engine is "oversquare" with a bore-to-stroke ratio of 1.5 whereas thermal efficiency should be optimum at values of less than unity. However, large bore areas permit large valves and are, hence, appropriate for high specific power engines. This is particularly important if strong Millerization is applied, as available boost pressure may be limited. The cylinder swept volume of the Formula 1 engine is a rather small 267 cc, and hence, combustion chambers remain compact. This has long been known to benefit knock. An increased cylinder count to reduce cylinder swept volume would, however, increase costs for road-car engines and also would increase friction, and hence reduce part-load efficiency. The high engine speed also reduces the time available for autoignition to occur and accelerates the flame front. One of the key Formula 1 hybrid technologies—the electrified turbo—allows significant waste heat recovery along with turbocharger lag compensation. This system has also been recently announced for production by Garrett and Mercedes-AMG [404]. Waste heat recovery is most effective at high speeds and loads although some recuperation may already be possible on emissions cycles, depending on turbo-matching and road load.

It can be seen, therefore, that the majority of knock-mitigating approaches in Formula 1 have an existing or potential road-car equivalent. The lack of exhaust aftertreatment due to no emissions limits[19] is an exception. A lean aftertreatment system for the full-load operation would not be desirable for road-car applications due to cost and packaging reasons; hence, stoichiometric operation with EGR is preferred. The lack of an aftertreatment system reduces exhaust backpressure, and hence trapped residual content. Knocking tendencies are therefore reduced.

Formula 1 has two other fundamental advantages over current road-car technology. One is the possibility to optimize the engine and turbocharger design for a narrow speed and load range. Compromises between competing objectives can therefore be avoided. Hybridization is a means of reducing the necessary operating range of road-car engines, but an extreme hybridization approach would be required to fully limit the engine to single-point operation—for example, a range extender. These engines are normally designed to be cheap rather than high performance, as strong powertrain electrification is already expensive. Catalyst heating is another operating point that must currently be performed by the combustion engine in road-car applications. The introduction of electrically heated catalysts may mean less need to bias the combustion system design to cover this point in the near future in comparison to the recent past, and hence, this compromise could maybe be avoided, or at least lessened. The second big advantage Formula 1 engines have is that continuous development with large budgets is invested into a single concept with a single target over a number of years. In some ways, this is similar to how WWII fighter aircraft piston engine development proceeded in the 1930s and 1940s, as described by Douglas [66]. Road-car engine development programs, on the other hand, need to match strict budgetary and time limitations and have many more targets and constraints to satisfy. The fact that 42.5% efficiency has been achieved in production and >45% efficiency demonstrated in near-production research is therefore very impressive.

Splitter et al. [405] of Oak Ridge National Laboratory and the University of Tennessee Knoxville published a paper in 2016 on the historical analysis of octane number and SI engine specifications. Five key development periods were identified with the "Fuel Improvement Period" said to be up until 1955. This was based on US market data over an extended period. Data from this report (together with the assumption that the Ford Model-T is representative of US vehicle sales in the 1920s) is shown in Figure 56. It can be seen that both compression ratio and specific output increased dramatically from the 1920s until the mid-1950s. Improvements in fuel quality made a large contribution in this period, as noted by Splitter et al. and already discussed in the current paper. Compression ratio stabilized at around 9:1 and specific output at 34 kW/L until 1970. Compression ratio and specific output then fell due primarily to the introduction of emissions legislation. This resulted in the consequent removal of leaded additives from gasoline, and hence a reduction in fuel octane values, as shown in Figure 20. From the late 1970s onwards, both compression ratios and specific output began increasing again. Fuel antiknock quality has not markedly changed; hence, since then these gains are mostly due to more knock-resistant engines. The increased specific output would normally require a compression ratio decrease for a given knock limit. This makes the improvements all the more impressive. These more recent gains have been primarily driven by a better understanding of knock, developments in engine hardware, and also improved powertrain calibration and control.

FIGURE 56 Changes in average compression ratio and specific output of US market cars 1925-2014. Data from Splitter et al. [405].

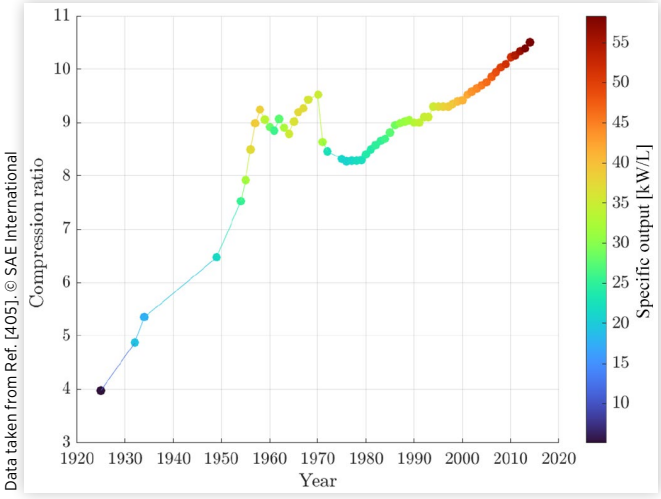

[19]Emissions are currently unregulated, but this is under consideration for future regulations [399].

Conclusions

Engineers have sought to improve the efficiency of the ICE for over 100 years and have been fighting against knock for all of that time. In the early period, a compression ratio of less than 5:1 was typical, and the ITE was around 30%. This was at just 600 rpm. In 2020, Geely reached 42.5% BTE at around 2700 rpm with a compression ratio of 13:1 [403], whereas Formula 1 is now over 50% BTE at 11000 rpm [402] with compression ratios believed to be not far from the regulatory limit of 18:1. Specific power outputs have also increased dramatically in the same period. Although much progress has been made, knock remains a key limitation to further efficiency gains today, just as it was 100 years ago. Any gain in ICE efficiency will translate to reduced CO_2 emissions in the near term. Even with non-fossil fuel sources in the future, energy will always be at a premium, and hence, efficiency will remain of critical importance. Knock as a phenomenon was already defined in the introduction of this paper. In the following section, knock mitigation strategies that have been developed over the last 100 years are presented. Much of this knowledge has been hard won over an extended period, as has already been described.

Knock Mitigation Strategies

Knock can be avoided if the flame front consumes all of the unburnt charge before autoignition has time to occur. Knock mitigation strategies, therefore, fall into two broad groups: those that seek to accelerate the rate of charge consumption by the flame front (this will be referred to as FFA) and those that aim to reduce reaction rates in the end gas (ERR, End-gas Reactivity Reduction). Guidelines for different component groups will now be given.

Charge Motion (Primarily FFA) Charge motion can assist in both mixture formation and FFA. In terms of cylinder head design, both swirl and tumble motions can be created. A combination is also possible. Increasing tumble or swirl will generally result in a reduction in volumetric efficiency. Charge motion is favored by high piston speeds and hence high stroke-to-bore ratios.

Tumble is effectively transformed into turbulence at the end of compression, and hence can accelerate especially the early phase of combustion. It is the predominant charge motion used with four-valve pent-roof-type cylinder heads.

Swirl persists longer into the cycle and can improve later burn rates, especially when combined with squish. It was more commonly applied on cylinder heads with a single intake valve. It can also be achieved with a four-valve head through obstructing flow to one of the intake valves.

Squish is achieved by having a large parallel area on the piston and combustion chamber roof with a small distance between them. A flow is generated in the direction of the piston bowl close to TDC. This increases turbulence. As the piston descends, an anti-squish flow is created where the flame may be pulled by vacuum into the expanding squish volume. A strong squish effect is difficult to combine with valve overlap as the necessary piston pockets for high overlap reduce the available squish area.

Whatever charge motion is adopted, care should be taken with undesirable secondary motions. These are flow tendencies that distort the flame front in an undesirable manner, and hence can locally slow its progress. This increases the time available for autoignition to occur. Care should also be taken with cyclic variability of charge motion.

Both the quantity of turbulence and its spatial and temporal distribution should be optimized for best effects on combustion.

Perhaps the most direct way of accelerating the flame front is to increase engine speed. This has a negative impact on friction and pumping work, however. Increasing engine speed also means the end gas is exposed to high temperatures and pressures for a shorter period of time, giving further knock benefits.

Charge Temperature Management (ERR) As knock is largely a temperature-driven phenomenon, all efforts should be taken to keep the charge as cool as possible until the flame front arrives.

Intake systems should, therefore, be thermally isolated from hot parts of the cylinder head, particularly in regions of high flow and, hence, high heat transfer coefficient.

Charge cooling systems can reduce the temperature of the intake charge, in particular after it has been increased by a compression process.

Expansion of the charge can also take place in the intake system through appropriately timed wave action and/or in the cylinder by adopting an EIVC strategy. Both of these techniques, however, reduce volumetric efficiency and tumble and so are limited by boost and combustion stability. A LIVC strategy can also be used to reduce the effective compression ratio.

Combustion chamber components should also be adequately cooled. Typically the exhaust valves are the hottest region, and this can be managed through sodium-filled valves and direct cooling of guides and seats. The coolant circuit can and should be optimized in coupled calculations of the water jacket and the knock behavior in the cylinder.

Cylinder flow motions and turbulence will also impact heat transfer behavior in the cylinder. Squish may have a positive impact on the cooling of the end gas if the piston temperature is lower than that of the charge during the squish and anti-squish period. Excessive cooling in the absence of knock will reduce overall efficiency. Careful use of coatings may enable a better compromise to be achieved between knocking tendency and excessive heat losses.

Mixture Formation (FFA and ERR) Early SI engines used carburetor systems to achieve an approximately homogeneous mixture distribution. Mixing occurred primarily in the intake system and lighter and heavier fuel fractions were prone to separation. Mixture distribution to the cylinders was

not necessarily even, and closed-loop control was difficult. Much of the fuel latent heat was lost to the walls of the intake system.

PFI creates a homogeneous distribution like a carburetor but has the advantage that the AFR can be tailored for each cylinder. However, most latent heat is still lost to the walls.

GDI systems create the possibility to tailor the mixture distribution to the operating point, and hence, a range of strategies can be applied. With correct timing of the injection event(s), maximum heat can be extracted from the charge, which reduces the knocking tendency. While late injection favors charge temperature reduction, there may be inadequate time for mixing. This can be alleviated somewhat with careful charge motion and spray pattern design. Extremely lean regions are unlikely to knock. Fuel concentration in the end gas is correlated negatively with temperature, however. Lean pockets may therefore be hotter and, combined with the fact that flame fronts will consume them more slowly, can be at increased risk of autoignition if they are not lean enough. It is generally advantageous to achieve a slightly rich mixture near the spark plug at the time of ignition to maximize early flame kernel growth rates and stability.

In theory it should be possible to manage reactivity gradients to reduce the risk of autoignition events transitioning to damaging developing detonations.

Fuel (Primarily ERR, Secondary Impact on FFA) The knock resistance of fuels was correlated with the highest compression ratio an engine could achieve over 100 years ago and, subsequently, with testing in comparison to PRF on a CFR research single-cylinder engine. These are known as the RON and MON tests.

The most common rating tests were conceived in the 1920s and 1930s when both fuel types and engine hardware were very different than they are today. Various methods have been proposed to correlate the rating values to modern engines with some success. The end gas in a modern engine tends to be at lower temperatures for a given pressure than in the RON, and particularly the MON test. Modern engines often perform best with fuels of high RON and low MON due to the combined effects of the rating method and the high sensitivity of modern fuels in comparison to the PRF test references.

The knock resistance of a fuel is correlated with its Ignition Delay Time. This can be characterized in experimental facilities, typically against temperature and pressure. The delay time characteristic against temperature exhibits non-Arrhenius behavior for many fuel types, especially paraffins, which make up the PRF scale. An NTC region exists for many fuels. This has an impact on the severity of knock in the engine as this depends on reactivity gradients. NTC behavior is also correlated to preflame reactions. Experimental results can be compared to delay time maps coming from facilities such as RCMs and shock tubes to better understand knocking behavior. However, modern engines frequently run at higher pressures than these facilities can reliably achieve. Results from such facilities are therefore normally used to calibrate chemical kinetics software that can be incorporated in 3D CFD packages.

Liquid fuels evaporate before combustion. In doing so, they cool the charge. This effect is strongest for DI engines. Oxygenated HCs, particularly alcohols, have higher latent HOV than other typical gasoline components. High latent heat is beneficial for knock mitigation. The RON test is with fixed inlet air temperature, and fuel is introduced to the intake system before the engine. There is therefore a partial charge cooling effect. The MON test, on the other hand, controls the air/fuel mixture temperature upstream of the engine to a high temperature and, hence, is not sensitive to fuel latent heat. The volatility characteristics of the individual fuel components may cause separation in the intake system. This is of less importance on modern engines than it was with carburetor fuel systems.

The flame speed of a fuel may also have an impact on knock as faster flame-front propagation results in a lower time for knock to occur. High flame speeds also mean more stable early flame kernel growth, and hence better cyclic variability. Fuel flame speed effects are generally second order to ignition delay times, however, at least for typical HCs currently used in gasoline blending.

Dilution (ERR) The benefits of charge dilution on knock were realized at an early point in the development of the ICE. Dilution renders the end gas less reactive. This is partly because a given amount of heat release from the flame front will result in a lower temperature rise in the chamber if the trapped mass is increased. Ignition delay time also depends on fuel/oxygen concentration, and this is reduced by adding an inert charge. Dilution can be with excess air, trapped or recirculated exhaust gas, and/or introduction of additional fluids. All of these will reduce flame speeds, and hence, there is a limit to how much can be applied.

EGR is commonly applied to increase the inert gas content in the cylinder. The exhaust gas should be cooled and ideally reactive species, such as NO, removed by catalysis before reintroduction to the engine. EGR cooling increases the total heat rejection requirement of the powertrain and may not be desirable for high-performance applications. EGR should be well distributed in the intake system to avoid further increases in cyclic variability. There is some evidence that EGR may be less effective at very high loads. Trapping of internal residuals has a detrimental effect on knock due to their high temperature and reactivity. This should be minimized by effective scavenging. Scavenging can be promoted by a combination of valve overlap and a favorable pressure gradient between the intake and exhaust systems. This is harder to achieve in a modern production engine, which features a restrictive exhaust system due to the necessity to aftertreat the gases to meet emissions limits.

Excess air is one of the simplest dilution strategies to apply. However, it is incompatible with emissions control by a three-way catalyst. It must therefore be used in conjunction with a lean aftertreatment system to meet modern emissions limits, which increases costs. In racing applications, notably Formula 1, excess air is applied to good effect to improve the knock limit at very high speeds and loads. It may be less

effective at lower speeds, and there is even evidence that it may be detrimental in some cases.

The most straightforward additional fluid to introduce is excess fuel. This was noted to benefit the knock limit in the early days of combustion research. Once again, three-way catalysts only operate effectively in stoichiometric conditions, and hence, this approach is currently only used to protect engine components from overheating in extreme operating conditions. Water injection may be used in addition or as an alternative. This was employed on WWII fighter aircraft and is enjoying renewed interest as a means of knock mitigation and as temperature reduction compliant with stoichiometric operation. As for enrichment fueling, there is both a chemical benefit and a latent heat benefit. DI of water gives maximum charge cooling for the same reasons that GDI systems mitigate knock more effectively. It is more complex and expensive to implement than low-pressure PWI.

Ignition System (FFA) Ignition can be initiated in a SI engine by a conventional spark plug and coil. A high-energy coil and large plug gap can result in a larger and more stable initial flame kernel. This is particularly important in dilute or stratified mixtures. A stable early flame kernel is key to guaranteeing low cyclic variability. Electrode design should aim to minimize kernel heat losses. Flow motion should aim to transport the kernel out of the gap, but not excessively as blow-off or short-circuiting may occur. Large gap sizes mean high voltages are required to achieve a spark. This may limit the gap size for highly boosted engines.

A distributed ignition system results in multiple combustion initiation sites. This will result in faster combustion with lower cyclic variability. Distributed ignition may be achieved by a number of means including multiple spark plugs, a corona discharge system, and prechamber jets.

Prechamber jets also result in higher turbulence and radical seeding in the main chamber and so can give an additional performance improvement over other distributed ignition systems.

Combustion Chamber Design (FFA and ERR) It has been known for at least 100 years that compact combustion chambers with short flame travel distances are beneficial for knock. The spark plug should therefore be arranged to minimize flame travel distance.

Smaller combustion chambers improve the knock limit. As knock generally occurs shortly after TDC, the bore size is the key dimension. Small bores are beneficial. For a given cylinder count and total swept volume, this implies a large stroke-to-bore ratio. This has a detrimental impact on volumetric efficiency, however.

Using an increased number of cylinders can be an effective strategy. But this increases cost, heat transfer, and potentially friction.

A bowl-in-piston design can be effective and was widely used in the past, combined with squish. However, this is difficult to achieve together with valve overlap.

Care should be taken to avoid protruding areas of the chamber that have poor heat transfer to the coolant jacket.

Exhaust System Design (ERR) Low exhaust system pressure drops should be aimed to minimize trapped residuals.

Pressure wave tuning in the exhaust system can be used to achieve low pressure at the exhaust valve during valve overlap to further reduce residuals.

High flow exhaust ports, early exhaust valve opening, and high exhaust valve lift may also contribute to more effective removal of burnt charge from the cylinder.

Closing Remarks If knocking is completely avoided, the engine is likely not running at its best possible efficiency. This may be due to excessively retarded combustion or an overly low compression ratio for the operating point. The target in the limiting condition should be to accept a given quantity of knock to permit the highest practicable compression ratio to be used. Control systems need to manage the combustion phasing and, hence, the knocking intensity to ensure an acceptable rate of damage accumulation in comparison to the engine's expected lifetime. Detailed combustion chamber design features and material choices may also lessen the damage that occurs for a given knocking intensity. Particular attention should be paid to the crevice zone and the piston rings.

Potential Future Research Directions

Powertrain engineering and the ICE is going through a seismic change. While the ICE is commonly described as a mature technology, areas where further research activity is required to improve knocking limits, and hence efficiency remain. There are many encouraging lines of research at the moment. An (incomplete) list of open points is as follows:

- The small spatial dimensions of exothermic centers that drive knock behavior, together with the extremely short timescales of autoignition chemistry in an ICE at elevated temperatures and pressures, mean that there is still much to understand here. DNS in CFD coupled with state-of-the-art reaction mechanisms can allow exploring the phenomenon, but more effort is required to arrive at a fully predictive methodology and the development of tools to robustly validate it. Consideration should also be given to the creation of a new generation of RCM and Shock Tube facilities to cover this experimental space. Downsizing has meant that many engines now operate outside of the current ranges of such devices.
- Standard methods of rating fuel knock resistance are long overdue for an overhaul. The researchers who created the RON and MON methods did not expect that they would still be in use almost 100 years later. A

number of suggestions on how such methods can be adapted have been proposed. A future rating scale should identify the possibility a fuel has to contribute to improved engine efficiency in a modern or near-future knock-limited powertrain. This will likely require testing at higher speeds than current RON and MON tests and over a range of dilution levels, compression ratios, and loads. The opportunity should also be taken to move to a more modern combustion chamber and charge motion with DI fueling and a high-energy ignition system. Modern cylinder pressure-based feedback should also be introduced. Burn rate data could therefore be produced together with knock limit results. Measurement of engine-out emissions should also be considered. The test procedure still needs to be possible in a relatively short time period. Modern automation systems and closed-loop controllers should make this possible, potentially combined with slow transient rather than stationary operation.

- Much engine manufacturer activity still focuses on avoiding running into knock. As efficiency gains become harder to realize, the engine must be controlled to greater than borderline knock conditions where performance can be improved. Work on knock control systems and damage modeling, together with detailed activity to improve engine hardware design combined with materials to permit increased knock robustness, should be explored. Further understanding of shock-wave behavior in engines and how to manage them to reduce damage is also needed.
- A number of potential future ICE fuels are currently being proposed including ethanol, methanol, methane, hydrogen, synthetic gasolines, and more. All of these have valid reasons for being studied, but it will be necessary to converge on a limited number of future fuels to permit engine manufacturers and energy companies to make the investments required to bring a new generation of products to market. There is a significant opportunity to improve the knock limit of the ICE, and hence its efficiency if the right solution is backed. The most appropriate solution should be based on WtW and Total Life-Cycle Analysis to have a maximum beneficial environmental impact. An appropriate regulatory framework needs to exist in order to enable this to happen.
- The large range of potential fuels combined with the numerous possibilities to hybridize the ICE means a predominantly experimental approach to identify the best solution would be prohibitively time consuming and expensive. A fully integrated simulation methodology starting from a systems level and working down to CFD with integrated kinetics is required. Many of the proposed fuels are single-component and, hence, from a reaction modeling point of view, significantly simpler than existing gasolines. A number of promising alternatives will doubtlessly be identified, and significant gains in knock-limited efficiency can be expected. These must then be validated experimentally. A large-scale international collaborative effort is likely needed, similar to what happened in the 1920s and 1930s driven by the CFR group. Such collaborations still exist today, but perhaps not at a sufficient scale. This is particularly important as vehicle manufacturers' budgets must now be divided between electrification and ICE research, and hence, there should be a greater impetus for a larger-scale collaboration than considered in the recent past. A problem on a global scale demands global collaboration to find the best solution.

Acknowledgments

My wife Elena and my girls Éila and Kiva for having supported me in writing this review despite all the time I needed to spend away from them!

Contact Information

daire.corrigan@me.com

Definitions, Acronyms, Abbreviations

ADC - Analog-to-Digital Converter
AFR - Air-Fuel Ratio
AKI - AntiKnock Index = (RON + MON)/2
AMOCO - AMerican Oil COmpany
ASTM - American Society of Testing and Materials
AVL - Anstalt für Verbrennungskraftmaschinen List
BDC - Bottom Dead Center
BEV - Battery Electric Vehicle
BMEP - Brake Mean Effective Pressure
BPF - Band-Pass Filter
BSFC - Brake-Specific Fuel Consumption
BTDC - Before Top Dead Center
CA - Crank Angle
CAI - Controlled AutoIgnition
CARS - Coherent Anti-Stokes Raman Spectroscopy
CCD - Charge-Coupled Device
CFD - Computation Fluid Dynamics
CFR - Cooperative Fuel Research
CIN - Chemical Ignition Number
CMOS - Complementary Metal Oxide Semiconductor
CNR - Consiglio Nazionale delle Ricerche
COV - Coefficient of Variation
CR - Compression Ratio
CRC - Coordinating Research Council
CRF - Centro Ricerche FIAT

CV - Metric horsepower
DD - Developing Detonation
DDT - Deflagration to Detonation Transition
DI - Direct Injection
DNS - Direct Numerical Simulation
DON - Distribution Octane Number
DWI - Direct Water Injection
ECFM - Extended Coherent Flamelet Model
ECU - Electronic Control Unit
EGR - Exhaust Gas Recirculation
EIVC - Early Intake Valve Closing
EPA - Environmental Protection Agency
ER - Expansion Ratio
EREV - Electric Range Extender Vehicle
ERR - End-gas Reactivity Reduction
ETBE - Ethyl Tert-Butyl Ether
EU - European Union
FCEV - Fuel Cell Electric Vehicle
FEM - Finite Element Method
FEV - Forschungsgesellschaft für Energietechnik und Verbrennungsmotoren
FFA - Flame-Front Acceleration
FFT - Fast Fourier Transform
FSR - Flame-Speed Ratio
GDI - Gasoline Direct Injection
GM - General Motors
GWDI - Gasoline Water Direct Injection
HC - Unburnt Hydrocarbons
HCCI - Homogeneous Charge Compression Ignition
HOV - Heat Of Vaporization
HPF - High-Pass Filter
IAV - Ingenieurgesellschaft Auto und Verkehr
ICCD - Intensified Charge-Coupled Device
ICE - Internal Combustion Engine
IDT - Ignition Delay Time
IFP - Institut Français du Pétrole
IMEP - Indicated Mean Effective Pressure
ITE - Indicated Thermal Efficiency
KLSA - Knock-Limited Spark Advance
LDV - Laser Doppler Velocimetry
LES - Large Eddy Simulations
LIF - Laser-Induced Fluorescence
LHV - Lower Heating Value
LIVC - Late Intake Valve Closing
LLNL - Lawrence Livermore National Laboratory
LPF - Low-Pass Filter
LPG - Liquefied Petroleum Gas
LSPI - Low-Speed Preignition
LTHR - Low-Temperature Heat Release
MACLO - Maximum Amplitude of Centroid Luminosity Oscillation
MAPO - Maximum Amplitude of Pressure Oscillation
MBT - Maximum Brake Torque
MFB - Mass Fraction Burned
MIT - Massachusetts Institute of Technology
MON - Motor Octane Number
MOT - Motorentechnik, Optik und Thermodynamik
MPG - Miles Per Gallon
MTBE - Methyl Tert-Butyl Ether
NA - Normally Aspirated
NACA - National Advisory Committee for Aeronautics
NG - Natural Gas
NMA - N-Methyl Aniline
NO_x - Oxides of nitrogen
NTC - Negative Temperature Coefficient
OHV - OverHead Valve
PDF - Probability Density Function
PFI - Port Fuel Injection
PHEV - Plug-in Hybrid Electric Vehicle
PIV - Particle Image Velocimetry
PLIF - Planar Laser-Induced Fluorescence
PRF - Primary Reference Fuel
PtG - Power to Gas
PtL - Power to Liquid
PWI - Port Water Injection
RANS - Reynolds-Averaged Navier-Stokes
RCEM - Rapid Compression and Expansion Machine
RCM - Rapid Compression Machine
RDE - Real Driving Emissions
RMS - Root Mean Square
ROHR - Rate Of Heat Release
RON - Research Octane Number
RWTH - Rheinisch-Westfalische Technische Hochschule
S - Sensitivity = RON − MON
SACI - Spark-Assisted Compression Ignition
SI - Spark Ignition
SNR - Signal-to-Noise Ratio
SPCCI - Spark-Controlled Compression Ignition
SRM - Stochastic Reactor Model
TDC - Top Dead Center
TEL - Tetra-Ethyl Lead
THIP - Toluene, Heptane, and Iso-Pentane

TML - Tetra Methyl Lead
TRF - Toluene Reference Fuel
US - United States
UV - UltraViolet
VVA - Variable Valve Actuation
WtW - Well to Wheel
WWII - World War II

References

1. United Nations Framework Convention on Climate Change, "Report of the Conference of the Parties on Its Twenty-First Session, Held in Paris from 30 November to 13 December 2015," 2016, https://unfccc.int/resource/docs/2015/cop21/eng/10a01.pdf.
2. European Environment Agency, "Monitoring of CO_2 Emissions from Passenger Cars—Regulation (EU) 2019/631," December 2020, https://www.eea.europa.eu/data-and-maps/data/co2-cars-emission-18.
3. European Automobile Manufacturers Association, "ACEA Press Release: Fuel Types of New Cars," November 2020, https://www.acea.auto/files/20201105_PRPC_fuel_Q3_2020_FINAL.pdf.
4. Ewing, J., *Faster, Higher, Farther: The Volkswagen Scandal* (New York: W. W. Norton & Company, 2017), ISBN:978-0393254501.
5. Clerk, D., "Cylinder Actions in Gas and Gasoline Engines," SAE Technical Paper 210043, 1921, https://doi.org/10.4271/210043.
6. Ricardo, H.R., "Recent Research Work on the Internal-Combustion Engine," SAE Technical Paper 220001, 1922, https://doi.org/10.4271/220001.
7. Towers, J.M. and Hoekstra, R.L., "Engine Knock, A Renewed Concern in Motorsports—A Literature Review," SAE Technical Paper 983026, 1998, https://doi.org/10.4271/983026.
8. Zhen, X., Wang, Y., Xu, S., Zhu, Y. et al., "The Engine Knock Analysis—An Overview," *Applied Energy* 92 (2012): 628-636.
9. Wang, Z., Liu, H., and Reitz, R.D., "Knocking Combustion in Spark-Ignition Engines," *Progress in Energy and Combustion Science* 61 (2017): 78-112.
10. Kalghatgi, G., "Knock Onset, Knock Intensity, Superknock and Preignition in Spark Ignition Engines," *International Journal of Engine Research* 19, no. 1 (2018): 7-20, https://doi.org/10.1177/1468087417736430.
11. Chapman, E.M. and Costanzo, V.S., "A Literature Review of Abnormal Ignition by Fuel and Lubricant Derivatives," *SAE Int. J. Engines* 9, no. 1 (2015): 107-142, https://doi.org/10.4271/2015-01-1869.
12. Kettering, C.F., "Fuel Research Developments," SAE Technical Paper 210012, 1921, https://doi.org/10.4271/210012.
13. Richards, P., *Automotive Fuels Reference Book*, 3rd ed. (Warrendale, PA: SAE International, 2014), ISBN:978-0-7680-0638-4.
14. Horning, H.L., "Effect of Compression on Detonation and Its Control," SAE Technical Paper 230033, 1923, https://doi.org/10.4271/230033.
15. Brooke, L., *Ford Model T: The Car That Put the World on Wheels* (Minneapolis, MN: Motorbooks, 2008), ISBN:978-0-7603-2728-9.
16. Dickinson, H.C., "Resume of Bureau of Standards Fuel Study," SAE Technical Paper 210004, 1921, https://doi.org/10.4271/210004.
17. Midgley, T. and Boyd, T.A., "Methods of Measuring Detonation in Engines," SAE Technical Paper 220004, 1922, https://doi.org/10.4271/220004.
18. Martin, E.J. and Caris, D.F., "A New Electrical Engine-Indicator," SAE Technical Paper 280050, 1928, https://doi.org/10.4271/280050.
19. Trowbridge, A., "Photographic Recording of Engine Data," SAE Technical Paper 220007, 1922, https://doi.org/10.4271/220007.
20. MacKenzie, D. and Honaman, R.K., "The Velocity of Flame Propagation in Engine Cylinders," SAE Technical Paper 200010, 1920, https://doi.org/10.4271/200010.
21. Clark, G.L. and Henne, A.L., "Ultraviolet Spectroscopy of Engine-Fuel Flames," SAE Technical Paper 270002, 1927, https://doi.org/10.4271/270002.
22. Cummings, H.K., "Methods of Measuring the Antiknock Value of Fuels," SAE Technical Paper 270003, 1927, https://doi.org/10.4271/270003.
23. Midgley, T. and Janeway, R., "Laws Governing Gaseous Detonation," SAE Technical Paper 230004, 1923, https://doi.org/10.4271/230004.
24. Bryson, B., *A Short History of Nearly Everything* (London: Transworld, 2003), ISBN:0-552-99704-8.
25. Hamilton, A., Reznikoff, P., and Burnham, G.M., "Tetra-Ethyl Lead," *Journal of the American Medical Association* 84, no. 20 (1925): 1481-1486, https://doi.org/10.1001/jama.1925.02660460017008.
26. Rosner, D. and Markowitz, G., "A 'Gift of God'?: The Public Health Controversy over Leaded Gasoline during the 1920s," *American Journal of Public Health* 75, no. 4 (1985): 344-352, https://doi.org/10.2105/ajph.75.4.344.
27. Sayers, R. and Fieldner, A., "Exhaust Gases from Engines Using Ethyl Gasoline," Tech. Rep., U.S. Bureau of Mines, February 1925.
28. Sayers, R., Fieldner, A., Yant, W., and Thomas, B., "Experimental Studies on the Effect of Ethyl Gasoline and Its Combustion Products," Tech. Rep. 597996515, U.S. Bureau of Mines, 1927.
29. Leake, J.P., Kolb, L., Schwartz, L., Lake, G.C. et al., "Investigation of Health Hazard from Tetraethyl Lead Gasoline," Tech. Rep. Public Health Bulletin No. 163, United States Public Health Service, June 1926.
30. Graham, E., "Detonation Specifications for Automotive Fuels," SAE Technical Paper 270006, 1927, https://doi.org/10.4271/270006.

31. Janeway, R.N., "Combustion Control by Cylinder-Head Design," SAE Technical Paper 290016, 1929, https://doi.org/10.4271/290016.
32. Barton, C.H., Sprake, C.H., and Stansfield, R., "Comparison of Antiknock Ratings Determined in Different Laboratories," SAE Technical Paper 300019, 1930, https://doi.org/10.4271/300019.
33. Campbell, J.M., Lovell, W.G., and Boyd, T.A., "Detonation Characteristics of Some of the Fuels Suggested as Standards of Antiknock Quality," SAE Technical Paper 300018, 1930, https://doi.org/10.4271/300018.
34. Barton, C.H., Sprake, C.H., Stansfield, R., and Thornycroft, O., "Knock Rating of Motor Fuels," SAE Technical Paper 310021, 1931, https://doi.org/10.4271/310021.
35. Kegerreis, C.S., "Carbureter Design for the C. F. R. Detonation Engine," SAE Technical Paper 310020, 1931, https://doi.org/10.4271/310020.
36. Graham, E., "Jacket and Cylinder-Head Temperature Effects upon Relative Knock-Ratings," SAE Technical Paper 310023, 1931, https://doi.org/10.4271/310023.
37. Campbell, J.M., Lovell, W.G., and Boyd, T.A., "Influence of Carbureter Setting and Spark Timing on Knock Ratings - Annual Meeting Paper," SAE Technical Paper 310025, 1931, https://doi.org/10.4271/310025.
38. Huf, H.F., Sabina, J.R., and Hill, J.B., "Effect of Sound Intensity on Knock Ratings," SAE Technical Paper 310026, 1931, https://doi.org/10.4271/310026.
39. Cooperative Fuel Research Committee, "CFR Research Method of Tests for Knock Characteristics of Motor Fuels," *SAE Transactions* 34 (1939): 277-280, http://www.jstor.org/stable/44467952.
40. ASTM International, "Standard Test Method for Research Octane Number of Spark-Ignition Engine Fuel," ASTM Standard 2699-19e1, Revised July 2019, www.astm.org.
41. Veal, C.B., Best, H.W., Campbell, J.M., and Holaday, W.M., "Antiknock Research Coordinates Laboratory and Road Tests," SAE Technical Paper 330015, 1933, https://doi.org/10.4271/330015.
42. ASTM International, "Standard Test Method for Motor Octane Number of Spark-Ignition Engine Fuel," ASTM Standard D2700-19e1, Revised July 2019, www.astm.org.
43. Veal, C.B., "C. F. R. Committee Report on 1934 Detonation Road Tests," SAE Technical Paper 350094, 1935, https://doi.org/10.4271/350094.
44. Boyd, T.A., "1937 Road Knock Tests," SAE Technical Paper 380145, 1938, https://doi.org/10.4271/380145.
45. Campbell, J.M. and Lovell, W.G., "Application of Statistical Concepts to the Knock-Rating Problem," SAE Technical Paper 380169, 1938, https://doi.org/10.4271/380169.
46. Beale, E. and Stansfield, R., "The Sunbury Knock Indicator," SAE Technical Paper 370118, 1937, https://doi.org/10.4271/370118.
47. Brooks, D.B. and Cleaton, R.B., "The Precision of Knock Rating - 1936-1938 - Report from Cooperative Fuel Research Committee," SAE Technical Paper 390176, 1939, https://doi.org/10.4271/390176.
48. Marvin, C.F., "Observations of Flame in an Engine," SAE Technical Paper 340112, 1934, https://doi.org/10.4271/340112.
49. Rassweiler, G.M. and Withrow, L., "Flame Temperatures Vary with Knock and Combustion-Chamber Position," SAE Technical Paper 350091, 1935, https://doi.org/10.4271/350091.
50. Withrow, L. and Rassweiler, G.M., "Slow Motion Shows Knocking and Non-Knocking Explosions," SAE Technical Paper 360126, 1936, https://doi.org/10.4271/360126.
51. Rassweiler, G.M. and Withrow, L., "Motion Pictures of Engine Flames Correlated with Pressure Cards," SAE Technical Paper 380139, 1938, https://doi.org/10.4271/380139.
52. Boyd, T.A., "Engine Flame Researches," SAE Technical Paper 390173, 1939, https://doi.org/10.4271/390173.
53. MacCoull, N. and Stanton, G.T., "The Measurement of Engine Knock by Electro-Acoustic Instruments," SAE Technical Paper 360104, 1936, https://doi.org/10.4271/360104.
54. Draper, C.S., "The Physical Effects of Detonation in a Closed Cylindrical Chamber," Tech. Rep. NACA-TR-493, National Advisory Committee for Aeronautics, 1935, https://ntrs.nasa.gov/citations/19930091567.
55. Draper, C., "Pressure Waves Accompanying Detonation in the Internal Combustion Engine," in *Power Plants and Propellers Session, Sixth Annual Meeting, I. Ae. S.*, Institute of Aeronautical Sciences, January 1938.
56. Rothrock, A.M. and Spencer, R.C., "A Photographic Study of Combustion and Knock in a Spark-Ignition Engine," Tech. Rep. NACA-TR-622, National Advisory Committee for Aeronautics, January 1938, https://ntrs.nasa.gov/citations/19930091697.
57. Heron, S.D., "Fuel Requirements of the Gasoline Aircraft-Engine," SAE Technical Paper 300024, 1930, https://doi.org/10.4271/300024.
58. Du Bois, R. and Cronstedt, V., "High Output in Aircraft Engines," SAE Technical Paper 370150, 1937, https://doi.org/10.4271/370150.
59. Nutt, A., "Detonation Rating of Aviation Fuels," SAE Technical Paper 330054, 1933, https://doi.org/10.4271/330054.
60. Veal, C.B., "Rating Aviation Fuels-in Full-Scale Aircraft Engines - A Report of the Cooperative Fuel Research Committee," SAE Technical Paper 360112, 1936, https://doi.org/10.4271/360112.
61. Cummings, H.K., "Rating Aviation Fuels in Full-Scale Aircraft Engines - Completion of First Program and Progress on Second Program-Report of the Cooperative Fuel Research Committee," SAE Technical Paper 380177, 1938, https://doi.org/10.4271/380177.
62. Stansfield, R. and Taylor, H.B., "A New Laboratory Method for Rating Aviation Fuels of High Octane Number," SAE Technical Paper 390018, 1939, https://doi.org/10.4271/390018.
63. ASTM International, "Standard Test Method for Supercharge Rating of Spark-Ignition Aviation Gasoline," ASTM Standard D909-18e1, Revised July 2018, www.astm.org.

64. Dillstrom, T., "A High-Power Spark-Ignition Fuel-Injection Engine," SAE Technical Paper 340117, 1934, https://doi.org/10.4271/340117.
65. Tsien, H.C., "Basic Problems in the Design of High-Output Aircraft Engines," SAE Technical Paper 380111, 1938, https://doi.org/10.4271/380111.
66. Douglas, C.E., *The Secret Horsepower Race—Western Front Fighter Engine Development* (Horncastle: Tempest Books, 2020), ISBN:978-1911658504.
67. Risk, T.H., "Factors Affecting the Antiknock Performance of Post-War Fuels," SAE Technical Paper 440169, 1944, https://doi.org/10.4271/440169.
68. Barnard, D.P. and Cragin, R.B., "Volatility Decreases and Availability of High Knock Rating Aviation Fuels," SAE Technical Paper 400120, 1940, https://doi.org/10.4271/400120.
69. Hives, E.W. and Smith, F.L., "High-Output Aircraft Engines," SAE Technical Paper 400133, 1940, https://doi.org/10.4271/400133.
70. Hubner, W.H., "Better Fuels for Better Engines …," SAE Technical Paper 400165, 1940, https://doi.org/10.4271/400165.
71. Campbell, J.M., Greenshields, R.J., and Holaday, W.M., "1940 Road Detonation Tests - (Compiled from Report 1 of The Cooperative Fuel Research Committee)," SAE Technical Paper 410107, 1941, https://doi.org/10.4271/410107.
72. Rothrock, A.M., "Fuel Rating - Its Relation to Engine Performance," SAE Technical Paper 410088, 1941, https://doi.org/10.4271/410088.
73. Brooks, D.B., "Development of Reference Fuel Scales for Knock Rating - Report of Coordinating Fuel Research Committee of Coordinating Research Council, Inc.," SAE Technical Paper 460230, 1946, https://doi.org/10.4271/460230.
74. Heron, S.D., "Mutual Adaptation of Aircraft Fuels and Engines," SAE Technical Paper 470214, 1947, https://doi.org/10.4271/470214.
75. Gay, E.J. and Mueller, H.T., "Fuel Antiknock Quality - A Basis for Selection of Compression Ratio," SAE Technical Paper 470238, 1947, https://doi.org/10.4271/470238.
76. Droegemueller, E.A., Hersey, D.S., and Kuhrt, W.A., "The Relation of Intake-Charge Cooling to Engine Performance," SAE Technical Paper 440214, 1944, https://doi.org/10.4271/440214.
77. Rowe, M.R. and Ladd, G.T., "Water Injection for Aircraft Engines," SAE Technical Paper 460192, 1946, https://doi.org/10.4271/460192.
78. Obert, E.F., "Detonation and Internal Coolants," SAE Technical Paper 480173, 1948, https://doi.org/10.4271/480173.
79. Miller, R., "Supercharging and Internal Cooling Cycle for High Output," *Transactions of the American Society of Mechanical Engineers* 69, no. 4 (1947): 453-464.
80. Streett, J.W., "The Detection of Detonation and Other Operating Abnormalities in Aircraft Engines by Means of Special Instrumentation," SAE Technical Paper 450012, 1945, https://doi.org/10.4271/450012.
81. Costa, P.J., "Detonation in Flight - Its Effect on Fuel Consumption and Engine Life," SAE Technical Paper 450191, 1945, https://doi.org/10.4271/450191.
82. Bogen, J.S. and Faust, W.J., "Aircraft Detonation Indicators," SAE Technical Paper 470233, 1947, https://doi.org/10.4271/470233.
83. Goffe, J.H. and Wheeler, J.W., "Development of Detonation Instrumentation for Automotive Vehicles," SAE Technical Paper 470245, 1947, https://doi.org/10.4271/470245.
84. Fiock, E.F., "The Present Status of Combustion Research," SAE Technical Paper 410122, 1941, https://doi.org/10.4271/410122.
85. Rothrock, A.M. and Spencer, R.C., "A High-Speed Motion-Picture Study of Normal Combustion, Knock and Preignition in a Spark-Ignition Engine," Tech. Rep. NACA-TR-704, National Advisory Committee for Aeronautics, January 1941, https://ntrs.nasa.gov/citations/19930091782.
86. Miller, C.D. and Olsen, H.L., "Identification of Knock in NACA High-Speed Photographs of Combustion in a Spark-Ignition Engine," Tech. Rep. NACA-TR-761, National Advisory Committee for Aeronautics, January 1943, https://ntrs.nasa.gov/citations/19930091840.
87. Miller, C.D., Olsen, H.L., Logan, J., Walter, O. et al., "Analysis of Spark-Ignition Engine Knock as Seen in Photographs Taken at 200,000 Frames Per Second," Tech. Rep. NACA-TR-857, National Advisory Committee for Aeronautics, January 1946, https://ntrs.nasa.gov/citations/19930091929.
88. Olsen, H.L. and Miller, C.D., "The Interdependence of Various Types of Autoignition and Knock," Tech. Rep. NACA-TR-912, National Advisory Committee for Aeronautics, January 1948, https://ntrs.nasa.gov/citations/19930091978.
89. Lovell, W.G., "Engine Knock and Molecular Structure of Hydrocarbons," SAE Technical Paper 480219, 1948, https://doi.org/10.4271/480219.
90. Kettering, C.F., "Fuels and Engines for Higher Power and Greater Efficiency," SAE Technical Paper 450195, 1945, https://doi.org/10.4271/450195.
91. Retailliau, E.R., Ricards, H.A., and Jones, M.C., "Precombustion Reaction in the Spark-Ignition Engine," SAE Technical Paper 500191, 1950, https://doi.org/10.4271/500191.
92. Pastell, D., "Precombustion Reactions in a Motored Engine," SAE Technical Paper 500198, 1950, https://doi.org/10.4271/500198.
93. Cornelius, W. and Caplan, J.D., "Some Effects of Fuel Structure, Tetraethyl Lead, and Engine Deposits on Precombustion Reactions in a Firing Engine," SAE Technical Paper 520250, 1952, https://doi.org/10.4271/520250.
94. Dauphin, R., Obiols, J., Serrano, D., Fenard, Y. et al., "Using RON Synergistic Effects to Formulate Fuels for Better Fuel Economy and Lower CO2 Emissions," SAE Technical Paper 2019-01-2155, 2019, https://doi.org/10.4271/2019-01-2155.

95. Levedahl, W.J. and Broida, H.P., "Emission Spectra on Autoignited Heptane-Air Mixtures," *Analytical Chemistry* 24, no. 11 (1952): 1776-1780, https://doi.org/10.1021/ac60071a019.
96. Mason, J. and Hesselberg, H., "Engine Knock as Influenced by Precombustion Reactions," SAE Technical Paper 540229, 1954, https://doi.org/10.4271/540229.
97. Sturgis, B.M., "Some Concepts of Knock and Antiknock Action," SAE Technical Paper 550249, 1955, https://doi.org/10.4271/550249.
98. Semenov, N., "Advances of Chemical Kinetics in the Soviet Union," *Nature* 151, no. 3824 (1943): 185-187, https://doi.org/10.1038/151185a0.
99. Taylor, C.F., Taylor, E.S., Livengood, J.C., Russell, W.A. et al., "Ignition of Fuels by Rapid Compression," SAE Technical Paper 500178, 1950, https://doi.org/10.4271/500178.
100. Livengood, J. and Wu, P., "Correlation of Autoignition Phenomena in Internal Combustion Engines and Rapid Compression Machines," *Symposium (International) on Combustion* 5, no. 1 (1955): 347-356.
101. Rifkin, E.B. and Walcutt, C., "A Basis for Understanding Antiknock Action," SAE Technical Paper 570046, 1957, https://doi.org/10.4271/570046.
102. Diggs, D., "Effect of Combustion Time on Knock in a Spark-Ignition Engine," SAE Technical Paper 530242, 1953, https://doi.org/10.4271/530242.
103. Meagher, R., Johnson, R.L., and Parthemore, K.G., "Correlation of Engine Noises With Combustion Phenomena," SAE Technical Paper 550269, 1955, https://doi.org/10.4271/550269.
104. Perry, R.H. and Lowther, H.V., "knock-knock: Spark Knock, Wild Ping, or Rumble?" SAE Technical Paper 590019, 1959, https://doi.org/10.4271/590019.
105. Hosteller, H.F. and Tuuri, W.R., "Knock, Rumble, and Ping," SAE Technical Paper 590020, 1959, https://doi.org/10.4271/590020.
106. Wiese, W.M., "If You Squeeze Them, Must They Scream?" SAE Technical Paper 590023, 1959, https://doi.org/10.4271/590023.
107. Warren, J.A. and Hinkamp, J.B., "New Instrumentation for Engine Combustion Studies," SAE Technical Paper 560059, 1956, https://doi.org/10.4271/560059.
108. Ricardo, H., "Some Early Reminiscences," SAE Technical Paper 550282, 1955, https://doi.org/10.4271/550282.
109. Pope, A.W., "Single-Cylinder Engine Fuel Research," SAE Technical Paper 590034, 1959, https://doi.org/10.4271/590034.
110. Buerstetta, F.D., Caputo, I.A., Corner, E.S., Korn, T.M. et al., "Are Octane Numbers and Hydrocarbon Type Enough?" SAE Technical Paper 600140, 1960, https://doi.org/10.4271/600140.
111. Bartholomew, E., "New Knock-Testing Methods Needed to Match Engine and Fuel Progress," SAE Technical Paper 610200, 1961, https://doi.org/10.4271/610200.
112. Brewster, B. and Kerley, R.V., "Automotive Fuels and Combustion Problems," SAE Technical Paper 630416, 1963, https://doi.org/10.4271/630416.
113. Gerard, P.L. and DiPerna, C.J., "Multifaceted Octane Numbers for Diverse Engine Requirements," SAE Technical Paper 650094, 1965, https://doi.org/10.4271/650094.
114. Fitch, F.B. and Thena, R.H., "Fuel Requirements of Passenger Cars Throughout the World," SAE Technical Paper 690210, 1969, https://doi.org/10.4271/690210.
115. Gluckstein, M. and Walcutt, C., "End-Gas Temperature-Pressure Histories and Their Relation to Knock," SAE Technical Paper 610044, 1961, https://doi.org/10.4271/610044.
116. Johnson, J.H., Myers, P.S., and Uyehara, O.A., "End-Gas Temperatures, Pressures, Reaction Rates, and Knock," SAE Technical Paper 650505, 1965, https://doi.org/10.4271/650505.
117. Hoffman, R.A., "A New Technique for Determining the Knocking Resistance of Fuels," SAE Technical Paper 610202, 1961, https://doi.org/10.4271/610202.
118. Taylor, C.F., "The Effects of Cylinder Size on Detonation and Octane Requirement," SAE Technical Paper 620522, 1962, https://doi.org/10.4271/620522.
119. Curry, S., "The Relationship Between Flame Propagation and Pressure Development During Knocking Combustion," SAE Technical Paper 630095, 1963, https://doi.org/10.4271/630095.
120. Haskell, W.W. and Bame, J.L., "Engine Knock - An End-Gas Explosion," SAE Technical Paper 650506, 1965, https://doi.org/10.4271/650506.
121. Graiff, L.B., "The Mode of Action of Tetraethyllead and Supplemental Antiknock Agents," SAE Technical Paper 660780, 1966, https://doi.org/10.4271/660780.
122. Patterson, C.C., "Contaminated and Natural Lead Environments of Man," *Archives of Environmental Health* 11, no. 3 (1965): 344-360, https://doi.org/10.1080/00039896.1965.10664229.
123. "An Act to Provide Research and Technical Assistance Relating to Air Pollution Control," *Public Law* 159, no. 360 (1955): 322-323.
124. "The Clean Air Act—An Act to Improve, Strengthen, and Accelerate Programs for the Prevention and Abatement of Air Pollution," *Public Law* 88, no. 206 (1963): 392-401.
125. "Motor Vehicle Air Pollution Control Act—An Act to Amend the Clean Air Act to Require Standards for Controlling the Emission of Pollutants from Certain Motor Vehicles, to Authorize a Research and Development Program with Respect to Solid-Waste Disposal, and for Other Purposes," *Public Law* 89, no. 271 (1965): 992-1001.
126. Burwell, W.G. and Olson, D.R., "The Spontaneous Ignition of Isooctane Air Mixtures under Steady Flow Conditions," SAE Technical Paper 650510, 1965, https://doi.org/10.4271/650510.
127. Jost, W. and Martinengo, A., "Recent Investigations of Reaction Processes by Means of Adiabatic Compression,"

SAE Technical Paper 660347, 1966, https://doi.org/10.4271/660347.

128. Quader, A.A., Myers, P.S., and Uyehara, O.A., "UV Absorbance Histories and Knock in a Spark Ignited Engine," SAE Technical Paper 690519, 1969, https://doi.org/10.4271/690519.
129. "Clean Air Amendments of 1970—An Act to Amend the Clean Air Act to Provide a More Effective Program to Improve the Quality of the Nation's Air," *Public Law* 91, no. 604 (1970): 1676-1713.
130. Engel, R., Hammer, D., Horton, R., Lane, N. et al., "Environmental Lead and Public Health," Tech. Rep. AP-90, Environmental Protection Agency, March 1971.
131. Office of Air Programs of the EPA and National Environmental Research Center, "Health Hazards of Lead," Tech. Rep. 400R72001, Environmental Protection Agency, April 1972.
132. Health Effects Branch of the EPA, "EPA's Position on the Health Effects of Airborne Lead," Tech. Rep. 736F72001, Environmental Protection Agency, November 1972.
133. EPA Office of Air Quality Planning and Standards, "National Ambient Air Quality Standard for Lead," Tech. Rep. EPA 600177502, Environmental Protection Agency, December 1977.
134. Angle, C.R. and McIntire, M.S., "Lead: Environmental Sources and Red Cell Toxicity in Urban Children," Tech. Rep. EPA-650/1-75-003, Environmental Protection Agency, June 1975.
135. Dage, E.L., "The Health and Environmental Impacts of Lead and an Assessment of a Need for Limitations," Tech. Rep. EPA-560/2-79-001, Environmental Protection Agency, April 1979.
136. Shelton, E.M., Whisman, M.L., and Woodward, P.W., "Trends in Motor Gasolines: 1942-1981," Tech. Rep. DOE/BETC/RI-82/4, United States of America Department of Energy, June 1982.
137. EPA Technology Assessment and Evaluation Branch, "Octane Requirements of 1975 Model Year Automobiles Fueled with Unleaded Gasoline," Tech. Rep. EPA-AA-TAEB 75-28, Environmental Protection Agency, August 1975.
138. Duke, L.C., Lestz, S.S., and Meyer, W.E., "The Relation Between Knock and Exhaust Emissions of a Spark Ignition Engine," SAE Technical Paper 700062, 1970, https://doi.org/10.4271/700062.
139. Hodges, J.L., "The Effect of Exhaust Recycle on Knock-Limited SI Engine Performance," SAE Technical Paper 750025, 1975, https://doi.org/10.4271/750025.
140. Morgan, C.R. and Hetrick, S.S., "The Effects of Engine Variables and Exhaust Gas Recirculation on Emissions, Fuel Economy, and Knock-Part II," SAE Technical Paper 760198, 1976, https://doi.org/10.4271/760198.
141. Gething, J.A. and Lestz, S.S., "Knocking and Performance Characteristics of Low Octane Primary Reference Fuels Blended with Methanol," SAE Technical Paper 780079, 1978, https://doi.org/10.4271/780079.
142. Roessler, W. and Muraszew, A., "Evaluation of Prechamber Spark Ignition Engine Concepts," Tech. Rep. EPA-650/2-75-023, Environmental Protection Agency, February 1975.
143. Blizard, N.C. and Keck, J.C., "Experimental and Theoretical Investigation of Turbulent Burning Model for Internal Combustion Engines," SAE Technical Paper 740191, 1974, https://doi.org/10.4271/740191.
144. Lancaster, D.R., "Effects of Engine Variables on Turbulence in a Spark-Ignition Engine," SAE Technical Paper 760159, 1976, https://doi.org/10.4271/760159.
145. Lancaster, D.R., Krieger, R.B., Sorenson, S.C., and Hull, W.L., "Effects of Turbulence on Spark-Ignition Engine Combustion," SAE Technical Paper 760160, 1976, https://doi.org/10.4271/760160.
146. Nagayama, I., Araki, Y., and Iioka, Y., "Effects of Swirl and Squish on S.I. Engine Combustion and Emission," SAE Technical Paper 770217, 1977, https://doi.org/10.4271/770217.
147. Allwood, H.I.S., Harrow, G.A., and Rose, L.J., "A Multichannel Electronic Gating and Counting System for the Study of Cyclic Dispersion, Knock and Weak Mixture Combustion in Spark Ignition Engines," SAE Technical Paper 700063, 1970, https://doi.org/10.4271/700063.
148. Barton, R.K., Lestz, S.S., and Duke, L.C., "Knock Intensity as a Function of Engine Rate of Pressure Change," SAE Technical Paper 700061, 1970, https://doi.org/10.4271/700061.
149. Chiampo, P., de Cristofaro, F., and Gozzelino, R., "Relationship of Flame Front Pattern to Pressure and High-Speed Knock on Commercial Engines," SAE Technical Paper 730087, 1973, https://doi.org/10.4271/730087.
150. Ferraro, C.V., "A Knock Intensity Meter Based on Kinetic Criterion," SAE Technical Paper 780154, 1978, https://doi.org/10.4271/780154.
151. Arrigoni, V., Cornetti, G.M., Spallanzani, G., Calvi, F. et al., "High Speed Knock in S.I. Engines," SAE Technical Paper 741056, 1974, https://doi.org/10.4271/741056.
152. Cornetti, G.M., De Cristofaro, F., and Gozzelino, R., "Engine Failure and High Speed Knock," SAE Technical Paper 770147, 1977, https://doi.org/10.4271/770147.
153. Arrigoni, V., Calvi, G.F., Gaetani, B., Giavazzi, F. et al., "Recent Advances in the Detection of Knock in S.I. Engines," SAE Technical Paper 780153, 1978, https://doi.org/10.4271/780153.
154. Randall, K.W. and Powell, J.D., "A Cylinder Pressure Sensor for Spark Advance Control and Knock Detection," SAE Technical Paper 790139, 1979, https://doi.org/10.4271/790139.
155. Kondo, M., Niimi, A., and Nakamura, T., "Indiscope—A New Combustion Pressure Indicator with Washer Transducers," SAE Technical Paper 750883, 1975, https://doi.org/10.4271/750883.
156. Kraus, B., Godici, P.E., and King, W., "Reduction of Octane Requirement by Knock Sensor Spark Retard System," SAE Technical Paper 780155, 1978, https://doi.org/10.4271/780155.

157. Wallace, T.F., "Buick's Turbocharged V-6 Powertrain for 1978," SAE Technical Paper 780413, 1978, https://doi.org/10.4271/780413.

158. Douaud, A.M. and Eyzat, P., "Four-Octane-Number Method for Predicting the Anti-Knock Behavior of Fuels and Engines," SAE Technical Paper 780080, 1978, https://doi.org/10.4271/780080.

159. Halstead, M.P., Kirsch, L.J., Prothero, A., and Quinn, C.P., "A Mathematical Model for Hydrocarbon Autoignition at High Pressures," *Proc. R. Soc. Lond. A* 346 (1975): 515-538.

160. Kirsch, L. and Quinn, C., "A Fundamentally Based Model of Knock in the Gasoline Engine," *Symposium (International) on Combustion* 16, no. 1 (1977): 233-244.

161. Boccadoro, Y. and Kizer, T., "Adaptive Spark Control with Knock Detection," SAE Technical Paper 840447, 1984, https://doi.org/10.4271/840447.

162. Decker, H. and Gruber, H.-U., "Knock Control of Gasoline Engines - A Comparison of Solutions and Tendencies, with Special Reference to Future European Emission Legislation," SAE Technical Paper 850298, 1985, https://doi.org/10.4271/850298.

163. Gillbrand, P., "Knock Detector System Controlling Turbocharger Boost Pressure," SAE Technical Paper 800833, 1980, https://doi.org/10.4271/800833.

164. Nakamura, N., Ohno, E., Kanamaru, M., and Funayama, T., "Detection of Higher Frequency Vibration to Improve Knock Controllability," SAE Technical Paper 871912, 1987, https://doi.org/10.4271/871912.

165. Priede, T. and Dutkiewicz, R.K., "The Effect of Normal Combustion and Knock on Gasoline Engine Noise," SAE Technical Paper 891126, 1989, https://doi.org/10.4271/891126.

166. Collings, N., Dinsdale, S., and Eade, D., "Knock Detection by Means of the Spark Plug," SAE Technical Paper 860635, 1986, https://doi.org/10.4271/860635.

167. Sawamoto, K., Kawamura, Y., Kita, T., and Matsushita, K., "Individual Cylinder Knock Control by Detecting Cylinder Pressure," SAE Technical Paper 871911, 1987, https://doi.org/10.4271/871911.

168. Amann, C.A., "Classical Combustion Diagnostics for Engine Research," SAE Technical Paper 850395, 1985, https://doi.org/10.4271/850395.

169. Amann, C., "Cylinder-Pressure Measurement and Its Use in Engine Research," SAE Technical Paper 852067, 1985, https://doi.org/10.4271/852067.

170. McNally, M.J., Benson, J.D., Callison, J.C., Graham, J.P. et al., "Coordinating Research Council Quantifying Performance of Knock-Sensor Equipped Vehicles with Varying Octane Level Fuels," SAE Technical Paper 892037, 1989, https://doi.org/10.4271/892037.

171. Sutton, D.L. and Williams, D., "Knock Protection—Future Fuels and Engines," SAE Technical Paper 841289, 1984, https://doi.org/10.4271/841289.

172. By, A., Kempinski, B., and Rife, J.M., "Knock in Spark Ignition Engines," SAE Technical Paper 810147, 1981, https://doi.org/10.4271/810147.

173. Leppard, W.R., "Individual-Cylinder Knock Occurrence and Intensity in Multicylinder Engines," SAE Technical Paper 820074, 1982, https://doi.org/10.4271/820074.

174. Chun, K.M. and Heywood, J.B., "Characterization of Knock in a Spark-Ignition Engine," SAE Technical Paper 890156, 1989, https://doi.org/10.4271/890156.

175. Iwata, T., Sakakibara, K., and Haragucti, H., "A New Method to Automatically Optimize the Knock Detection Level in the Knock Control System," SAE Technical Paper 891964, 1989, https://doi.org/10.4271/891964.

176. Lee, W. and Schaefer, H.J., "Analysis of Local Pressures, Surface Temperatures and Engine Damages under Knock Conditions," SAE Technical Paper 600140, 1983, https://doi.org/10.4271/830508.

177. Nakagawa, Y., Takagi, Y., Itoh, T., and Iijima, T., "Laser Shadowgraphic Analysis of Knocking in S.I. Engine," SAE Technical Paper 845001, 1984, https://doi.org/10.4271/845001.

178. Najt, P.M., "Evaluating Threshold Knock with a Semi-Empirical Model—Initial Results," SAE Technical Paper 872149, 1987, https://doi.org/10.4271/872149.

179. Spicher, U. and Kollmeier, H.-P., "Detection of Flame Propagation During Knocking Combustion by Optical Fiber Diagnostics," SAE Technical Paper 861532, 1986, https://doi.org/10.4271/861532.

180. Checkel, M.D. and Dale, J.D., "Computerized Knock Detection from Engine Pressure Records," SAE Technical Paper 860028, 1986, https://doi.org/10.4271/860028.

181. Ando, H., Takemura, J., and Koujina, E., "A Knock Anticipating Strategy Basing on the Real-Time Combustion Mode Analysis," SAE Technical Paper 890882, 1989, https://doi.org/10.4271/890882.

182. Harrington, J.A., "Water Addition to Gasoline-Effect on Combustion, Emissions, Performance, and Knock," SAE Technical Paper 820314, 1982, https://doi.org/10.4271/820314.

183. Klimstra, J., "The Knock Severity Index - A Proposal for a Knock Classification Method," SAE Technical Paper 841335, 1984, https://doi.org/10.4271/841335.

184. Iwashita, Y. and Saito, A., "Observation of Knock Using a High Speed Shutter TV Camera System," SAE Technical Paper 831696, 1983, https://doi.org/10.4271/831696.

185. Hayashi, T., Taki, M., Kojima, S., and Kondo, T., "Photographic Observation of Knock with a Rapid Compression and Expansion Machine," SAE Technical Paper 841336, 1984, https://doi.org/10.4271/841336.

186. Takagi, Y., Itoh, T., and Iijima, T., "An Analytical Study on Knocking Heat Release and Its Control in a Spark Ignition Engine," SAE Technical Paper 880196, 1988, https://doi.org/10.4271/880196.

187. Sakai, H., Noguchi, H., Kawauchi, M., and Kanesaka, H., "A New Type of Miller Supercharging System for High-Speed Engines - Part 1 Fundamental Considerations and Application to Gasoline Engines," SAE Technical Paper 851522, 1985, https://doi.org/10.4271/851522.

188. Schäpertöns, H. and Lee, W., "Multidimensional Modelling of Knocking Combustion in SI Engines," SAE Technical Paper 850502, 1985, https://doi.org/10.4271/850502.
189. Zeldovich, Y., "Regime Classification of an Exothermic Reaction with Nonuniform Initial Conditions," *Combustion and Flame* 39, no. 2 (1980): 211-214.
190. Oppenheim, A.K., "The Knock Syndrome—Its Cures and Its Victims," SAE Technical Paper 841339, 1984, https://doi.org/10.4271/841339.
191. Oppenheim, A., "Dynamic Features of Combustion," *Philosophical Transactions of the Royal Society of London. Series A* 315 (1985): 471-508.
192. Maly, R. and Ziegler, G., "Thermal Combustion Modeling — Theoretical and Experimental Investigation of the Knocking Process," SAE Technical Paper 820759, 1982, https://doi.org/10.4271/820759.
193. Cuttler, D. and Girgis, N., "Photography of Combustion During Knocking Cycles in Disc and Compact Chambers," SAE Technical Paper 880195, 1988, https://doi.org/10.4271/880195.
194. Witze, P.O., Martin, J.K., and Borgnakke, C., "Measurements and Predictions of the Precombustion Fluid Motion and Combustion Rates in a Spark Ignition Engine," SAE Technical Paper 831697, 1983, https://doi.org/10.4271/831697.
195. Gosman, A.D., Tsui, Y.Y., and Vafidis, C., "Flow in a Model Engine with a Shrouded Valve—A Combined Experimental and Computational Study," SAE Technical Paper 850498, 1985, https://doi.org/10.4271/850498.
196. Kent, J.C., Mikulec, A., Rimal, L., Adamczyk, A. et al., "Observations on the Effects of Intake-Generated Swirl and Tumble on Combustion Duration," SAE Technical Paper 892096, 1989, https://doi.org/10.4271/892096.
197. Heywood, J.B., *Internal Combustion Engine Fundamentals* (New York: McGraw Hill Education, 2017), ISBN:978-0070286375.
198. Otobe, Y., Goto, O., Miyano, H., Kawamoto, M. et al., "Honda Formula One Turbo-Charged V-6 1.5L Engine," SAE Technical Paper 890877, 1989, https://doi.org/10.4271/890877.
199. Maly, R.R., Klein, R., Peters, N., and Konig, G., "Theoretical and Experimental Investigation of Knock Induced Surface Destruction," SAE Technical Paper 900025, 1990, https://doi.org/10.4271/900025.
200. Konig, G. and Sheppard, C.G.W., "End Gas Autoignition and Knock in a Spark Ignition Engine," SAE Technical Paper 902135, 1990, https://doi.org/10.4271/902135.
201. König, G., Maly, R.R., Bradley, D., Lau, A.K.C. et al., "Role of Exothermic Centres on Knock Initiation and Knock Damage," SAE Technical Paper 902136, 1990, https://doi.org/10.4271/902136.
202. Herweg, R. and Maly, R.R., "A Fundamental Model for Flame Kernel Formation in S. I. Engines," SAE Technical Paper 922243, 1992, https://doi.org/10.4271/922243.
203. Pan, J., Sheppard, C.G.W., Tindall, A., Berzins, M. et al., "End Gas Inhomogeneity, Autoignition and Knock," SAE Technical Paper 982616, 1998, https://doi.org/10.4271/982616.
204. Spicher, U., Kröger, H., and Ganser, J., "Detection of Knocking Combustion Using Simultaneously High-Speed Schlieren Cinematography and Multi Optical Fiber Technique," SAE Technical Paper 912312, 1991, https://doi.org/10.4271/912312.
205. Westbrook, C.K., Pitz, W.J., and Leppard, W.R., "The Autoignition Chemistry of Paraffinic Fuels and Pro-Knock and Anti-Knock Additives: A Detailed Chemical Kinetic Study," SAE Technical Paper 912314, 1991, https://doi.org/10.4271/912314.
206. Ronney, P., Shoda, M., Waida, S., Westbrook, C. et al., "Knock Characteristics of Liquid and Gaseous Fuels in Lean Mixtures," SAE Technical Paper 912311, 1991, https://doi.org/10.4271/912311.
207. Brussovansky, S., Heywood, J.B., and Keck, J.C., "Predicting the Effects of Air and Coolant Temperature, Deposits, Spark Timing and Speed on Knock in Spark Ignition Engines," SAE Technical Paper 922324, 1992, https://doi.org/10.4271/922324.
208. Nakano, M., Nakahara, S., Akihama, K., Kubo, S. et al., "Predictions of the Knock Onset and the Effects of Heat Release Pattern and Unburned Gas Temperature on Torque at Knock Limit in S.I. Engines," SAE Technical Paper 952408, 1995, https://doi.org/10.4271/952408.
209. Blunsdon, C.A. and Dent, J., "The Simulation of Autoignition and Knock in a Spark Ignition Engine with Disk Geometry," SAE Technical Paper 940524, 1994, https://doi.org/10.4271/940524.
210. Kalghatgi, G.T., Snowdon, P., and McDonald, C.R., "Studies of Knock in a Spark Ignition Engine with "CARS" Temperature Measurements and Using Different Fuels," SAE Technical Paper 950690, 1995, https://doi.org/10.4271/950690.
211. Shoji, H., Saima, A., and Shiino, K., "Simultaneous Measurement of Light Emission and Absorption Behavior of Unburned Gas During Knocking Operation," SAE Technical Paper 932754, 1993, https://doi.org/10.4271/932754.
212. Golombok, M., Kalghatgi, G.T., and Tindall, A., "Heat Release and Knock in Paraffinic and Aromatic Fuels and the Effect of an Ashless Anti-knock Additive," SAE Technical Paper 952405, 1995, https://doi.org/10.4271/952405.
213. Kaneyasu, M., Kurihara, N., Katogi, K., and Tokuda, H., "Engine Knock Detection Using Multi-Spectrum Method," SAE Technical Paper 920702, 1992, https://doi.org/10.4271/920702.
214. Samimy, B., Rizzoni, G., and Leisenring, K.C., "Improved Knock Detection by Advanced Signal Processing," SAE Technical Paper 950845, 1995, https://doi.org/10.4271/950845.
215. Scholl, D., Russ, S., and Stockhausen, W., "Detection of Spark Knock Oscillations: Dependence on Combustion Temperature," SAE Technical Paper 970038, 1997, https://doi.org/10.4271/970038.

216. Burgdorf, K. and Karlström, A., "Using Multi-Rate Filter Banks to Detect Internal Combustion Engine Knock," SAE Technical Paper 971670, 1997, https://doi.org/10.4271/971670.
217. Burgdorf, K. and Denbratt, I., "Comparison of Cylinder Pressure Based Knock Detection Methods," SAE Technical Paper 972932, 1997, https://doi.org/10.4271/972932.
218. Burgdorf, K., "A Contribution to Knock Statistics," SAE Technical Paper 982475, 1998, https://doi.org/10.4271/982475.
219. Burgdorf, K. and Chomiak, J., "A New Knock Form - An Experimental Study," SAE Technical Paper 982589, 1998, https://doi.org/10.4271/982589.
220. Stiebels, B., Schreiber, M., and Sakak, A.S., "Development of a New Measurement Technique for the Investigation of End-Gas Autoignition and Engine Knock," SAE Technical Paper 960827, 1996, https://doi.org/10.4271/960827.
221. Liiva, P.M., Valentine, J.N., Cobb, J.M., and Acker, W.P., "Use of Multiple Pressure Transducers to Find In-Cylinder Knock Location," SAE Technical Paper 922368, 1992, https://doi.org/10.4271/922368.
222. Gschweitl, K., Gotthard, E., and Kampitsch, A., "Real Time Knock Analysis for Automatic Engine Mapping and Calibration," SAE Technical Paper 942399, 1994, https://doi.org/10.4271/942399.
223. Grandin, B., Ångström, H.-E., Stålhammar, P., and Olofsson, E., "Knock Suppression in a Turbocharged SI Engine by Using Cooled EGR," SAE Technical Paper 982476, 1998, https://doi.org/10.4271/982476.
224. Ueda, T., Okumura, T., Sugiura, S., and Kojima, S., "Effects of Squish Area Shape on Knocking in a Four-Valve Spark Ignition Engine," SAE Technical Paper 1999-01-1494, 1999, https://doi.org/10.4271/1999-01-1494.
225. Goto, T., Hatamura, K., Takizawa, S., Hayama, N. et al., "Development of V6 Miller Cycle Gasoline Engine," SAE Technical Paper 940198, 1994, https://doi.org/10.4271/940198.
226. Hitomi, M., Sasaki, J., Hatamura, K., and Yano, Y., "Mechanism of Improving Fuel Efficiency by Miller Cycle and Its Future Prospect," SAE Technical Paper 950974, 1995, https://doi.org/10.4271/950974.
227. Ueda, N., Sakai, H., Iso, N., and Sasaki, J., "A Naturally Aspirated Miller Cycle Gasoline Engine - Its Capability of Emission, Power and Fuel Economy," SAE Technical Paper 960589, 1996, https://doi.org/10.4271/960589.
228. Iwamoto, Y., Noma, K., Nakayama, O., Yamauchi, T. et al., "Development of Gasoline Direct Injection Engine," SAE Technical Paper 970541, 1997, https://doi.org/10.4271/970541.
229. Harada, J., Tomita, T., Mizuno, H., Mashiki, Z. et al., "Development of Direct Injection Gasoline Engine," SAE Technical Paper 970540, 1997, https://doi.org/10.4271/970540.
230. Yang, J. and Anderson, R.W., "Fuel Injection Strategies to Increase Full-Load Torque Output of a Direct-Injection SI Engine," SAE Technical Paper 980495, 1998, https://doi.org/10.4271/980495.
231. Anderson, W., Yang, J., Brehob, D.D., Vallance, J.K. et al., "Understanding the Thermodynamics of Direct Injection Spark Ignition (DISI) Combustion Systems: An Analytical and Experimental Investigation," SAE Technical Paper 962018, 1996, https://doi.org/10.4271/962018.
232. Willand, J., Nieberding, R.-G., Vent, G., and Enderle, C., "The Knocking Syndrome - Its Cure and Its Potential," SAE Technical Paper 982483, 1998, https://doi.org/10.4271/982483.
233. Töpfer, G., Reissing, J., Weimar, H.-J., and Spicher, U., "Optical Investigation of Knocking Location on S.I.-Engines with Direct-Injection," SAE Technical Paper 2000-01-0252, 2000, https://doi.org/10.4271/2000-01-0252.
234. Philipp, H., Hirsch, A., Baumgartner, M., Fernitz, G. et al., "Localization of Knock Events in Direct Injection Gasoline Engines," SAE Technical Paper 2001-01-1199, 2001, https://doi.org/10.4271/2001-01-1199.
235. Westin, F., Grandin, B., and Ångström, H.-E., "The Influence of Residual Gases on Knock in Turbocharged SI-Engines," SAE Technical Paper 2000-01-2840, 2000, https://doi.org/10.4271/2000-01-2840.
236. Stenlåås, O., Einewall, P., Egnell, R., and Johansson, B., "Measurement of Knock and Ion Current in a Spark Ignition Engine with and without NO Addition to the Intake Air," SAE Technical Paper 2003-01-0639, 2003, https://doi.org/10.4271/2003-01-0639.
237. Burluka, A.A., Liu, K., Sheppard, C., Smallbone, A.J. et al., "The Influence of Simulated Residual and NO Concentrations on Knock Onset for PRFs and Gasolines," SAE Technical Paper 2004-01-2998, 2004, https://doi.org/10.4271/2004-01-2998.
238. Grandin, B. and Denbratt, I., "The Effect of Knock on Heat Transfer in SI Engines," SAE Technical Paper 2002-01-0238, 2002, https://doi.org/10.4271/2002-01-0238.
239. Grandin, B., Denbratt, I., Bood, J., Brackmann, C. et al., "Heat Release in the End-Gas Prior to Knock in Lean, Rich and Stoichiometric Mixtures With and Without EGR," SAE Technical Paper 2002-01-0239, 2002, https://doi.org/10.4271/2002-01-0239.
240. Gogan, A., Sundén, B., Lehtiniemi, H., and Mauss, F., "Stochastic Model for the Investigation of the Influence of Turbulent Mixing on Engine Knock," SAE Technical Paper 2004-01-2999, 2004, https://doi.org/10.4271/2004-01-2999.
241. Sjöberg, M. and Dec, J.E., "Effects of Engine Speed, Fueling Rate, and Combustion Phasing on the Thermal Stratification Required to Limit HCCI Knocking Intensity," SAE Technical Paper 2005-01-2125, 2005, https://doi.org/10.4271/2005-01-2125.
242. Aleiferis, P.G., Taylor, A.M.K.P., Whitelaw, J.H., Ishii, K. et al., "Cyclic Variations of Initial Flame Kernel Growth in a Honda VTEC-E Lean-Burn Spark-Ignition Engine," SAE Technical Paper 2000-01-1207, 2000, https://doi.org/10.4271/2000-01-1207.
243. Zhao, F., Harrington, D.L., and Lai, M.D., *Automotive Gasoline Direct-Injection Engines* (Warrendale, PA: SAE International, 2002), ISBN:978-0-7680-0882-1.

244. Yi, J., Wooldridge, S., Coulson, G., Hilditch, J. et al., "Development and Optimization of the Ford 3.5L V6 EcoBoost Combustion System," *SAE Int. J. Engines* 2, no. 1 (2009): 1388-1407, https://doi.org/10.4271/2009-01-1494.

245. Bradley, D., Morley, C., Gu, X.J., and Emerson, D.R., "Amplified Pressure Waves During Autoignition: Relevance to CAI Engines," SAE Technical Paper 2002-01-2868, 2002, https://doi.org/10.4271/2002-01-2868.

246. Eng, J.A., "Characterization of Pressure Waves in HCCI Combustion," SAE Technical Paper 2002-01-2859, 2002, https://doi.org/10.4271/2002-01-2859.

247. Bradley, D. and Kalghatgi, G., "Influence of Autoignition Delay Time Characteristics of Different Fuels on Pressure Waves and Knock in Reciprocating Engines," *Combustion and Flame* 156, no. 12 (2009): 2307-2318.

248. Hyvönen, J., Haraldsson, G., and Johansson, B., "Operating Conditions Using Spark Assisted HCCI Combustion During Combustion Mode Transfer to SI in a Multi-Cylinder VCR-HCCI Engine," SAE Technical Paper 2005-01-0109, 2005, https://doi.org/10.4271/2005-01-0109.

249. Urushihara, T., Yamaguchi, K., Yoshizawa, K., and Itoh, T., "A Study of a Gasoline-Fueled Compression Ignition Engine - Expansion of HCCI Operation Range Using SI Combustion as a Trigger of Compression Ignition," SAE Technical Paper 2005-01-0180, 2005, https://doi.org/10.4271/2005-01-0180.

250. Suzuki, T., Ohara, H., Kakishima, A., Yoshida, K. et al., "A Study of Knocking Using Ion Current and Light Emission," SAE Technical Paper 2003-32-0038, 2003, https://doi.org/10.4271/2003-32-0038.

251. Hirooka, H., Mori, S., and Shimizu, R., "Effects of High Turbulence Flow on Knock Characteristics," SAE Technical Paper 2004-01-0977, 2004, https://doi.org/10.4271/2004-01-0977.

252. Shinagawa, T., Okumura, T., Furuno, S., and Kim, K.-O., "Effects of Hydrogen Addition to SI Engine on Knock Behavior," SAE Technical Paper 2004-01-1851, 2004, https://doi.org/10.4271/2004-01-1851.

253. Zhang, Z. and Tomota, E., "A New Diagnostic Method of Knocking in a Spark-Ignition Engine Using the Wavelet Transform," SAE Technical Paper 2000-01-1801, 2000, https://doi.org/10.4271/2000-01-1801.

254. Carstens-Behrens, S., Urlaub, M., Böhme, J.F., Förster, J. et al., "FEM Approximation of Internal Combustion Chambers for Knock Investigations," SAE Technical Paper 2002-01-0237, 2002, https://doi.org/10.4271/2002-01-0237.

255. Noubari, H.A. and Dumont, G.A., "Towards an Improved Knock Detection and Quantification Using Wavelets and Entropy-Based Noise Compensation," SAE Technical Paper 2005-01-2269, 2005, https://doi.org/10.4271/2005-01-2269.

256. Borg, J.M., Saikalis, G., Oho, S., and Cheok, K.C., "Knock Signal Analysis Using the Discrete Wavelet Transform," SAE Technical Paper 2006-01-0226, 2006, https://doi.org/10.4271/2006-01-0226.

257. Borg, J.M. and Alkidas, A.C., "Characterization of Autoignition in a Knocking SI Engine Using Heat Release Analysis," SAE Technical Paper 2006-01-3341, 2006, https://doi.org/10.4271/2006-01-3341.

258. Worret, R., Bernhardt, S., Schwarz, F., and Spicher, U., "Application of Different Cylinder Pressure Based Knock Detection Methods in Spark Ignition Engines," SAE Technical Paper 2002-01-1668, 2002, https://doi.org/10.4271/2002-01-1668.

259. Corti, E. and Moro, D., "Knock Indexes Thresholds Setting Methodology," SAE Technical Paper 2007-01-1508, 2007, https://doi.org/10.4271/2007-01-1508.

260. Hettinger, A. and Kulzer, A., "A New Method to Detect Knocking Zones," SAE Technical Paper 2009-01-0698, 2009, https://doi.org/10.4271/2009-01-0698.

261. Cavina, N., Corti, E., Minelli, G., Moro, D. et al., "Knock Indexes Normalization Methodologies," SAE Technical Paper 2006-01-2998, 2006, https://doi.org/10.4271/2006-01-2998.

262. Naber, J., Blough, J.R., Frankowski, D., Goble, M. et al., "Analysis of Combustion Knock Metrics in Spark-Ignition Engines," SAE Technical Paper 2006-01-0400, 2006, https://doi.org/10.4271/2006-01-0400.

263. Mittal, V., Revier, B.M., and Heywood, J.B., "Phenomena that Determine Knock Onset in Spark-Ignition Engines," SAE Technical Paper 2007-01-0007, 2007, https://doi.org/10.4271/2007-01-0007.

264. Abhijit, A. and Naber, J., "Ionization Signal Response during Combustion Knock and Comparison to Cylinder Pressure for SI Engines," SAE Technical Paper 2008-01-0981, 2008, https://doi.org/10.4271/2008-01-0981.

265. Zhu, G.G., Haskara, I., and Winkelman, J., "Stochastic Limit Control and Its Application to Knock Limit Control Using Ionization Feedback," SAE Technical Paper 2005-01-0018, 2005, https://doi.org/10.4271/2005-01-0018.

266. Castagné, M., Dumas, J.P., Henriot, S., Lafossas, F.A. et al., "New Knock Localization Methodology for SI Engines," SAE Technical Paper 2003-01-1118, 2003, https://doi.org/10.4271/2003-01-1118.

267. Rothe, M., Heidenreich, T., Spicher, U., and Schubert, A., "Knock Behavior of SI-Engines: Thermodynamic Analysis of Knock Onset Locations and Knock Intensities," SAE Technical Paper 2006-01-0225, 2006, https://doi.org/10.4271/2006-01-0225.

268. Kalghatgi, G., "Fuel Anti-Knock Quality - Part I. Engine Studies," SAE Technical Paper 2001-01-3584, 2001, https://doi.org/10.4271/2001-01-3584.

269. Kalghatgi, G.T., "Fuel Anti-Knock Quality - Part II. Vehicle Studies - How Relevant Is Motor Octane Number (MON) in Modern Engines?" SAE Technical Paper 2001-01-3585, 2001, https://doi.org/10.4271/2001-01-3585.

270. Mittal, V. and Heywood, J.B., "The Shift in Relevance of Fuel RON and MON to Knock Onset in Modern SI Engines Over the Last 70 Years," SAE Technical Paper 2009-01-2622, 2009, https://doi.org/10.4271/2009-01-2622.

271. Milpied, J., Jeuland, N., Plassat, G., Guichaous, S. et al., "Impact of Fuel Properties on the Performances and Knock Behaviour of a Downsized Turbocharged DI SI Engine -

Focus on Octane Numbers and Latent Heat of Vaporization," SAE Technical Paper 2009-01-0324, 2009, https://doi.org/10.4271/2009-01-0324.

272. Nakama, K., Kusaka, J., and Daisho, Y., "Effect of Ethanol on Knock in Spark Ignition Gasoline Engines," SAE Technical Paper 2008-32-0020, 2008, https://doi.org/10.4271/2008-32-0020.
273. Topinka, J.A., Gerty, M.D., Heywood, J.B., and Keck, J.C., "Knock Behavior of a Lean-Burn, H2 and CO Enhanced, SI Gasoline Engine Concept," SAE Technical Paper 2004-01-0975, 2004, https://doi.org/10.4271/2004-01-0975.
274. Swarts, A., Yates, A., Viljoen, C., and Coetzer, R., "Standard Knock Intensity Revisited: Atypical Burn Rate Characteristics Identified in the CFR Octane Rating Engine," SAE Technical Paper 2004-01-1850, 2004, https://doi.org/10.4271/2004-01-1850.
275. Elmqvist, C., Lindström, F., Ångström, H.-E., Grandin, B. et al., "Optimizing Engine Concepts by Using a Simple Model for Knock Prediction," SAE Technical Paper 2003-01-3123, 2003, https://doi.org/10.4271/2003-01-3123.
276. Noda, T., Hasegawa, K., Kubo, M., and Itoh, T., "Development of Transient Knock Prediction Technique by Using a Zero-Dimensional Knocking Simulation with Chemical Kinetics," SAE Technical Paper 2004-01-0618, 2004, https://doi.org/10.4271/2004-01-0618.
277. Yates, A.D.B., Swarts, A., and Viljoen, C.L., "Correlating Auto-Ignition Delays and Knock-Limited Spark-Advance Data for Different Types of Fuel," SAE Technical Paper 2005-01-2083, 2005, https://doi.org/10.4271/2005-01-2083.
278. Mehl, M., Faravelli, T., Ranzi, E., Lucchini, T. et al., "Kinetic Modeling of Knock Properties in Internal Combustion Engines," SAE Technical Paper 2006-01-3239, 2006, https://doi.org/10.4271/2006-01-3239.
279. D'Errico, G., Lucchini, T., Onorati, A., Mehl, M. et al., "Development and Experimental Validation of a Combustion Model with Detailed Chemistry for Knock Predictions," SAE Technical Paper 2007-01-0938, 2007, https://doi.org/10.4271/2007-01-0938.
280. Bozza, F., Siano, D., and Torella, E., "Cycle-by-Cycle Analysis, Knock Modeling and Spark-Advance Setting of a "Downsized" Spark-Ignition Turbocharged Engine," SAE Technical Paper 2009-24-0020, 2009, https://doi.org/10.4271/2009-24-0020.
281. Hattrell, T., Sheppard, C.G.W., Burluka, A.A., Neumeister, J. et al., "Burn Rate Implications of Alternative Knock Reduction Strategies for Turbocharged SI Engines," SAE Technical Paper 2006-01-1110, 2006, https://doi.org/10.4271/2006-01-1110.
282. Liang, L., Reitz, R.D., Iyer, C.O., and Yi, J., "Modeling Knock in Spark-Ignition Engines Using a G-equation Combustion Model Incorporating Detailed Chemical Kinetics," SAE Technical Paper 2007-01-0165, 2007, https://doi.org/10.4271/2007-01-0165.
283. Eckert, P., Kong, S.-C., and Reitz, R.D., "Modeling Autoignition and Engine Knock Under Spark Ignition Conditions," SAE Technical Paper 2003-01-0011, 2003, https://doi.org/10.4271/2003-01-0011.
284. Corti, E. and Forte, C., "Combination of In-Cylinder Pressure Signal Analysis and CFD Simulation for Knock Detection Purposes," SAE Technical Paper 2009-24-0019, 2009, https://doi.org/10.4271/2009-24-0019.
285. Kleemann, A.P., Menegazzi, P., Henriot, S., and Marchal, A., "Numerical Study on Knock for an SI Engine by Thermally Coupling Combustion Chamber and Cooling Circuit Simulations," (2003), https://doi.org/10.4271/2003-01-0563.
286. Shih, S., Itano, E., Xin, J., Kawamoto, M. et al., "Engine Knock Toughness Improvement Through Water Jacket Optimization," SAE Technical Paper 2003-01-3259, 2003, https://doi.org/10.4271/2003-01-3259.
287. Couet, S., Higelin, P., and Moreau, B., "APIR: A New Firing Concept for the Internal Combustion Engines - Sensitivity to Knock and In-Cylinder Aerodynamics," SAE Technical Paper 2001-01-1954, 2001, https://doi.org/10.4271/2001-01-1954.
288. Kettner, M., Rothe, M., Velji, A., Spicher, U. et al., "A New Flame Jet Concept to Improve the Inflammation of Lean Burn Mixtures in SI Engines," SAE Technical Paper 2005-01-3688, 2005, https://doi.org/10.4271/2005-01-3688.
289. Getzlaff, J., Pape, J., Gruenig, C., Kuhnert, D. et al., "Investigations on Pre-Chamber Spark Plug with Pilot Injection," SAE Technical Paper 2007-01-0479, 2007, https://doi.org/10.4271/2007-01-0479.
290. Kawabata, Y. and Mori, D., "Combustion Diagnostics & Improvement of a Prechamber Lean-Burn Natural Gas Engine," SAE Technical Paper 2004-01-0979, 2004, https://doi.org/10.4271/2004-01-0979.
291. Winter, H., Kogler, G., Schnessl, E., Wimmer, A. et al., "Investigations on Combustion and Heat Transfer in a Large Gaseous Fuelled Engine," SAE Technical Paper 2003-01-0562, 2003, https://doi.org/10.4271/2003-01-0562.
292. Toulson, E., Watson, H.C., and Attard, W.P., "Modeling Alternative Prechamber Fuels in Jet Assisted Ignition of Gasoline and LPG," SAE Technical Paper 2009-01-0721, 2009, https://doi.org/10.4271/2009-01-0721.
293. Hoepke, B., Jannsen, S., Kasseris, E., and Cheng, W.K., "EGR Effects on Boosted SI Engine Operation and Knock Integral Correlation," SAE Technical Paper 2012-01-0707, 2012, https://doi.org/10.4271/2012-01-0707.
294. Alger, T., Mangold, B., Roberts, C., and Gingrich, J., "The Interaction of Fuel Anti-Knock Index and Cooled EGR on Engine Performance and Efficiency," SAE Technical Paper 2012-01-1149, 2012, https://doi.org/10.4271/2012-01-1149.
295. Roberts, P. and Sheppard, C., "The Influence of Residual Gas NO Content on Knock Onset of Iso-Octane, PRF, TRF and ULG Mixtures in SI Engines," SAE Technical Paper 2013-01-9046, 2013, https://doi.org/10.4271/2013-01-9046.
296. Alger, T., Walls, M., Chadwell, C., Joo, S. et al., "The Interaction between Fuel Anti-Knock Index and Reformation Ratio in an Engine Equipped with Dedicated EGR," SAE Technical Paper 2016-01-0712, 2016, https://doi.org/10.4271/2016-01-0712.
297. Szybist, J.P., Wagnon, S.W., Splitter, D., Pitz, W.J. et al., "The Reduced Effectiveness of EGR to Mitigate Knock at High

Loads in Boosted SI Engines," SAE Technical Paper 2017-24-0061, 2017, https://doi.org/10.4271/2017-24-0061.

298. Sjöberg, M., Vuilleumier, D., Kim, N., Yokoo, N. et al., "On the Role of Nitric Oxide for the Knock-Mitigation Effectiveness of EGR in a DISI Engine Operated with Various Gasoline Fuels," SAE Technical Paper 2019-01-2150, 2019, https://doi.org/10.4271/2019-01-2150.
299. Turner, J., Popplewell, A., Patel, R., Johnson, T. et al., "Ultra Boost for Economy: Extending the Limits of Extreme Engine Downsizing," SAE Technical Paper 2014-01-1185, 2014, https://doi.org/10.4271/2014-01-1185.
300. Adomeit, P., Jakob, M., Pischinger, S., Brunn, A. et al., "Effect of Intake Port Design on the Flow Field Stability of a Gasoline DI Engine," SAE Technical Paper 2011-01-1284, 2011, https://doi.org/10.4271/2011-01-1284.
301. Baum, E., Peterson, B., Surmann, C., Michaelis, D. et al., "Investigation of the 3D Flow Field in an IC Engine Using Tomographic PIV," *Proceedings of the Combustion Institute* 34, no. 2 (2013): 2903-2910.
302. Yoshihara, Y., Nakata, K., Takahashi, D., Omura, T. et al., "Development of High Tumble Intake-Port for High Thermal Efficiency Engines," SAE Technical Paper 2016-01-0692, 2016, https://doi.org/10.4271/2016-01-0692.
303. Itabashi, S., Murase, E., Tanaka, H., Yamaguchi, M. et al., "New Combustion and Powertrain Control Technologies for Fun-to-Drive Dynamic Performance and Better Fuel Economy," SAE Technical Paper 2017-01-0589, 2017, https://doi.org/10.4271/2017-01-0589.
304. Suzuki, K., Uehera, K., Murase, E., and Nogawa, S., "Study of Ignitability in Strong Flow Field," in *Ignition Systems for Gasoline Engines*, Günther, S.M., Ed. (Cham: Springer, 2016), ch. 4, 69-84, https://doi.org/10.1007/978-3-319-45504-4 4.
305. Hayashi, N., Sugiura, A., Abe, Y., and Suzuki, K., "Development of Ignition Technology for Dilute Combustion Engines," *SAE Int. J. Engines* 10, no. 3 (2017): 984-995, https://doi.org/10.4271/2017-01-0676.
306. Corrigan, D.J., Pascolini, E., Zecchetti, D., and Titus, F., "Ignition System Development for High Speed, High Load, Lean Boosted Engines," in *Ignition Systems for Gasoline Engines*, Günther, S.M., Ed. (Cham: Springer, 2016), ch. 13, 217-242, https://doi.org/10.1007/978-3-319-45504-4 13.
307. Idicheria, C.A. and Najt, P.M., "Potential of Advanced Corona Ignition System (ACIS) for Future Engine Applications," in *Ignition Systems for Gasoline Engines*, Günther, S.M., Ed. (Cham: Springer, 2016), ch. 19, 315-331, https://doi.org/10.1007/978-3-319-45504-4_19.
308. Singleton, D., Sanders, J.M., Thomas, M.A., Söjberg, M. et al., "Demonstration of Improved Dilution Tolerance Using a Production-Intent Compact Nanosecond Pulse Ignition System," in *Ignition Systems for Gasoline Engines*, Günther, S.M., Ed. (Cham: Springer, 2016), ch. 3, 315-331, https://doi.org/10.1007/978-3-319-45504-4 3.
309. d'Adamo, A., Berni, F., Breda, S., Lugli, M. et al., "A Numerical Investigation on the Potentials of Water Injection as a Fuel Efficiency Enhancer in Highly Downsized GDI Engines," SAE Technical Paper 2015-01-0393, 2015, https://doi.org/10.4271/2015-01-0393.
310. Hermann, I., Glahn, C., Kluin, M., Paroll, M. et al., "Water Injection for Gasoline Engines - Quo Vadis?" in *Knocking in Gasoline Engines*, Günther, M. and Sens, M., Eds. (Cham: Springer, 2017), 299-321, https://doi.org/10.1007/978-3-319-69760-4_18.
311. Heinrich, C., Dörksen, H., Esch, A., and Krämer, K., "Gasoline Water Direct Injection (GWDI) as a Key Feature for Future Gasoline Engines," in *Knocking in Gasoline Engines*, Günther, M. and Sens, M., Eds. (Cham: Springer International Publishing, 2018), 322-337, https://doi.org/10.1007/978-3-319-69760-4_19.
312. Hunger, M., Böcking, T., Walther, U., Günther, M. et al., "Potential of Direct Water Injection to Reduce Knocking and Increase the Efficiency of Gasoline Engines," in *Knocking in Gasoline Engines*, Günther, M. and Sens, M., Eds. (Cham: Springer International Publishing, 2018), 338-359, https://doi.org/10.1007/978-3-319-69760-4_20.
313. Paltrinieri, S., Mortellaro, F., Silvestri, N., Rolando, L. et al., "Water Injection Contribution to Enabling Stoichiometric Air-to-Fuel Ratio Operation at Rated Power Conditions of a High-Performance DISI Single Cylinder Engine," SAE Technical Paper 2019-01-0173, 2019, https://doi.org/10.4271/2019-24-0173.
314. Vacca, A., Bargende, M., Chiodi, M., Franken, T. et al., "Analysis of Water Injection Strategies to Exploit the Thermodynamic Effects of Water in Gasoline Engines by Means of a 3D-CFD Virtual Test Bench," SAE Technical Paper 2019-24-0102, 2019, https://doi.org/10.4271/2019-24-0102.
315. Franken, T., Seidel, L., Matrisciano, A., Mauss, F. et al., "Analysis of the Water Addition Efficiency on Knock Suppression for Different Octane Ratings," SAE Technical Paper 2020-01-0551, 2020, https://doi.org/10.4271/2020-01-0551.
316. ANSYS, "CHEMKIN Pro Homepage," accessed April 12, 2021, https://www.ansys.com/products/fluids/ansys-chemkin-pro.
317. Convergent Science, "Converge Homepage," accessed April 12, 2021, https://convergecfd.com.
318. SIEMENS, "Simcenter STAR-CCM+ Homepage," accessed April 12, 2021, https://www.plm.automation.siemens.com/global/en/products/simcenter/STAR-CCM.html.
319. Atef, N., Kukkadapu, G., Mohamed, S.Y., Rashidi, M.A. et al., "A Comprehensive Iso-Octane Combustion Model with Improved Thermochemistry and Chemical Kinetics," *Combustion and Flame* 178 (2017): 111-134.
320. Miller, J.A., Sivaramakrishnan, R., Tao, Y., Goldsmith, C.F. et al., "Combustion Chemistry in the Twenty-First Century: Developing Theory-Informed Chemical Kinetics Models," *Progress in Energy and Combustion Science* 83 (2021): 100886.
321. Luisi, S., Doria, V., Stroppiana, A., Millo, F. et al., "Experimental Investigation on Early and Late Intake Valve Closures for Knock Mitigation through Miller Cycle in a Downsized Turbocharged Engine," SAE Technical Paper 2015-01-0760, 2015, https://doi.org/10.4271/2015-01-0760.

322. Ketterer, J.E., Gautier, E., and Keating, E.J., "The Development and Evaluation of Robust Combustion Systems for Miller Cycle Engines," SAE Technical Paper 2018-01-1416, 2018, https://doi.org/10.4271/2018-01-1416.
323. Blair, G.P., *Design and Simulation of Four-Stroke Engines* (Warrendale, PA: SAE International, 1999), ISBN:978-0-7680-0440-3.
324. Taylor, J., Gurney, D., Freeland, P., Dingelstadt, R. et al., "Intake Manifold Length Effects on Turbocharged Gasoline Downsizing Engine Performance and Fuel Economy," SAE Technical Paper 2012-01-0714, 2012, https://doi.org/10.4271/2012-01-0714.
325. Toulson, E., Schock, H.J., and Attard, W.P., "A Review of Pre-Chamber Initiated Jet Ignition Combustion Systems," SAE Technical Paper 2010-01-2263, 2010, https://doi.org/10.4271/2010-01-2263.
326. Attard, W.P. and Parsons, P., "Flame Kernel Development for a Spark Initiated Pre-Chamber Combustion System Capable of High Load, High Efficiency and Near Zero NOx Emissions," SAE Technical Paper 2010-01-2260, 2010, https://doi.org/10.4271/2010-01-2260.
327. Attard, W.P. and Blaxill, H., "A Single Fuel Pre-Chamber Jet Ignition Powertrain Achieving High Load, High Efficiency and Near Zero NOx Emissions," SAE Technical Paper 2011-01-2023, 2011, https://doi.org/10.4271/2011-01-2023.
328. Attard, W.P., Bassett, M., Parsons, P., and Blaxill, H., "A New Combustion System Achieving High Drive Cycle Fuel Economy Improvements in a Modern Vehicle Powertrain," SAE Technical Paper 2011-01-0664, 2011, https://doi.org/10.4271/2011-01-0664.
329. Attard, W.P. and Blaxill, H., "A Lean Burn Gasoline Fueled Pre-Chamber Jet Ignition Combustion System Achieving High Efficiency and Low NOx at Part Load," SAE Technical Paper 2012-01-1146, 2012, https://doi.org/10.4271/2012-01-1146.
330. Attard, W.P., Blaxill, H., Anderson, E.K., and Litke, P., "Knock Limit Extension with a Gasoline Fueled Pre-Chamber Jet Igniter in a Modern Vehicle Powertrain," *SAE Int. J. Engines* 5, no. 3 (2012): 1201-1215, https://doi.org/10.4271/2012-01-1143.
331. Mazzoni, D., Musu, E., Bedogni, F., Pivetti, G. et al., "Gasoline Internal Combustion Engine Having Precombustion Chamber and Two Spark Plugs," JP2019049258A, March 2019, https://worldwide.espacenet.com/patent/search?q=pn%3DJP2019049258A.
332. Maserati, "Maserati Presents Nettuno: The New 100% Maserati Engine That Adopts F1 Technology for a Road Car," 2020, accessed January 2021, https://www.media.maserati.com/en-ww/releases/1575.
333. Corrigan, D.J., Di Sacco, M., Medda, M., Paltrinieri, S. et al., "High-Performance Internal Combustion Engine with Improved Handling of Emissions and Method for Controlling Such Engine," EP3561255A1, October 2019, https://worldwide.espacenet.com/patent/search?q=pn%3DEP3561255A1.
334. Yun, H., Wermuth, N., and Najt, P., "Extending the High Load Operating Limit of a Naturally-Aspirated Gasoline HCCI Combustion Engine," *SAE Int. J. Engines* 3, no. 1 (2010): 681-699, https://doi.org/10.4271/2010-01-0847.
335. Manofsky, L., Vavra, J., Assanis, D.N., and Babajimopoulos, A., "Bridging the Gap between HCCI and SI: Spark-Assisted Compression Ignition," SAE Technical Paper 2011-01-1179, 2011, https://doi.org/10.4271/2011-01-1179.
336. Dec, J.E. and Yang, Y., "Boosted HCCI for High Power without Engine Knock and with Ultra-Low NOx Emissions - Using Conventional Gasoline," SAE Technical Paper 2010-01-1086, 2010, https://doi.org/10.4271/2010-01-1086.
337. Maria, A., Cheng, W.K., Kar, K., and Cannella, W., "Understanding Knock Metric for Controlled Auto-Ignition Engines," SAE Technical Paper 2013-01-1658, 2013, https://doi.org/10.4271/2013-01-1658.
338. Iijima, A., Ito, N., Shimada, T., Yamada, M. et al., "A Study of HCCI Knocking Accompanied by Pressure Oscillations Based on Visualization of the Entire Bore Area," SAE Technical Paper 2014-01-2664, 2014, https://doi.org/10.4271/2014-01-2664.
339. Iijima, A., Shoji, H., Yoshida, Y., Rin, C. et al., "A Study of the Behavior of In-Cylinder Pressure Waves under HCCI Knocking by Using an Optically Accessible Engine," SAE Technical Paper 2015-01-1795, 2015, https://doi.org/10.4271/2015-01-1795.
340. Nakai, E., Goto, T., Ezumi, K., Tsumura, Y. et al., "Mazda SKYACTIV-X 2.0L Gasoline Engine," in *28th Aachen Colloquium Automobile and Engine Technology*, Aachen, Germany, 2019.
341. Kasseris, E. and Heywood, J.B., "Charge Cooling Effects on Knock Limits in SI DI Engines Using Gasoline/Ethanol Blends: Part 2-Effective Octane Numbers," SAE Technical Paper 2012-01-1284, 2012, https://doi.org/10.4271/2012-01-1284.
342. Steurs, K., Blomberg, C., and Boulouchos, K., "Formulation of a Knock Model for Ethanol and Iso-Octane under Specific Consideration of the Thermal Boundary Layer within the End-Gas," SAE Technical Paper 2014-01-2607, 2014, https://doi.org/10.4271/2014-01-2607.
343. Steurs, K., Blomberg, C.K., and Boulouchos, K., "Knock in an Ethanol Fueled Spark Ignition Engine: Detection Methods with Cycle-Statistical Analysis and Predictions Using Different Auto-Ignition Models," SAE Technical Paper 2014-01-1215, 2014, https://doi.org/10.4271/2014-01-1215.
344. Leone, T.G., Olin, E.D., Anderson, J.E., Jung, H.H. et al., "Effects of Fuel Octane Rating and Ethanol Content on Knock, Fuel Economy, and CO2 for a Turbocharged DI Engine," SAE Technical Paper 2014-01-1228, 2014, https://doi.org/10.4271/2014-01-1228.
345. Chupka, G.M., Christensen, E., Fouts, L., Alleman, T.L. et al., "Heat of Vaporization Measurements for Ethanol Blends Up To 50 Volume Percent in Several Hydrocarbon Blendstocks and Implications for Knock in SI Engines," SAE Technical Paper 2015-01-0763, 2015, https://doi.org/10.4271/2015-01-0763.
346. Binder, E., Grigoriadis, P., Sens, M., Kitte, J. et al., "A Clean Methane ICE Concept with >45% Efficiency for Hybrid Powertrains," in *29th Aachen Colloquium Sustainable Mobility*, Aachen, Germany, 2020.

347. Stoffels, H., Weber, C., Graf, F., Lauer, S. et al., "The Methane Fuel Based Turbocharged Direct Injection Engine in a Hybrid Powertrain - An Efficient Synergy," SAE Technical Paper 2019-24-0201, 2019, https://doi.org/10.4271/2019-24-0201.

348. Johnson, K., Veenstra, M.J., Gotthold, D., Simmons, K. et al., "Advancements and Opportunities for On-Board 700 Bar Compressed Hydrogen Tanks in the Progression Towards the Commercialization of Fuel Cell Vehicles," *SAE Int. J. Alt. Power.* 6, no. 2 (2017): 201-218, https://doi.org/10.4271/2017-01-1183.

349. Matthias, N.S., Wallner, T., and Scarcelli, R., "A Hydrogen Direct Injection Engine Concept that Exceeds U.S. DOE Light-Duty Efficiency Targets," *SAE Int. J. Engines* 5, no. 3 (2012): 838-849, https://doi.org/10.4271/2012-01-0653.

350. Kalghatgi, G., *Fuel/Engine Interactions* (Warrendale, PA: SAE International, 2013), ISBN:978-0-7680-6458-2.

351. Heuser, B., "Closed Carbon Cycle Mobility," November 2020, http://www.c3-mobility.de/wp-content/uploads/2020/11/2020 08 C3 Mobility Projektvorstellung Englisch.pdf.

352. Williams, J. and Hamje, H., "Testing and Modelling the Effect of High Octane Petrols on an Adapted Vehicle," Tech. Rep., Concawe, May 2020, ISBN:978-2-87567-119-6, https://www.concawe.eu/wp-content/uploads/Rpt 20-8.pdf.

353. Valdenaire, D. and Mennecier, S., "High Octane Petrol Study," Tech. Rep., Concawe, September 2020, ISBN:978-2-87567-125-5, https://www.concawe.eu/wp-content/uploads/Rpt 20-17.pdf.

354. Amer, A., Babiker, H., Chang, J., Kalghatgi, G. et al., "Fuel Effects on Knock in a Highly Boosted Direct Injection Spark Ignition Engine," SAE Technical Paper 2012-01-1634, 2012, https://doi.org/10.4271/2012-01-1634.

355. Kalghatgi, G., Head, R., Chang, J., Viollet, Y. et al., "An Alternative Method Based on Toluene/n-Heptane Surrogate Fuels for Rating the Anti-Knock Quality of Practical Gasolines," SAE Technical Paper 2014-01-2609, 2014, https://doi.org/10.4271/2014-01-2609.

356. Kalghatgi, G., Babiker, H., and Badra, J., "A Simple Method to Predict Knock Using Toluene, N-Heptane and Iso-Octane Blends (TPRF) as Gasoline Surrogates," SAE Technical Paper 2015-01-0757, 2015, https://doi.org/10.4271/2015-01-0757.

357. Gail, S., Cracknell, R.F., Corrigan, D., Festa, A. et al., "Evaluating a Novel Gasoline Surrogate Containing Isopentane Using a Rapid Compression Machine and an Engine," *Proceedings of the Combustion Institute* 38, no. 4 (2020): 5643-5653.

358. Mehl, M., Pitz, W.J., Westbrook, C.K., and Curran, H.J., "Kinetic Modeling of Gasoline Surrogate Components and Mixtures under Engine Conditions," *Proceedings of the Combustion Institute* 33, no. 1 (2011): 193-200.

359. Kitada, T., Kuchita, M., Hayashi, S., Shirota, T. et al., "A Study on Knocking Prediction Improvement Using Chemical Reaction Calculation," SAE Technical Paper 2015-01-1905, 2015, https://doi.org/10.4271/2015-01-1905.

360. Fandakov, A., Grill, M., Bargende, M., and Kulzer, A.C., "Two-Stage Ignition Occurrence in the End Gas and Modeling Its Influence on Engine Knock," SAE Technical Paper 2017-24-0001, 2017, https://doi.org/10.4271/2017-24-0001.

361. Kim, N., Vuilleumier, D., Sjöberg, M., Yokoo, N. et al., "Using Chemical Kinetics to Understand Effects of Fuel Type and Compression Ratio on Knock-Mitigation Effectiveness of Various EGR Constituents," SAE Technical Paper 2019-01-1140, 2019, https://doi.org/10.4271/2019-01-1140.

362. Fontanesi, S., Paltrinieri, S., D'Adamo, A., Cantore, G. et al., "Knock Tendency Prediction in a High Performance Engine Using LES and Tabulated Chemistry," SAE Technical Paper 2013-01-1082, 2013, https://doi.org/10.4271/2013-01-1082.

363. Robert, A., Richard, S., Colin, O., and Poinsot, T., "Les Study of Deflagration to Detonation Mechanisms in a Downsized Spark Ignition Engine," *Combustion and Flame* 162, no. 7 (2015): 2788-2807.

364. Ritter, M., Malbec, L.-M., and Laget, O., "Assessment and Validation of Internal Aerodynamics and Mixture Preparation in Spark-Ignition Engine Using LES Approach," *SAE Int. J. Adv. Curr. Pract. in Mobility* 3, no. 1 (2020): 95-112, https://doi.org/10.4271/2020-01-2009.

365. Corti, E., Forte, C., Bianchi, G.M., and Moro, D., "Relating Knocking Combustions Effects to Measurable Data," SAE Technical Paper 2015-24-2429, 2015, https://doi.org/10.4271/2015-24-2429.

366. D'Adamo, A., Breda, S., Fontanesi, S., and Cantore, G., "A RANS-Based CFD Model to Predict the Statistical Occurrence of Knock in Spark-Ignition Engines," SAE Technical Paper 2016-01-0581, 2016, https://doi.org/10.4271/2016-01-0581.

367. D'Adamo, A., Breda, S., Iaccarino, S., Berni, F. et al., "Development of a RANS-Based Knock Model to Infer the Knock Probability in a Research Spark-Ignition Engine," SAE Technical Paper 2017-01-0551, 2017, https://doi.org/10.4271/2017-01-0551.

368. Breda, S., D'Adamo, A., Fontanesi, S., Giovannoni, N. et al., "CFD Analysis of Combustion and Knock in an Optically Accessible GDI Engine," SAE Technical Paper 2016-01-0601, 2016, https://doi.org/10.4271/2016-01-0601.

369. Bjerkborn, S., Frojd, K., Perlman, C., and Mauss, F., "A Monte Carlo Based Turbulent Flame Propagation Model for Predictive SI In-Cylinder Engine Simulations Employing Detailed Chemistry for Accurate Knock Prediction," SAE Technical Paper 2012-01-1680, 2012, https://doi.org/10.4271/2012-01-1680.

370. Kozarac, D., Tomic, R., Taritas, I., Chen, J.-Y. et al., "A Model for Prediction of Knock in the Cycle Simulation by Detail Characterization of Fuel and Temperature Stratification," SAE Technical Paper 2015-01-1245, 2015, https://doi.org/10.4271/2015-01-1245.

371. De Bellis, V., Teodosio, L., Siano, D., Minarelli, F. et al., "Knock and Cycle by Cycle Analysis of a High Performance V12 Spark Ignition Engine. Part 1: Experimental Data and Correlations Assessment," SAE Technical Paper 2015-01-2392, 2015, https://doi.org/10.4271/2015-24-2392.

372. Bozza, F., De Bellis, V., Minarelli, F., and Cacciatore, D., "Knock and Cycle by Cycle Analysis of a High Performance V12 Spark Ignition Engine. Part 2: 1D Combustion and Knock Modeling," SAE Technical Paper 2015-24-2393, 2015, https://doi.org/10.4271/2015-24-2393.

373. Fontanesi, S., Severi, E., Siano, D., Bozza, F. et al., "Analysis of Knock Tendency in a Small VVA Turbocharged Engine Based on Integrated 1D-3D Simulations and Auto-Regressive Technique," SAE Technical Paper 2014-01-1065, 2014, https://doi.org/10.4271/2014-01-1065.

374. Kikusato, A., Jin, K., and Daisho, Y., "A Numerical Simulation Study on Improving the Thermal Efficiency of a Spark Ignited Engine Part 1: Modeling of a Spark Ignited Engine Combustion to Predict Engine Performance Considering Flame Propagation, Knock, and Combustion Chamber Wall," *SAE Int. J. Engines* 7, no. 1 (2014): 96-105, https://doi.org/10.4271/2014-01-1073.

375. Kikusato, A., Terahata, K., Jin, K., and Daisho, Y., "A Numerical Simulation Study on Improving the Thermal Efficiency of a Spark Ignited Engine Part 2: Predicting Instantaneous Combustion Chamber Wall Temperatures, Heat Losses and Knock," SAE Technical Paper 2014-01-1066, 2014, https://doi.org/10.4271/2014-01-1066.

376. Peters, N., Kerschgens, B., and Paczko, G., "Super-Knock Prediction Using a Refined Theory of Turbulence," SAE Technical Paper 2013-01-1109, 2013, https://doi.org/10.4271/2013-01-1109.

377. Lauer, T., Heiss, M., Bobicic, N., and Pritze, S., "Model Approach for Pre-Ignition Mechanisms," *MTZ Worldwide* 75 (2014): 44-49, https://doi.org/10.1007/s38313-014-0010-6.

378. Liu, H., Wang, Z., Wooldridge, M., Fatouraie, M. et al., "Highly Turbocharged Gasoline Engine and Rapid Compression Machine Studies of Super-Knock," SAE Technical Paper 2016-01-0686, 2016, https://doi.org/10.4271/2016-01-0686.

379. Kalghatgi, G., Algunaibet, I., and Morganti, K., "On Knock Intensity and Superknock in SI Engines," SAE Technical Paper 2017-01-0689, 2017, https://doi.org/10.4271/2017-01-0689.

380. Ohtomo, M., Suzuoki, T., Yamamoto, S., and Miyagawa, H., "Effect of Fuel-Air Mixture Dilution on Knock Intensity in an SI Engine," SAE Technical Paper 2018-01-0211, 2018, https://doi.org/10.4271/2018-01-0211.

381. Cho, J. and Song, H.H., "Understanding the Effect of Inhomogeneous Mixing on Knocking Characteristics of Iso-Octane by Using Rapid Compression Machine," SAE Technical Paper 2018-01-0212, 2018, https://doi.org/10.4271/2018-01-0212.

382. Catapano, F., Costa, M., Marseglia, G., Sementa, P. et al., "Experimental and Numerical Investigation in a Turbocharged GDI Engine Under Knock Condition by Means of Conventional and Non-Conventional Methods," SAE Technical Paper 2015-01-0397, 2015, https://doi.org/10.4271/2015-01-0397.

383. Catapano, F., Sementa, P., and Vaglieco, B.M., "Characterization of Knock Tendency and Onset in a GDI Engine by Means of Conventional Measurements and a Non-Conventional Flame Dynamics Optical Analysis," SAE Technical Paper 2017-24-0099, 2017, https://doi.org/10.4271/2017-24-0099.

384. Imaoka, Y., Shouji, K., Inoue, T., and Noda, T., "A Study of Combustion Technology for a High Compression Ratio Engine: The Influence of Combustion Chamber Wall Temperature on Knocking," SAE Technical Paper 2016-01-0703, 2016, https://doi.org/10.4271/2016-01-0703.

385. Iijima, A., Izako, T., Ishikawa, T., Yamashita, T. et al., "Analysis of Interaction between Autoignition and Strong Pressure Wave Formation during Knock in a Supercharged SI Engine Based on High Speed Photography of the End Gas," *SAE Int. J. Engines* 10, no. 5 (2017): 2616-2623.

386. Huber K. and Hauber J., "Cylinder Pressure-Based Knock Detection—Challenges in Cylinder Pressure Indication and Application in a New Engine-Based Fuel Test Method," in *Knocking in Gasoline Engines*, Kratzsch, M. and Günther, M., Eds.(Cham: Springer, 2013), 119-141.

387. Pal, P., Kolodziej, C.P., Choi, S., Som, S. et al., "Development of a Virtual CFR Engine Model for Knocking Combustion Analysis," SAE Technical Paper 2018-01-0187, 2018, https://doi.org/10.4271/2018-01-0187.

388. Rockstroh, T., Kolodziej, C.P., Jespersen, M.C., Goldsborough, S.S. et al., "Insights into Engine Knock: Comparison of Knock Metrics across Ranges of Intake Temperature and Pressure in the CFR Engine," SAE Technical Paper 2018-01-0210, 2018, https://doi.org/10.4271/2018-01-0210.

389. Hoth, A., Pulpeiro Gonzalez, J., Kolodziej, C.P., and Rockstroh, T., "Effects of Lambda on Knocking Characteristics and RON Rating," SAE Technical Paper 2019-01-0627, 2019, https://doi.org/10.4271/2019-01-0627.

390. Xiao, B., Wang, S., and Prucka, R.G., "Virtual Combustion Phasing Target Correction in the Knock Region for Model-Based Control of Multi-Fuel SI Engines," SAE Technical Paper 2013-01-0307, 2013, https://doi.org/10.4271/2013-01-0307.

391. Corti, E., Forte, C., Bianchi, G.M., and Zoffoli, L., "A Control-Oriented Knock Intensity Estimator," SAE Technical Paper 2017-24-0055, 2017, https://doi.org/10.4271/2017-24-0055.

392. Spelina, J.M., Peyton Jones, J.C., and Frey, J., "Recent Advances in Knock Analysis, Simulation, and Control," SAE Technical Paper 2014-01-1349, 2014, https://doi.org/10.4271/2014-01-1349.

393. Peyton Jones, J.C. and Frey, J., "Threshold Optimization and Performance Evaluation of a Classical Knock Controller," SAE Technical Paper 2015-01-0871, 2015, https://doi.org/10.4271/2015-01-0871.

394. Peyton Jones, J., Spelina, J.M., and Frey, J., "Control-Oriented Knock Simulation," SAE Technical Paper 2016-01-0821, 2016, https://doi.org/10.4271/2016-01-0821.

395. Siano, D., Panza, M.A., and D'Agostino, D., "Knock Detection Based on MAPO Analysis, AR Model and Discrete Wavelet Transform Applied to the In-Cylinder Pressure Data: Results and Comparison," SAE Technical Paper 2014-01-2547, 2014, https://doi.org/10.4271/2014-01-2547.

396. Rosetti, A., Iotti, C., and Cantore, G., "Intake Manifold Primary Trumpet Tuning Options for Fuel Flow Limited High Performance I.C.E," SAE Technical Paper 2019-24-0005, 2019, https://doi.org/10.4271/2019-24-0005.

397. Sassi, L., Kitsopanidis, I., and Lovett, G., "Evolutions in F1 Engine Technology: Pursuing Performance from Today's Power Unit through Efficiency," Presented at the in *37th Engine Symposium*, Vienna, 2016.

398. Clasen, K.H. and Koopmans, L., "Investigation of Homogeneous Lean SI Combustion in High Load Operating Conditions," *SAE Int. J. Adv. & Curr. Prac. in Mobility* 2, no. 4 (2020): 2051-2066, https://doi.org/10.4271/2020-01-0959.

399. Symonds, P., "Future Powertrains in F1," Presented at the in *IMechE High Performance Powertrains Conference*, Online, 2020.

400. Burke, U., Cracknell, R., Evans, M., Poulet, B. et al., "Use of a Rapid Compression Machine to Characterize the Anti-Knock Properties of High Octane Fuels," Presented at the in *36th International Symposium on Combustion*, Seoul, 2016.

401. Fédération Internationale de l'Automobile, "FIA Formula 1 Regulations 2021," 2021, https://www.fia.com/regulation/category/110.

402. Mercedes-AMG Petronas Formula One Team, "Mercedes AMG F1 INSIGHT: Five Examples Why F1 Is Accelerating the Future," 2018, accessed January 2021, https://www.mercedesamgf1.com/en/news/2018/10/insight-five-examples-why-f1-is-accelerating-the-future/.

403. Zhang, G., Wang, Q., Chen, G., de Oliveira, D. et al., "Geely Hybrid Engine: World Class Efficiency for Hybrid Vehicles," in *29th Aachen Colloquium Sustainable Mobility*, Aachen, Germany, 2020.

404. Garrett, "Garrett E-Turbo Technology Accelerating Global Powertrain Electrification Trends Beginning with Mercedes-AMG," July 2020, https://www.garrettmotion.com/news/media-materials/press-releases/.

405. Splitter, D.A., Pawlowski, A.E., and Wagner, R.M., "A Historical Analysis of the Co-Evolution of Gasoline Octane Number and Spark-Ignition Engines," *Frontiers in Mechanical Engineering* 1, no. 21 (2016): 1-22, https://www.frontiersin.org/article/10.3389/fmech.2015.00016.